A Case Study of Wave Power Integration into the Ucluelet Area Electrical Grid

by

Louise Anne St.Germain
B. Eng., Carleton University, 2003

A Thesis Submitted in Partial Fulfillment of the
Requirements for the Degree of

MASTER OF APPLIED SCIENCE

in the Department of Mechanical Engineering

University of Victoria

Supervisors: Dr. Andrew Rowe
Dr. Peter Wild

Abstract

Technologies exist that can capture and convert wave energy but there are few studies examining systemic integration of wave energy devices. This work examines the potential to use wave energy as a renewable energy resource on Vancouver Island, specifically in the Tofino/Ucluelet area. A model of a wave energy conversion (WEC) device was developed as a module within TRNSYS™ where it can be coupled to a load as well as to a storage medium. For this particular study, wave profiles generated from hourly average data for a location on the west coast of Vancouver Island are used as a resource input. An analysis of the potential to use wave energy is carried out with an emphasis on overall system efficiency and resulting device scaling. The results of the wave energy conversion with and without storage, as well as the general economics of these scenarios, are used to make recommendations regarding technical feasibility of wave power projects on Vancouver Island.

Supervisors: Dr. Andrew Rowe, (Department of Mechanical Engineering)
Dr. Peter Wild, (Department of Mechanical Engineering)

Table of Contents

List of Figures

List of Tables

Acknowledgements

I would like to thank my supervisors, Drs. Andrew Rowe and Peter Wild, who were patient with me as my thesis idea(s) morphed from one thing to another until we settled on this topic. I would especially like to thank Dr. Andrew Rowe for still considering me for the M.A.Sc., even after the incident with his car!

A big thanks also to my parents, Rick and Suzanne, particularly Mom, whose constant nagging got me in gear to actually finish this thing. Their financial support was also very helpful.

Thanks to Ron Songprakorp, my office-mate, whose incredible generosity kept me well-fed with amazingly good food (why is it that everything they cook is fantastic, and everything I cook is barely edible?), as well as with interesting stories and insight into life in Thailand.

Thanks also to S/Lt Thomas Kliem for the encouragement, optimism, and incentive to get this done.

Last but not least, thanks to Christina Ianniciello, my “partner in crime” here at UVic, whose friendship, ready smile, and ability to commiserate were essential to my survival in my time here.

1 Introduction

Vancouver Island, with a population of approximately 665,000 people [1], is responsible for 26% of BC's yearly residential electricity demand [2]. Six hydroelectric facilities totalling 450 MW exist on the island, as well as a 99.7 MW combustion turbine which runs on diesel [3]. As Vancouver Island's total load fluctuates between 1.2 and 1.8 GW [4], the rest of the electricity comes from mainland British Columbia via submarine cables. The cables linking Southern Vancouver Island to the mainland are now approximately 50 years old, and starting in late 2006, a program of cable replacement and equipment upgrade will lead to the temporary decommissioning of certain cables [5]. This, along with a demand for power growing at a rate of 1.6% per year, would lead to a shortage of power on the Island [6]. Therefore, in October 2003, BC Hydro issued a Call For Tender (CFT) to find a way to meet the demand for power [7]. As a result, on February 17, 2005, the British Columbia Utilities Commission (BCUC) approved a plan to build a 265 MW natural gas power plant at Duke Point on Vancouver Island [8]. Four months later, the project was cancelled due to continuing appeals which made the process too risky for BC Hydro [9].

Given Vancouver Island's dependence on electricity from mainland British Columbia, BC Hydro has invited proposals from independent power producers (IPPs) on the island for contracts to purchase electricity from these installations. Though BC Hydro has withdrawn its backing of a joint venture for a demonstration wave power project near Ucluelet, it continues to encourage the development of wave power projects on the Island [10].

Wave energy, like most resources, is not spread evenly throughout the world. In general, equatorial areas tend to have weaker waves than areas closer to the poles. A sampling of average wave power values is shown on the world map in Figure 1.1.

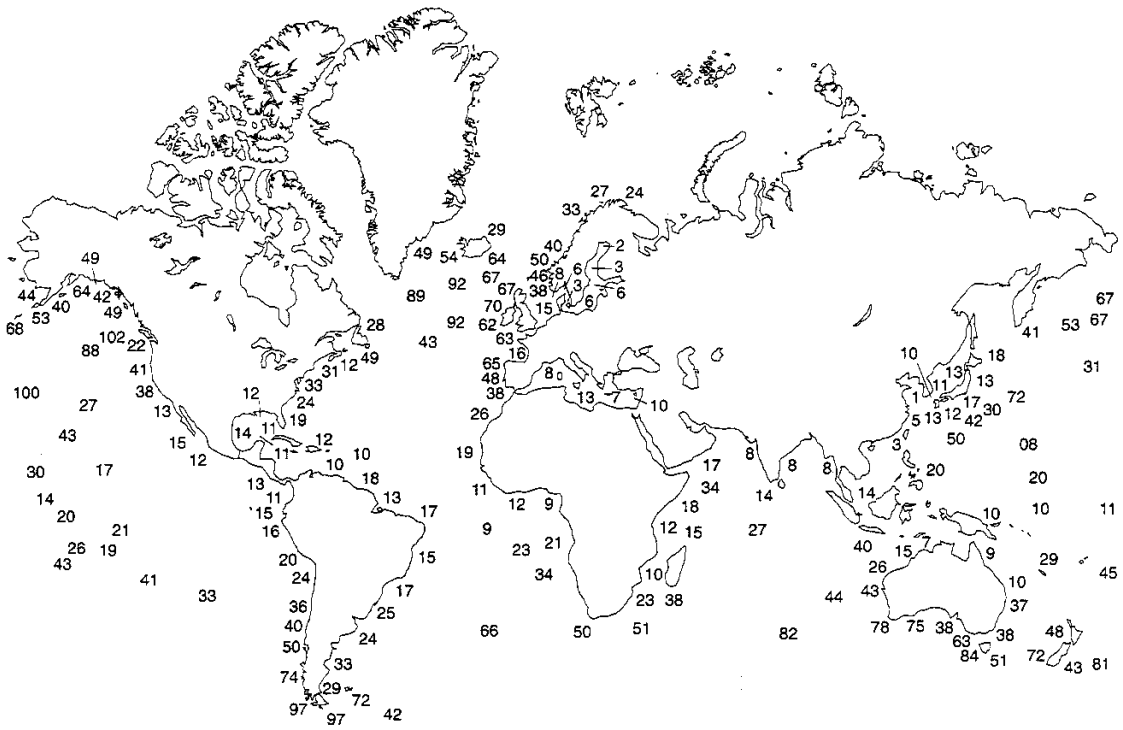

Figure 1.1 - Wave power values, given in kW/m crest length, in various locations worldwide [11]

Given Canada's lengthy coastlines and northerly location, this gives Canada generous amounts of wave energy resources compared to other countries.

While Canada has coastlines on three oceans – namely, the Pacific, Atlantic, and Arctic oceans, all with potentially useful wave energy, this work focuses only on the Pacific Ocean, and in particular the West coast of Vancouver Island. In the future, this case study can be extended to larger areas of Canada.

BC Hydro has identified two locations on Vancouver Island that would be suitable for wave energy installations: one at Amphitrite Point, near Ucluelet, and the other at Winter Harbour in the Northwest of Vancouver Island. These two locations are indicated on the map in Figure 1.2. In 20 years' time, BC Hydro had anticipated that each site could be developed to 100 MW of installed capacity, at a unit energy cost of $100/MWh at each site [12]. By 2002, an initial demonstration project of 3 to 4 MW capacity was planned for Vancouver Island [13]. In February 2002, BC Hydro signed a Memorandum of Understanding with Energetech Australia Pty Ltd, an Australian company, to enter a joint

venture in the development of 2 MW of wave power capacity on Vancouver Island [14]. By the end of 2003, BC Hydro had officially abandoned the project [15]. However, as of June 2004, Energetech claimed to still be involved with the Vancouver Island project, indicating that the project may still proceed independent of BC Hydro [16].

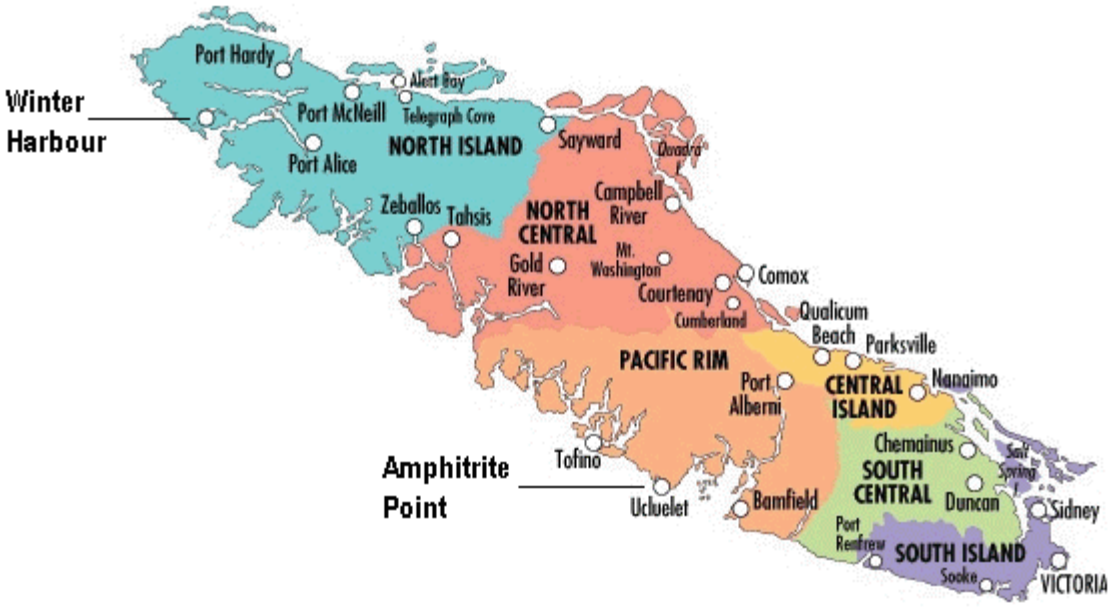

Figure 1.2 - Map of Vancouver Island showing two candidate locations for wave power installations - Amphitrite Point (Ucluelet) and Winter Harbour (map modified from [17])

The objective of this research is to determine how much wave power can feasibly be converted for use in servicing the residential load in the Tofino/Ucluelet area of Vancouver Island, and the infrastructure required for such an undertaking. The problem has been broken down into three sections, which address:

- The magnitudes of the energy resource and the residential load;
- The energy capture capability of current technology;
- The viability of such an endeavour, from the perspective of an investor.

If such a project could be undertaken, it could reduce Vancouver Island's dependence on transmission cables from the mainland, and the renewable nature of the resouce could increase the likelihood of acceptance of a project, avoiding the lengthy succession of appeals which ultimately caused the cancellation of the Duke Point gas-fired plant [9].

2 Status of the Industry

2.1 Introduction

To gain a better understanding of the rationale for wave energy conversion and the types of devices chosen for simulation over the course of this thesis, this chapter presents information which will be useful in placing the research in context. The first section describes some of the wave projects which exist worldwide. The second section presents the variety of storage options for electricity generated from intermittent resources such as wind and wave, while the next two sections present reasons why the use of storage could mitigate problems related to grid integration of renewables. The last section describes a few economic studies which have been perfomed relating to wave energy.

2.2 Existing Wave Energy Conversion Projects

While both wave and tidal energy exist in significant quantities, wave energy conversion technologies are not as well-known as those which capture tidal energy. Several large tidal barrage facilities exist worldwide, and devices which capture energy from tidal currents are also in development [18]. However, this thesis focuses only on wave energy conversion technologies, which are summarized in this section.

There are nearly as many ideas for wave energy conversion (WEC) devices as there are research groups, and it would therefore be a difficult and lengthy process to describe each one in this thesis. Therefore, some of the larger projects will be briefly described in this section, and Chapter 4 is dedicated to more detailed descriptions of the two major technologies which will be simulated – the oscillating water column (OWC), and the Pelamis, which is a heaving and pitching device.

A common type of WEC design is the point absorber, whose dimensions are small compared to the wavelength of the incident waves [11]. One of these point absorbers, the

Salter Duck, was one of the original modern WEC device designs. Salter's device, also called a Nodding Duck, is a tear-shaped hydraulic device that converts the motion of the waves into rotational motion, causing an internal fluid to run unidirectionally through a specially designed pump to generate electricity [19]. This device is illustrated in Figure 2.1. Though the Salter Duck project ran into financial difficulties and never did get to the commercialization stage, many other point absorbers exist which are based on the concept of using hydraulics to convert wave motion into rotational motion and then to electricity.

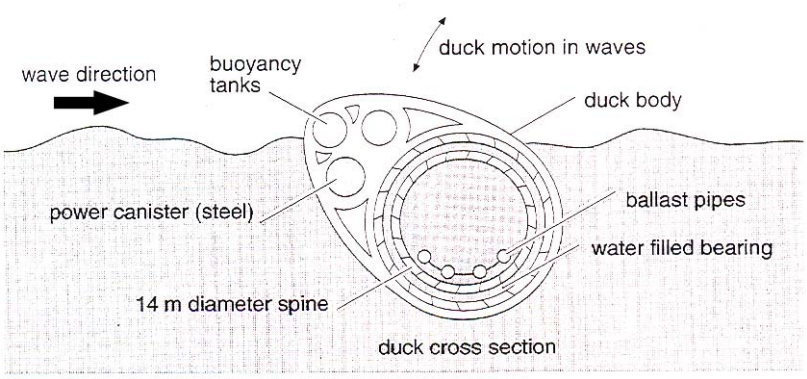

Figure 2.1 - Salter Duck point absorber [11]

Another type of device is the overtopping device, of which the Wave Dragon is one. In this type of device, waves are focused onto a ramp, such that the wave height increased enough to spill water into a floating reservoir. Electricity is then extracted by using a low-head turbine similar to those used in hydroelectric facilities. The Wave Dragon, developed in Denmark, will eventually have a rated power of 4 to 10 MW. A 1:4.5 scale prototype is currently in the water off the coast of Denmark, and is also one of the few grid-connected wave energy devices [20].

OWCs are the most mature of the wave technologies, though they are still in their infancy compared to other energy conversion devices such as photovoltaic arrays and wind turbines. OWCs are pneumatic devices which convert water motion to air motion within an enclosed chamber, and this reciprocating motion of the air is run through a turbine attached to a generator to produce electricity. The principle will be described in more

detail in section 4.2. A floating OWC in Japan called the Mighty Whale was built and moored in 1998, and its four generators have a total rated output of 120 kW. It was found that the maximum efficiency, comparing electrical output with wave energy input, was only 15% [21].

Further information on a number of other devices is available in Thorpe's comprehensive report "A Brief Review of Wave Energy" [22].

2.3 Storage Media

There are many options available for the storage of electricity, some of which are more suited for short term events whereas others can provide larger and longer-term capacity. These include:

- hydrogen
- batteries
- flow batteries (such as VRB)
- supercapacitors
- flywheels
- pumped hydro
- superconducting magnets
- compressed air

Flywheels, supercapacitors, and superconducting magnets are very short-term storage technologies and will not be considered in this study.

2.3.1 Flow Batteries

The vanadium redox battery (VRB) is one option for chemical storage of electrical energy. It operates on a principle similar to that of a fuel cell, with an ion-selective membrane separating the oxidizing reaction from the reduction reaction. The electrolytes on both sides are contained in tanks and the fluid is circulated through the membrane

stack via pumps. As with a fuel cell system, electrons travel through an external circuit, which produces electricity. Alternatively, the system can be run in reverse, allowing the storage of energy in the electrolytes [23]. Figure 2.2 shows a general schematic of a VRB system.

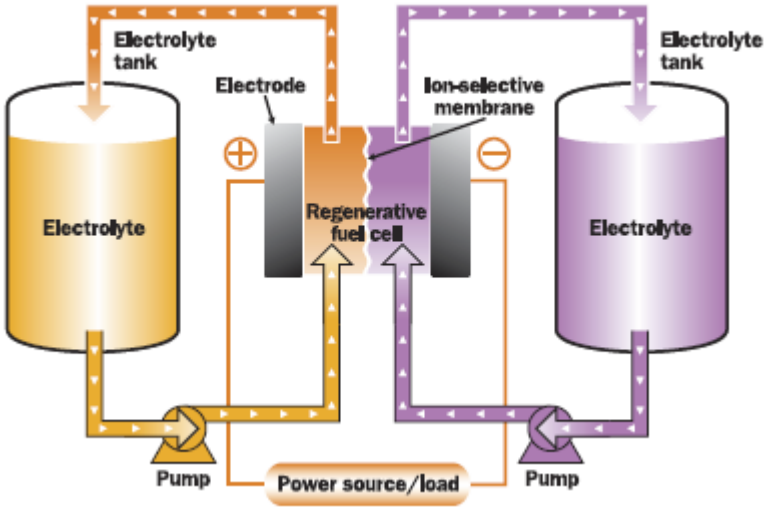

Figure 2.2 - Vanadium Redox Battery (VRB) schematic [23]

One of its main advantages over conventional lead-acid batteries is its tolerance for deep discharge [24]. While its main application would be for load levelling, it is also suitable for power quality control and the stabilization of renewable energy outputs, due to its quick response and overload capacity, which allows it to provide more than its rated output for short periods of time [25].

Since the storage capacity and power input/output of VRB systems are independent of each other, unlike conventional batteries, the specifications of a VRB system are usually given as rated output times the number of hours this output could be maintained given the storage size. Therefore, multiplying the power output by the number of hours gives the storage capacity.

Several VRB projects have been implemented in Japan, with the largest being a semiconductor factory whose system includes a 3 MW/1.5s voltage sag protection system

as well as a 1.5 MW/1h load-leveling system [25, 26]. Sumitomo is also experimenting with a 275 kW wind turbine, which includes a VRB storage system of 175 kW/ 6h [26]. VRB Power Systems, a Vancouver company, has installed a VRB system in Moab Valley, Utah, rated at 350 kW with a storage capacity of 2 MWh [27], which appears to be currently one of the largest installations in the world.

The VRB system will be used as the basic model for storage in this thesis, due to the independence of storage capacity and power output, and also because of the relative simplicity of basing the storage performance on a nominal efficiency. VRB power systems has claimed a system round-trip efficiency of 70-78% [23], while HILTech uses a more optimistic value of 85% [28]. A moderate efficiency within VRB's range will be used in this model, and will be discussed further in section 6.6.3.

2.3.2 Hydrogen system

Though VRB flow batteries are a promising method of energy storage, other methods exist as well. Several attempts have been made to use hydrogen storage for renewable energy systems, including the IRENE system at the University of Victoria [29] and the Hydrogen Research Institute's system at the Université du Québec à Trois-Rivières [30]. Simulations for other similar systems have been attempted by numerous groups worldwide [31-34]. One of the main concerns in designing a wave energy conversion system with hydrogen storage is that the experimental results of the IRENE system, for example, shows a round-trip efficiency of approximately 15%, far lower than is claimed by literature based on simulations. There have also been difficulties in producing a cost-effective system based on off-the-shelf components [29].

To date, no hydrogen-and-wave systems have been built, though the Scottish Fuel Cell Consortium has made a proposal to the Highlands and Islands Enterprise for a project combining a hydrogen storage system with the output of the LIMPET oscillating water column (OWC) on the Isle of Islay in Scotland [35]. Currently, no further information is available as the proposal is confidential.

2.3.3 Pumped hydro

Pumped hydro is a method of energy storage which converts energy in the form of electricity into potential energy as water is pumped from a lower reservoir to a higher one. The Rocky Mountain Institute in conjunction with BC Hydro agree that potential pumped hydro sites exist on Vancouver Island [36], so this could be a viable alternative if a wave energy project were to be built off the coast of the island. The round-trip efficiency of this process is in the range of 75% [37], which is in the same range as the VRB flow batteries.

2.3.4 Batteries

A large number of renewable energy projects use electrochemical storage in the form of batteries (such as lead-acid), particularly in smaller-scale or off-grid applications. This is mainly because batteries are a relatively mature technology, and are available in a variety of sizes and capacities. The round-trip efficiency of lead-acid batteries is typically between 65% and 80% [38], though in their study Perrin et al. claim it could be slightly higher than 80% [39]. The efficiency is, however, dependent on the life cycle of the battery and decreases over time, particularly in the case of deep discharging [40].

2.3.5 Compressed air

Excess energy from a renewable resource such as wind or wave can be used to compress air. Depending on the amount of air, it can be stored in small containers, such as gas bottles, or in large structures, such as underground salt caverns or aquifers. When the energy is needed again, the compressed air can be used in conjunction with a turbine and natural gas to generate electricity [38, 41]. Though a large amount of energy could be stored depending on the availability of suitable geological features, the round-trip efficiency of the process is approximately 40-50% [38], which is much lower than the estimates for VRB or pumped hydro. Therefore, for the purposes of this study, compressed air storage was not simulated, though it could potentially be an option for future developments if a site proved suitable for this technology.

The next section describes the impacts of renewable energy on the grid. Problems associated with grid integration provide an incentive to use storage in hopes of mitigating

some or all of the problems encountered when attempting to integrate renewable energy with an electrical distribution network.

2.4 Impacts of Intermittent Renewable Energy on Grid

Solar energy, like most renewables, is an intermittent resource, but has some predictability due to patterns of night and day. Wave energy and wind energy, though intermittent, are also more irregular, with energy levels fluctuating substantially from hour to hour and even minute to minute. In the absence of large-scale wave energy conversion installations, the inherent similarity between wind and wave resources leads to the conclusion that any issues encountered with large-scale wind installations will likely also be encountered with large-scale wave energy facility. To quantify the effects of intermittent and irregular energy on transmission networks, the literature on grid-connected wind energy installations was surveyed, as experience in these installations is considerable. Following that, Section 2.4.2 describes what is known of wave energy impacts on the grid.

2.4.1 Wind Energy

One important case study in wind energy is the Danish transmission network, where 50% of the electricity generation in 2001 came from wind turbines and combined heat and power (CHP) plants. According to Jensen [42], the only reason this system functions is because of Denmark's high-capacity transmission lines to other countries whose electricity is principally generated by other means. Costs were incurred from upgrading the weak networks often found in areas suitable for wind power generation. Jensen notes that Denmark requires a solution for the long-term, but does not suggest solutions.

Østergaard [43] confirms that the present distribution network, originally meant for unidirectial transmission of electricity from central stations, cannot support large-scale integration of intermittent distributed generation sources such as wind. He concluded that grid reinforcements in both Denmark and neighbouring countries would be necessary in

order to be able to export enough electricity in times of peak generation, unless power-balancing were to be applied.

The introduction of renewables such as wind into small or isolated transmission networks also poses challenges [44, 45]. Weisser and Garcia [45] discuss the effect of introduction of wind energy in isolated communities originally dependent on diesel power generation. Wind penetration, which is the amount of electricity generated by wind as a percentage fo the total grid capacity, is limited. High penetration levels require system management changes and infrastructure upgrades, which are costly and can reduce overall system performance. The solutions proposed for increasing penetration while reducing disruptions include grid reinforcement, grid voltage-controlled wind power production, inclusion of storage as wind output buffer, and better wind velocity forecasting.

Several other researchers [43, 46-48] have recognized the difficulties with reactive power introduced to the transmission network due to the induction generators used in wind turbines. While Østergaard [43] identifies its negative impact on the quality of power in the Danish distribution network, Tande [48] contends that current power system simulation tools do not include models of wind farms, and the effects are therefore difficult for utilities to anticipate and account for in their designs.

Jardan et al. [46] take the next step, recognizing that reactive power from renewable sources could be used to the advantage of a distribution network, by providing power factor correction that would normally have separate correction. This paper describes the technical approach to the design of a converter which can be controlled to deliver the proper amount of active and reactive power, to maintain an overall system power factor close to unity.

2.4.2 Wave Energy

It is apparent that numerous issues exist in the integration of wind farms into distribution networks which were designed for centralized plants. As previously mentioned, few wave

energy projects are grid-connected, and only three studies have been identified which address integration effects. Falcao [49] describes the development of a control strategy for the Pico OWC, since the dynamic effects of turbine stall and power oscillations were determined to be detrimental to the grid. Glendenning [50] recognized the potential grid connection problems back in 1978, and proposed short-term storage as a requirement in wave energy devices to even out the power fluctuations. The LIMPET OWC is grid-connected through a grid protection system, and it was found that while the LIMPET has never caused any grid faults, on numerous occasions faults originating from the grid have caused the shutdown of the LIMPET [51].

2.5 Wave Economics

Several studies have touched on the economics of wave power conversion projects, but due to the lack of data, these studies are, generally speaking, based on assumptions and estimates. The following paragraphs describe the differing approaches of each of three papers which focus specifically on economic aspects of wave energy.

The Danish Wave Energy programme uses a very rough estimation of structural cost based on the quantity of materials and the unit costs of standard materials. The cost of power take-off was calculated in general terms, using a common unit value per kW [52].

Stallard et al. at Lancaster University are developing a model which will predict which type of device is suitable for a given scale of an installation, by determining the lifetime costs of installation, maintenance, operation, and disposal. At present the model is not complete but does provide a foundation for the connection between the number of devices required and the overall cost of a plant encompassing them [53].

In Europe, the European Wave Energy Thematic Network (EWEN) examined some of the economic aspects of wave energy, specifically focusing on the future scenario where R&D challenges have been overcome and the technologies can benefit from economies of scale [54]. While this is not currently the situation with wave energy technologies and

is therefore not directly applicable to the economic overview which will be conducted for this thesis, their conclusion that new OWCs and point absorbers are the least costly of the devices they studied lends support to the choice in this paper to focus on these two types of device.

2.6 Summary

This chapter gives an overview of the status of wave energy projects, and the similarities between wind and wave resources highlight concerns which may be common to both. The next step is to begin the process of examining a particular scenario for wave energy conversion implementation. In the next chapter, the analysis of such a project on Vancouver Island begins with a quantification of the wave resource available.

3 Wave Resource Quantification

3.1 Introduction

To determine whether wave energy conversion devices would be suitable for power production on the west coast of Vancouver Island, it is necessary to understand wave formation and energy transport. Furthermore, it is important to understand the changes which occur to waves as they enter shallow water and approach shore.

In this chapter, these points are covered as much as will be necessary for the purposes of wave energy conversion simulation. The chapter begins with a discussion of how waves are formed, and where the energy lies. Deep water waves, which are unaffected by interaction with the sea floor are considered and the main governing equations are introduced. This is followed by a discussion of the effects of shallow water on waves, particularly regarding mechanisms by which waves lose energy in shallow water, which will be important in the discussion of shallow water wave energy conversion devices such as shoreline oscillating water columns. Finally, the specific wave climate near Tofino and Ucluelet is examined, using data from BC Hydro and Environment Canada wave buoys.

3.2 Wave Formation

Ocean waves come in a variety of sizes and periods, from small capillary waves with a period of less than a second, up to planetary waves, which are due to differential rotation effects of the earth and whose periods are on the order of a hundred days [55]. The total wave energy in the ocean is distributed among the waves of different wavelengths, as shown in Figure 3.1. A significant amount of energy is transferred from the wind to the ocean in the form of capillary waves, wind waves, and swell.

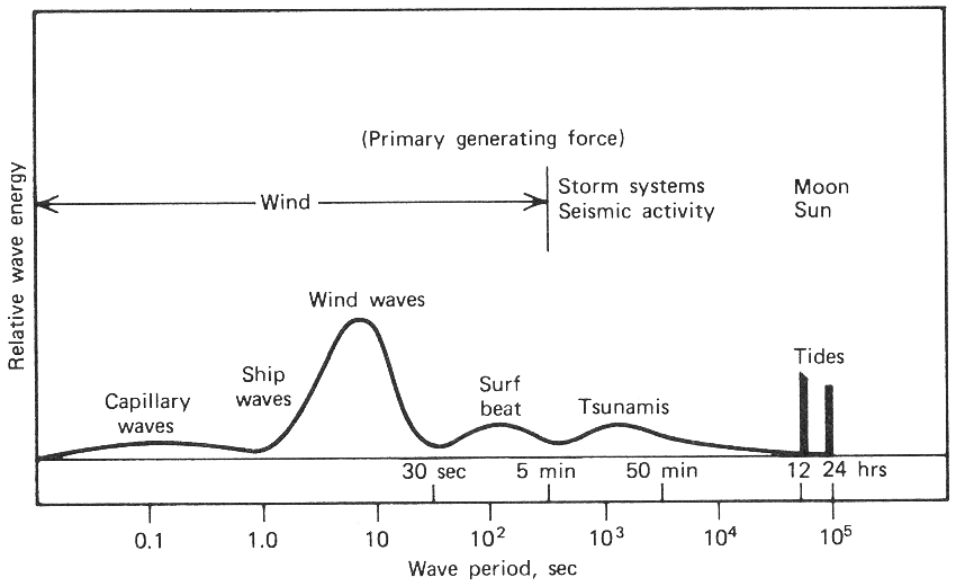

Figure 3.1 - Schematic energy spectrum of ocean variability (the energy along the y axis is in arbitrary units) [56]

While the exact interactions between the wind and the water can be complex and are not always well understood, at least three different mechanisms are involved in the development of wind waves [11]:

1. The wind exerts a tangential stress on the water surface of the sea, causing wave formation and growth.
2. Near the water surface, air flow may cause further wave development if the pressure fluctuations are in phase with existing waves.
3. When a wave is large enough, wind can exert more direct force on the upwind side of the wave, leading to further growth of the wave.

3.3 Deep Water Waves

The behaviour of waves in water is often quite complex, particularly in shallow waters where there are interactions between the water, the ocean floor, and the shore. For the purposes of determining the behaviour of waves, water is considered deep when the depth is over half the wavelength of the water [57]. In this case, the waves on the surface of the water do not “feel” the ocean floor, and thus simplifications can be made to the equations which characterize the wave motion. This section describes the behaviour of waves in

deep water, and begins with a further simplification, assuming that the wave train is monochromatic, or that all waves are of uniform height and wavelength. Later, in Section 3.3.2, the irregularities of oceanic wave trains will be discussed.

3.3.1 Energy in Deep Water Waves

Characteristic parameters of a wave include the wave height (H), the wave length (L), and the period of the wave (T). These characteristics, as well as a few others which will be touched on shortly, are illustrated in Figure 3.2 [55]. One important point to note in dealing with water wave calculations is the use of wave height, which is the height from trough to crest, while wave amplitude (a) is the height from the mean water level to either trough or crest.

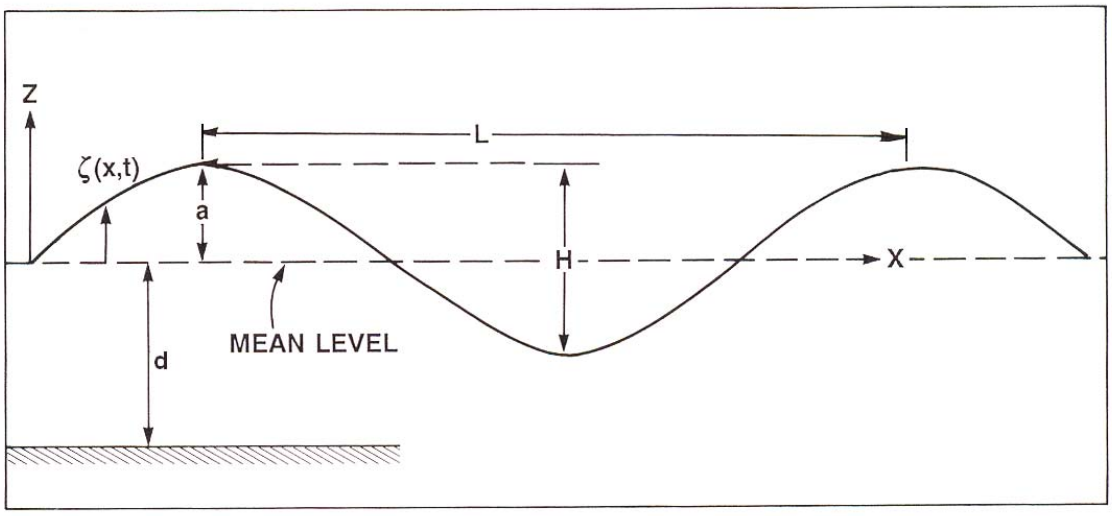

Figure 3.2 - Characteristics of a wave (modified from [55])

The wave number, *k*, is a measure often used in the quantitative analysis of waves. It is the reciprocal of the wavelength or, in other words, the number of wave cycles per metre. The following two equations for wave number are equivalent and both are commonly used [58].

$$k = \frac{2\pi}{L} \quad [\mathrm{m}^{-1}] \tag{3.1}$$

$$k = \frac{\omega}{c} \quad [\mathrm{m}^{-1}] \tag{3.2}$$

The angular frequency in equation (3.2) is given by:

$$\omega = \frac{2\pi}{T} \tag{3.3}$$

The wave celerity, c, is the speed of propagation, and is given in equation (3.15).

The waves which are formed on the surface of the ocean vary in height, wavelength, and period. To understand the properties of ocean waves, a monochromatic wave train is assumed, where all waves are of uniform height, period, and wavelength. $\zeta(x,t)$, which represents the height of a specific point on the wave surface, can be expressed as [59]:

$$\zeta = a\cos(kx - \omega t) \tag{3.4}$$

where

a = amplitude of the wave [m]

T = angular frequency [rad/sec]

k = wave number [m^{-1}]

x = horizontal displacement in the direction of propagation of the wave [m]

The potential energy per unit horizontal surface area of the wave is given by [55]:

$$E_p = \frac{1}{L}\int_0^L \frac{\rho g}{2}\zeta^2 dx \tag{3.5}$$

where

L = wavelength [m]

ρ = density of seawater, taken to be a constant 1025 kg/m^3

Performing this integration and simplifying results in the following relationship:

$$E_p = \frac{\rho g a^2}{4} \tag{3.6}$$

If the wave height (H) rather than the amplitude is used, the equation becomes

$$E_p = \frac{\rho g H^2}{16} \tag{3.7}$$

The kinetic energy per unit surface area of one wavelength is given by:

$$E_k = \frac{\rho}{2L} \int_0^L \int_{-d}^{\zeta} (u^2 + w^2) dz dx \tag{3.8}$$

where *u* and *v* are the horizontal and vertical components of the fluid velocity respectively, and *d* is the water depth.

In deep water, *u* and *w* are given by:

$$u = a\omega e^{kz} \cos(kx - \omega t) \tag{3.9}$$

$$w = a\omega e^{kz} \sin(kx - \omega t) \tag{3.10}$$

Substituting equations (3.9) and (3.10) into (3.8) and solving, using the deep water limit (water depth, d, tends to infinity) yields the following equation for the kinetic energy per unit surface area:

$$E_k = \frac{\rho g a^2}{4} e^{2k\zeta} \tag{3.11}$$

This can be further simplified with the small amplitude assumption, which states that the wave height is small compared to the wave length (H/L << 1). This reduces the exponential term to 1 and brings the equation for kinetic energy to:

$$E_k = \frac{\rho g a^2}{4} \text{ or}$$

$$E_k = \frac{\rho g H^2}{16} \tag{3.12}$$

The total energy in the wave is given by the sum of the kinetic and potential energies:

$$E = E_p + E_k = \frac{\rho g H^2}{8} \tag{3.13}$$

The mean wave power per unit crest width over a wave period is simply the energy in the wave multiplied by the rate of transmission, which is equal to the group velocity of the wave, c_g.

$$P = E \cdot c_g \tag{3.14}$$

For deep water, the group velocity c_g is approximately c/2, or half of the wave celerity, which is the wave's propagation velocity. The celerity in deep water is:

$$c = \frac{g}{\omega} \tag{3.15}$$

Inserting (3.15) and (3.3) into (3.14) yields the power per unit crest length:

$$P = \frac{\rho g^2 H^2 T}{32\pi} \quad \text{[W/m]} \tag{3.16}$$

This equation for wave power in deep water, as derived in [55], is also found either exactly or in equivalent forms in several other sources [11, 38, 56, 60, 61]. This is therefore the equation used in the simulations for this study, where wave height and period are measurements gathered from a buoy.

3.3.2 Properties of Oceanic Waves

While the previous sub-section concludes with the power for a monochromatic wave train, in reality, ocean waves are not monochromatic due to the superposition of waves from different sources [11]. Figure 3.3 is an example of a typical wave record, showing the irregular nature of the waves.

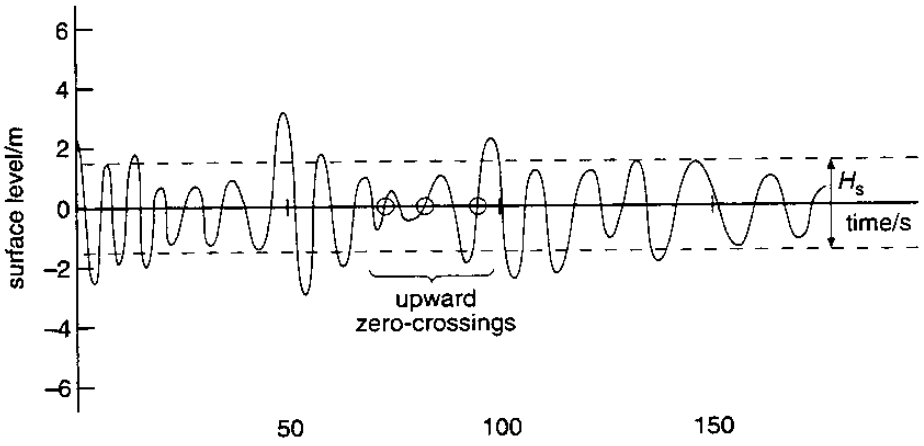

Figure 3.3 - A wave record showing the irregularities in ocean waves [11]

To make calculations using wave data, statistical measures are used. Of these, the most frequently encountered are the significant wave height, H_{sig} (also denoted by H_s or H_{33}), and the significant period, T_{sig} or T_s. The significant wave height is the average height of the highest 1/3 of the waves, and roughly corresponds to the wave height as would be estimated by a human observer [11]. The significant wave period is the average wave period of the highest 1/3 of the waves. Other measures often encountered include the average wave height (H_{ave}), and peak period (T_p).

For the work in this thesis, the significant wave height and significant wave period as recorded by a measurement buoy are used in the hourly calculation of wave power through equation (3.16).

3.4 Shallow Water Waves

Depending on the WEC technology used in a project, it may be necessary to determine the wave conditions in shallow water. For example, both the Energetech and OSPREY OWCs are shallow water or nearshore devices, with the Energetech device operating ideally in waters 5 to 50 m deep [62], and ideally 14 m deep for the OSPREY [22].

One of the first considerations is determining whether the nearshore devices are within the surf zone. A WEC device which is within range of breaking waves can be exposed to large and potentially damaging forces from breaking waves [63]. Furthermore, the type of wave breaking can affect the amount of energy dissipated during the breaking [64], and in turn affect the amount of useful energy left in the wave by the time it reaches a near-shore or shoreline WEC device. The following section briefly explains the wave breaking phenomenon in general terms, and then indicates the specific conditions which could be expected in the area near Ucluelet.

3.4.1 Wave Breaking

While the amount of energy or power in deep water waves can be relatively easily approximated using equations (3.13) and (3.16), determining the power left in the waves as they approach the shore can be much more difficult. The breaking of waves, which can dissipate up to 85% of the energy in the waves [64], is a mechanism which is poorly understood and difficult to quantify [65].

There are several categories of breaking waves, as shown in Figure 3.4. In the case of spilling breakers, the bottom slope is usually quite shallow and the water continuously spills down the front face of the wave [56]. Plunging waves usually occur when the bottom slope is steeper – in this case, there is not enough water in the trough ahead of the wave to fill in the oncoming crest [66]. The front face of the wave becomes concave [56], leading to the curling and plunging of the wave. This type of breaker dissipates the most energy [64], due to the large amount of turbulent activity.

While it is not a main objective of this study to look at the mechanics of wave breaking, it is useful to know which type of breaking occurs in the Ucluelet area, and also the depth at which breaking begins to occur. Knowing the type of wave breaker allows the use of a parameter in the model to scale the power incident on a WEC device, according to the estimated energy loss due to breakers. The depth at which breaking is likely to occur

gives an indication as to which devices would be situated in the surf zone, and would therefore be affected by these energy losses.

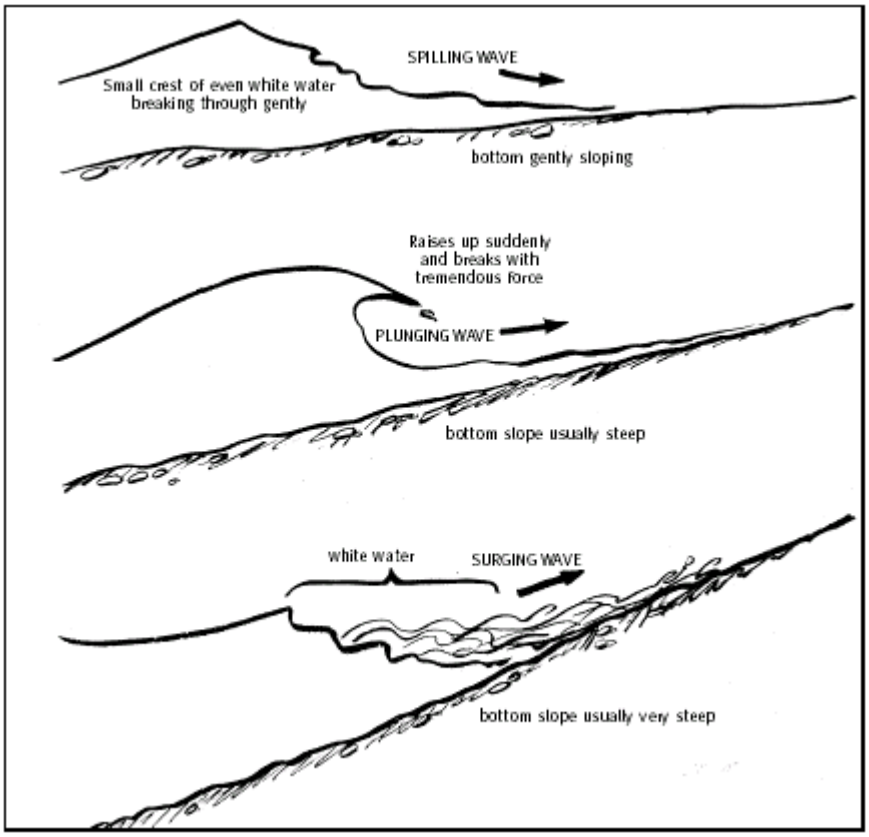

Figure 3.4 - Three different forms of breaking waves [66]

In [67], Nicoll studied the bathymetry of the coastal waters at several locations between Tofino and Ucluelet. At the area near BC Hydro's Amphitrite Point buoy, Nicoll determined that the waves begin to break at a water depth between 13 and 15 m, depending on the wave height and period. The waves were also found to be of the spilling breaker type, and Kabdasli et al. [64] determined experimentally that approximately 40% of the wave energy is dissipated in a spilling breaker.

3.4.2 Other Shallow Water Considerations

Other than breaking, several other phenomena contribute to the loss of energy in waves as they enter shallow water. These include:

- Wind effects, where an opposing wind can attenuate waves
- Bottom friction, caused by the development of a turbulent boundary layer near the ocean floor due to the motion of the waves
- Bottom percolation, where there is water flow in and out of a porous sea bed
- Bottom movement, which is transport of sediment from the ocean floor.

The relative importance of these is dependent on the bottom geometry and composition, bottom movement and bottom friction are the two main energy dissipation phenomena in shallow water when there is no wave breaking involved [61].

3.5 Wave Resource in British Columbia and Vancouver Island

Figure 3.5 shows a plot of the wave climate of a typical year at the La Perouse Bank buoy site. The colours indicate the number of hours per year that the wave conditions at that point in the graph exist.

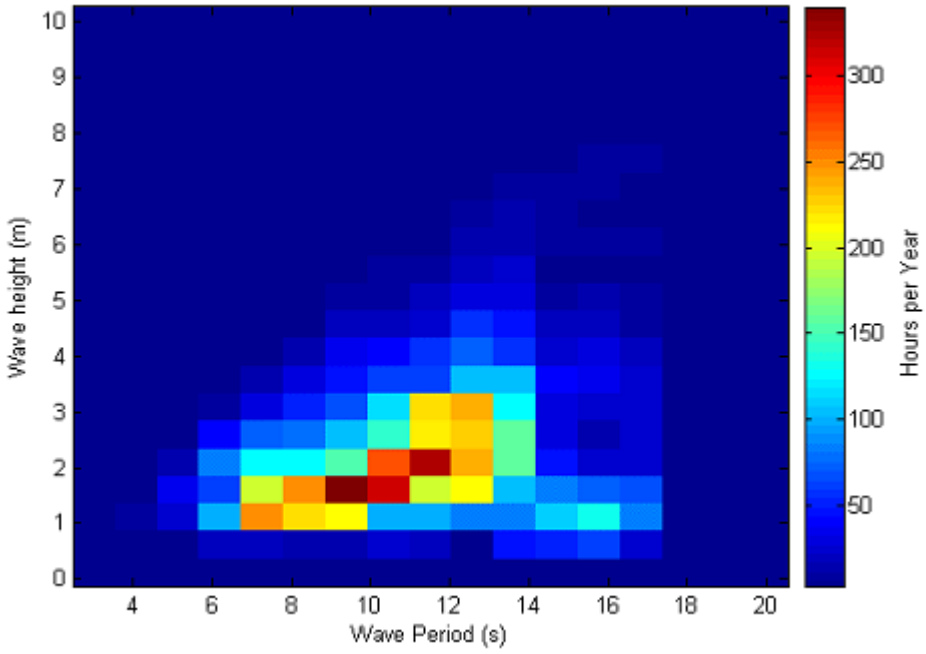

Figure 3.5 - Wave climate for La Perouse Bank buoy, 2003

The Electric Power Research Institute (EPRI) conducted studies of the potential for wave energy conversion devices in five states, and produced system level design reports for five states – Maine, Massachussetts, Hawaii, California, and Oregon. Of these states, Oregon was deemed to have the most similar wave climate to Vancouver Island, as it is geographically the closest state of the five and also has West-facing shores. A similar diagram to that of Vancouver Island's wave climate in Figure 3.5 was created, and is shown in Figure 3.6. While the overall shape is similar and also shows a that wave periods of 8 to 11 seconds and wave heights of 1 to 2 m are most commonly seen, Oregon sea states are less variable than Vancouver Island's. For example, for 471 hours of the year, the average wave height is in the vicinity of 1.5 m and the average period is in the vicinity of 9 seconds, making that combination the most frequent over the course of the year. For Vancouver Island, that same combination is also the most frequent, but only 343 hours are spent in that state, or 73% of the Oregon maximum. Instead, the wave powers are more widely distributed.

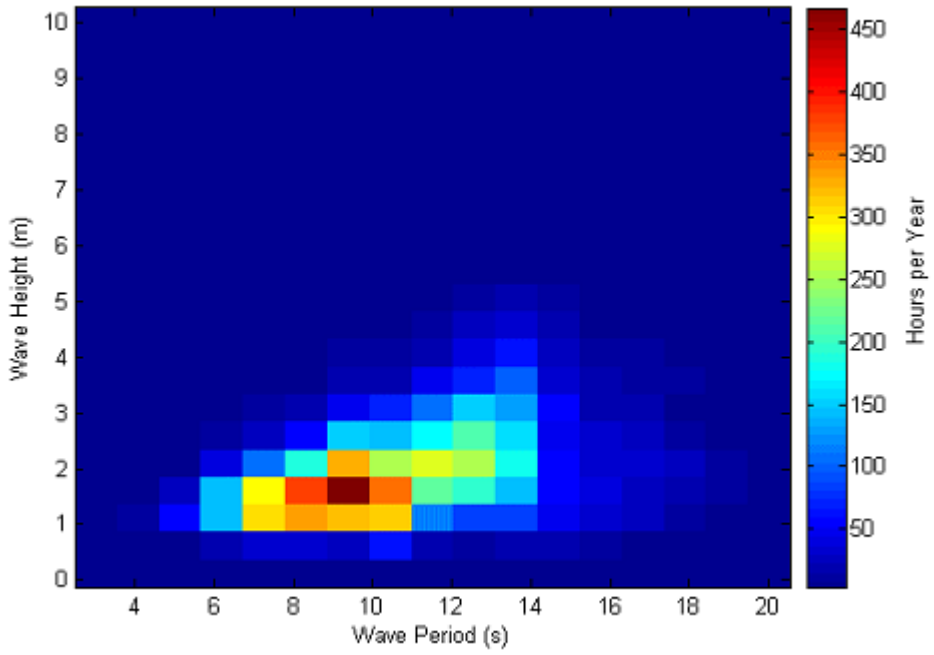

Figure 3.6 - Wave climate in Oregon, from EPRI data [68]

Figure 3.7 shows the absolute difference between the Vancouver Island and Oregon wave climates, which is generated by subtracting the values in Figure 3.6 (Oregon) from those in Figure 3.5 (Vancouver Island). The areas in blue show where Vancouver Island wave climates are less frequent than in Oregon, and the red areas show where they are more frequent. From this figure it can be seen that Vancouver Island tends towards longer wave periods and higher wave heights than Oregon. This is important to note in the future when comparing studies made on wave energy conversion potential based on U.S. wave data, such as the studies performed by the EPRI.

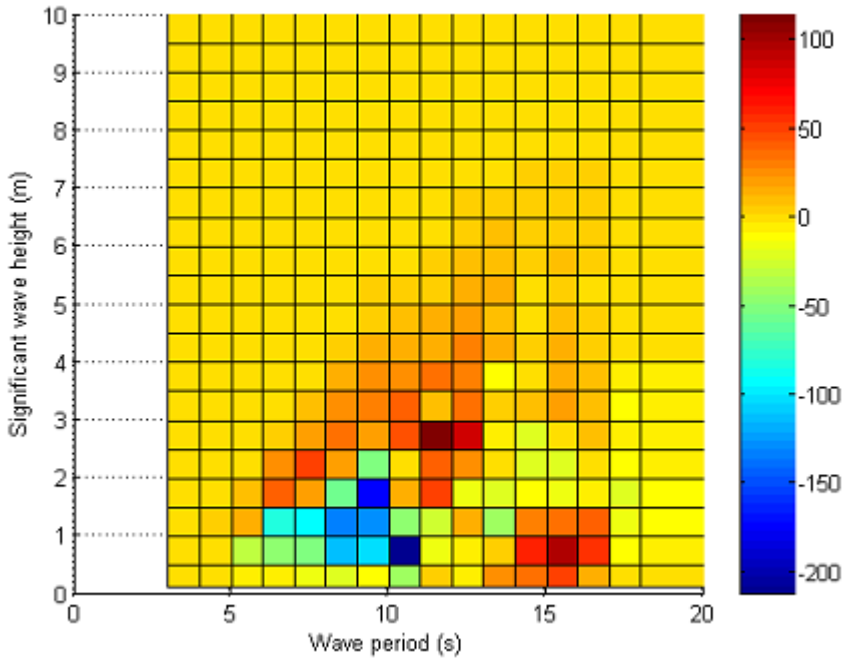

Figure 3.7 - Absolute difference (in hours per year) between La Perouse Bank and Oregon

3.6 Measurement of Wave Properties

The wave data used for the simulations in this study is taken from Environment Canada's buoy 46206, a 3-metre discus buoy moored at La Perouse Bank, roughly Southwest of Ucluelet and Amphitrite Point. The coordinates of the buoy are 48°50'2" N, 126°0'0" W, and Figure 3.8 shows its location relative to the shore. The buoy is approximately 30 km offshore and sits in a water depth of 78 m (73 m until early October 2003) [69]. Also

visible in Figure 3.8 is Cape Beale, on the East side of Barkley Sound, the location at which the wind measurements used in this thesis were taken.

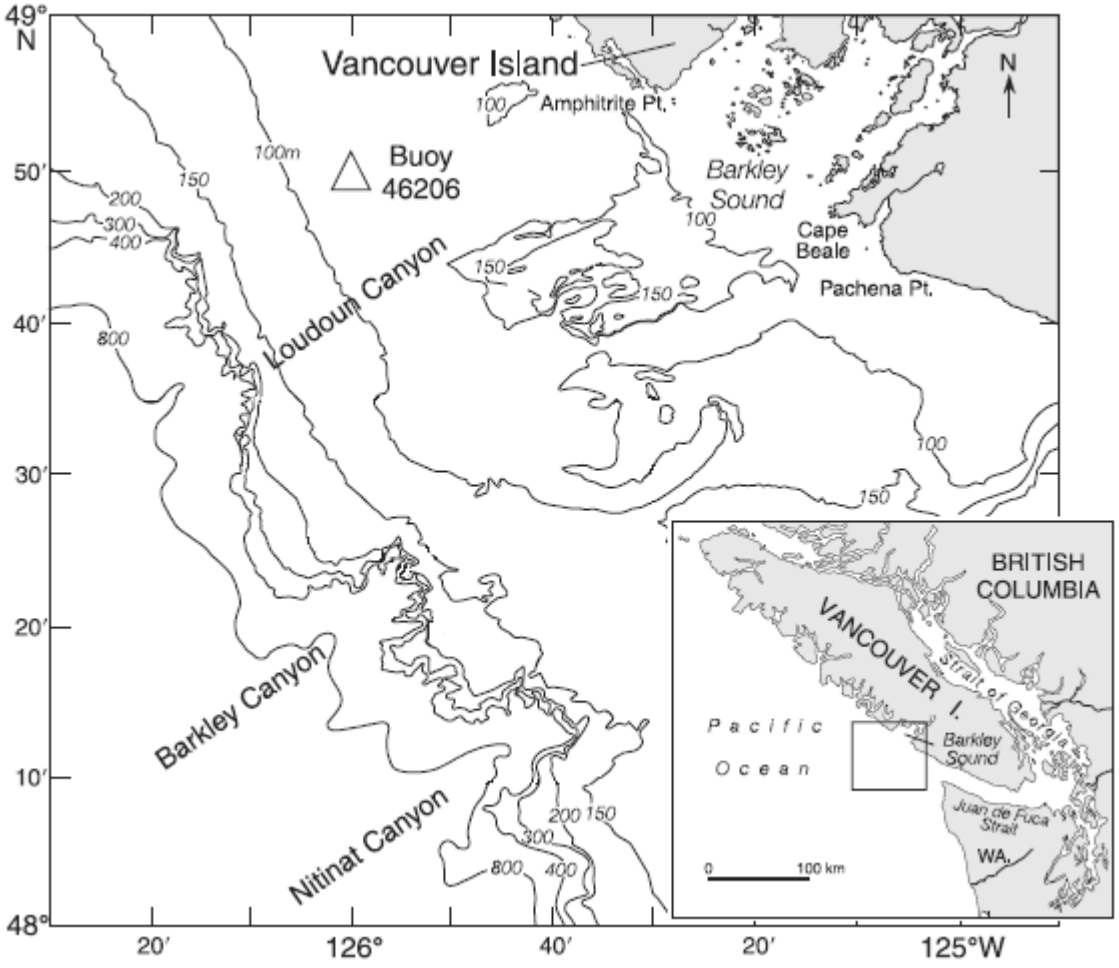

Figure 3.8 - Location of La Perouse Bank Buoy 46206 relative to coast of Vancouver Island [70] (image adapted to remove items of no consequence to this study)

A data set is recorded hourly by buoy 46206, and each data set consists of the items as listed in Table 3.1.

Name	Description	Units
STN_ID	Station ID. This is the buoy's ID number – 46206	-
DATE	Date and time in format MM/DD/YYYY HH:MM (Note that the time is UTC time, such that the local time is 8 hours behind UTC)	-
Q_FLAG	Quality code indicating validity of data. (The value is	-

	usually 1, meaning data appears valid and consistent) For a full list of codes, refer to [71]	
LATITUDE	Latitude of buoy – always recorded as 48.83	degrees North
LONGITUDE	Longitude of buoy – always recorded as 126	degrees West
DEPTH	Depth of water	m
VCAR	Characteristic significant wave height	m
VTPK	Characteristic significant wave period	s
VCMX	Maximum zero crossing wave height	m
WDIR	Wind direction (*from* which wind is blowing)	degrees
WSPD	Horizontal wind speed	m/s
GSPD	Gust wind speed	m/s
ATMS	Sea level atmospheric pressure	mb
DRYT	Dry bulb air temperature	°C
SSTP	Sea surface temperature	°C

Table 3.1 - Parameters recorded hourly by La Perouse Bank buoy 46206 [71]

From March 1st to November 4th 2003, measurements are also available from a second buoy in the area, owned by BC Hydro. This buoy, an Axys TRIAXYS, is located near Amphitrite Point at coordinates 48°56'N and 125°36' W, roughly 2.2 km offshore, and sits in approximately 55 m of water. Although this data was used in the preliminary stages of this study, and is useful for estimating the power from waves in shallower water, the data set available does not include the winter months, which would be crucial information, given that the residential load in the area peaks in the winter months. Therefore, the decision was made to use the information from the buoy at La Perouse Bank, as year-round data was available from that source.

3.7 Tides

Another consideration when dealing with shoreline WEC devices is the pattern of the tides in that particular location. It has been shown that the tides have an effect on the power output of OWCs, as the incident wave power is higher with the higher tides and thus deeper waters at the device [72].

The tides and therefore the mean sea level at a particular location along a shoreline are regionally dependent, and may or may not have the same pattern as a nearby location. For example, Winter Harbour and Tofino, separated by just over 200 km have nearly the same tidal pattern [73]. Victoria, which is almost the same distance from Tofino, however, has a very different tidal profile, as shown in Figure 3.9.

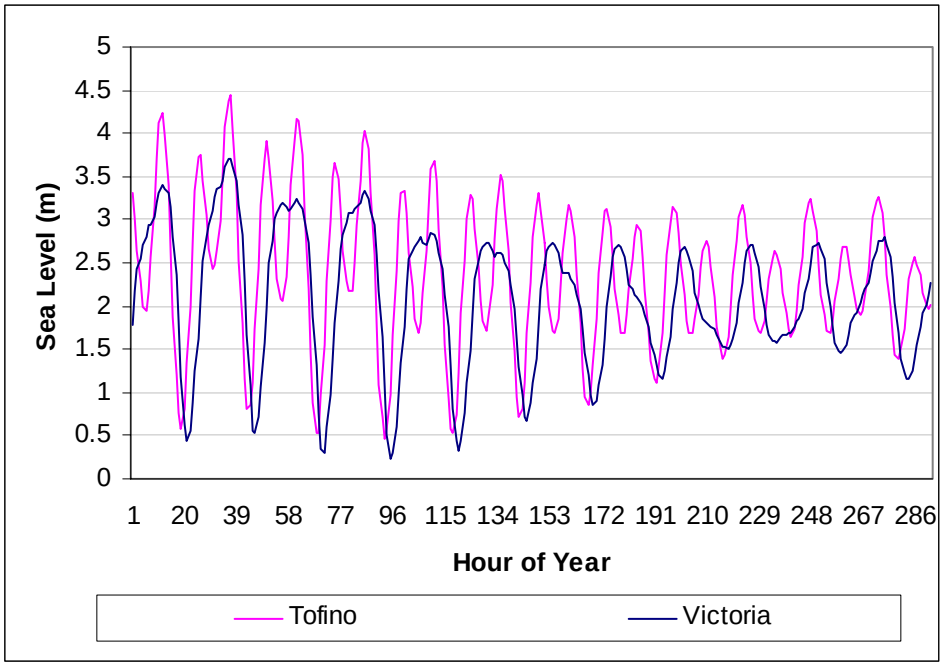

Figure 3.9 - Comparison of tidal regimes of Tofino and Victoria, January 1-11, 2003 [73]

While the tides may have an effect on the performance of shoreline OWCs, in the simulation models developed for this study, the tides were not considered. This was done to maintain the simplicity of the system model, particularly since the model can accommodate both shoreline and offshore devices as the main WEC component. For further details about this decision and the assumptions made, refer to section 6.6.2.

3.8 Storms

When undertaking a project such as the design and construction of a wave energy conversion system, storms must be taken into account for at least three reasons – device design, system design, and cost. Device design for survivability is not a focus of this

thesis and will therefore not be covered here. System design and cost considerations are each discussed in the following sub-sections.

3.8.1 System Considerations

A second consideration related to storms when considering wave energy conversion devices is system design with regard to device availability. Availability is the percentage of time the device is serviceable and can produce electricity if the renewable resource is present. Since WEC devices are mainly still either in the research or prototype phases, a survey of the literature on these devices has not produced any quantitative values for either their experimental or estimated availability. However, issues related to the impact of device availability in offshore applications have been encountered in offshore wind turbine applications.

While commercial onshore wind turbines commonly have an availability of 98%, van Bussel et al. [74, 75] determined that for an offshore wind turbine to have the same availability, the turbine failure rate must be reduced by at least 25%, and the number of maintenance personnel must also be increased. Otherwise, a significant decrease in availability results, due to the inability of maintenance crews to safely travel to the turbine location and conduct repairs during stormy periods with high seas. Therefore, any failure occurring in these conditions incurs large penalties to availability because of the increased downtime, as compared to similar onshore turbines.

This issue is also likely to exist for wave energy conversion devices, since the increased downtime is not a function of the type of device that has failed, but of its location and the method by which maintenance crews must access the device. To compensate for any devices which may not be functioning, the device availability must be accounted for in a system design. Since availability numbers are not known for WEC devices, a 100% availability has been assumed as a simplification, meaning that the devices are assumed to be operational at all times. Therefore, since availability can never realistically be 100%, due to preventative maintenance measures and any failures which may occur, the

real-life scenario will have to account for these facts. Since the wave climate used in these simulations is for one year only, and that climates change slightly from year to year, the uncertainty in the actual climate from year to year is likely to overcome the simulation errors caused by the small fraction of time that any particular device may be out of service. Furthermore, since the system is assumed to be grid-tied, and the likelihood of all devices failing at the same time is minimal, any fluctuations in output due to a device failure is assumed to be an event which can be compensated for through the grid connection, if necessary.

3.8.2 Economic Considerations

In [75], van Bussel indicated that the operation and maintenance (O&M) costs for offshore wind farms could be responsible for as much as 25% of the final energy cost. This is due to the fact that adverse weather reduces the ability of maintenance crews to reach the offshore devices, and therefore extends the amount of time a device is out of commission if a failure occurs during bad weather. Shoreline devices such as the LIMPET would be able to avoid some of these problems, though it is likely that depending on the type of failure and the severity of the sea state, the device may not be approachable. For example, a severe storm hit the LIMPET device in 2001, taking out several components and flooding the main equipment housing with 1.3 m of water, even though this housing sits well above the water line [51].

3.9 Summary

In this chapter, the wave resource in both deep and shallow water was determined within limits reasonable for the scope of this thesis. The next step is to identify technologies which can convert this wave energy into a more useful form. These technologies are identified and described in the next chapter.

4 Wave Energy Conversion Devices

4.1 Introduction

Having described the wave resource in Chapter 3, the next step is to determine which technologies might be useful in harnessing this wave energy. The following sections describe the two main technologies which were examined in this study – the Oscillating Water Column (OWC), and the Pelamis device. Although other devices exist, as outlined in the literature review, these two are currently entering the commercialization stage and would therefore be the most likely to be available for commercial purposes if a wave energy project on Vancouver Island were to go ahead.

4.2 Oscillating Water Column

An OWC consists of a chamber that extends both under and above the water line, thus containing a water surface that can move upwards or downwards as a result of the motion of waves. This moving water surface causes the displacement of air. At the top of the OWC is a horizontal-axis turbine through which air flows, driven by the movement of the water. This turbine captures some of the energy transferred to the air by the water, and a generator attached to the turbine shaft produces electricity from the rotational movement of the turbine. This principle is illustrated in Figure 4.1, and the system power conversion chain is shown in Figure 4.2.

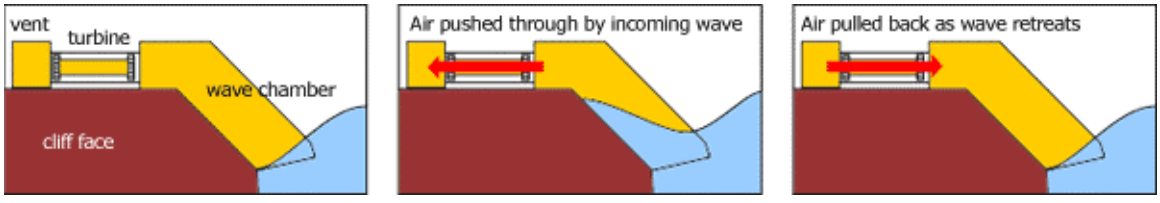

Figure 4.1 - OWC principle of operation [76]

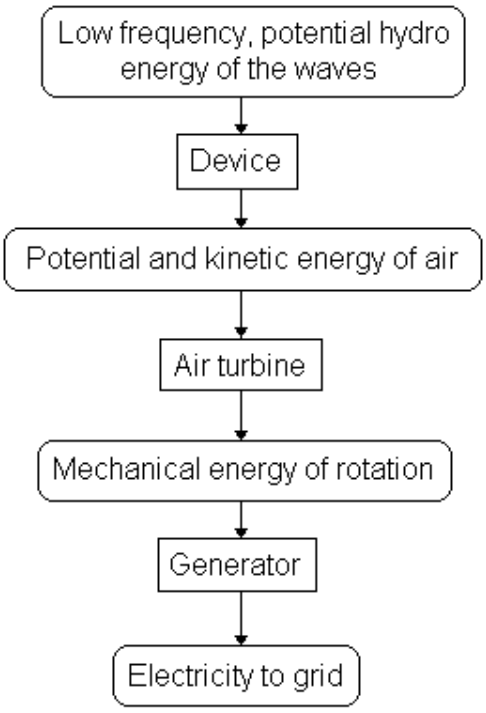

Figure 4.2 - Typical wave energy conversion system (OWC) [77]

Many of the major OWC installations are onshore, though floating OWCs (such as the Mighty Whale in Japan) [11] and tethered OWCs (the Port Kembla project currently under construction) also exist and have been proven to work. This discussion will focus mainly with onshore OWCs, as the experiences of onshore plants such as the Islay OWCs and the Pico plant have proven to be an invaluable source of reference data.

Two of the leading onshore OWCs are the LIMPET on the Isle of Islay, and the Pico device in the Portuguese Azores. Energetech also has an up-and-coming OWC design verging on commercialization, the first of which has been installed at Port Kembla in Australia. The next three sections briefly describes these designs before progressing to a description of the Pelamis device.

4.2.1 Isle of Islay OWCs – LIMPET and its Predecessor

Two OWCs have been built on the Isle of Islay, which is an island off the West coast of Scotland, due west from Glasgow. The original Islay OWC was built in 1988 and

commissioned with a turbine in 1991, while the second Islay OWC, the LIMPET installation, was operational in 2000 and still operates today. The original Islay OWC had a 75 kW installed capacity, which is quite low, but useful for testing and research. The LIMPET installation is much larger, with an installed capacity of 500 kW [78],[79]. Figure 4.3 shows an image of the LIMPET OWC.

Figure 4.3 - LIMPET OWC on the Isle of Islay [80]

The LIMPET uses a counter-rotating Wells turbine to convert the air's kinetic energy into rotational motion. Wells turbines are frequently used in wave energy devices because the rotor (or rotors) moves in the same direction regardless of the direction of the airflow through the turbine. Counter-rotating turbines, where two rotors travel in opposite directions, are sometimes used to increase the operational range of the turbine, as stalling can be a problem at higher airflows [77].

Many difficulties arose with this OWC, beginning with construction, which was difficult and expensive as a result of the custom-fitting to the shape of the rock gully. Once the plant was in operation, it was found that the generator, which had been sized to handle the large storm waves, was usually operating at reduced efficiency due to the prevalence

of comparatively calmer seas. This led to the recommendation for the installation of a smaller generator with blow off valves for protection from larger water column oscillations. Another recommendation stemming from the variability of sea states was the installation of a flywheel on the shaft connecting the generator and the turbine, to maintain output despite variations in wave groups. This was especially important in the case of the Isle of Islay, where the small grid capacity cannot tolerate large oscillations [78].

It was also observed that the turbine rotors had been subjected to water ingestion during operation. From this observation came the recommendation that the geometry of the OWC structure be carefully designed in order to minimize sloshing of the water column surface and/or the generation of surface waves [78].

In 2000, after the decommissioning of the original Isle of Islay OWC, the larger LIMPET project was commissioned on the Isle of Islay. Designed by Wavegen in the UK, it is 6 m long by 6 m wide, and has a counter-rotating Wells turbine. Each of the rotors in the LIMPET's turbine is attached to a 250 kW generator, giving a nominal capacity of 500 kW [81]. From operational experience, however, the conversion efficiency of the LIMPET project was far lower than expected, as summarized in Table 4.1.

Table 4.1 – Annual Average Operational Data from LIMPET, Isle of Islay [79]

	Units	**Initial Estimate**	**Current Performance**	**Achievable Target**
Incident Power	kW/m	20	12	20
Pneumatic Capture Efficiency	%	80	64	80
Pneumatic Capture	kW	336	161	336
Turbine Efficiency	%	60	40	70
Turbine Shaft Power	kW	202	65	235
Losses	kW	0	44	22
Net Output	**kW**	**202**	**21**	**214**

The achievable target column indicates Wavegen's expected performance of a next-generation LIMPET, in which solutions to known problems are addressed. As shown in the last row of the table, the actual net output of the current LIMPET OWC is roughly 10% of the expected value. The low turbine efficiency was attributed not to problems with the turbine, but of high, idealistic values published in previous papers regarding the performance of fixed-pitch Wells turbines. The achievable target of 70% was estimated for a new design of variable-pitch Wells turbine being developed by Energetech. Research into geometric configurations of the OWC and the surrounding seabed are expected to lead to improvements in pneumatic capture and incident power [79].

Another Wavegen OWC is slated for the Faroe Islands [82], which are approximately halfway between Iceland and Norway. Wave tank performance modelling has been conducted for this project [83], and the power capture curve used in this thesis is based on the results of these experiments.

4.2.2 Pico Azores

An OWC has also been built on another remote island, this time on the island of Pico in the Portuguese Azores. Construction on this OWC began in the mid-1990s, and the plant is currently operating. Its rated capacity is 400 kW and is expected to supply 8%-9% of the island's electricity requirements for the next 25 years [84]. Figure 4.4 is an image of the Pico OWC, which is similar in many aspects to the LIMPET installation at the Isle of Islay. A single-rotor Wells turbine provides approximately 0.6 to 0.8 GWh/year, if used on a permanent basis [85].

Figure 4.4 - OWC at Pico in the Portuguese Azores [86]

4.2.3 Energetech OWC

Energetech's OWC is a nearshore device which includes parabolic walls to focus the energy of the incoming waves into the opening of the OWC. The structure is not built into the shoreline but rests on feet tethered to the sea floor, as shown in Figure 4.5 [87]. The first of these OWCs has been built in Port Kembla, near Sydney, Australia, and was installed and tested in June 2005 [88]. Unfortunately, no academic papers have been found regarding the design of this structure, and the performance will not be known until results from the Port Kembla project become available.

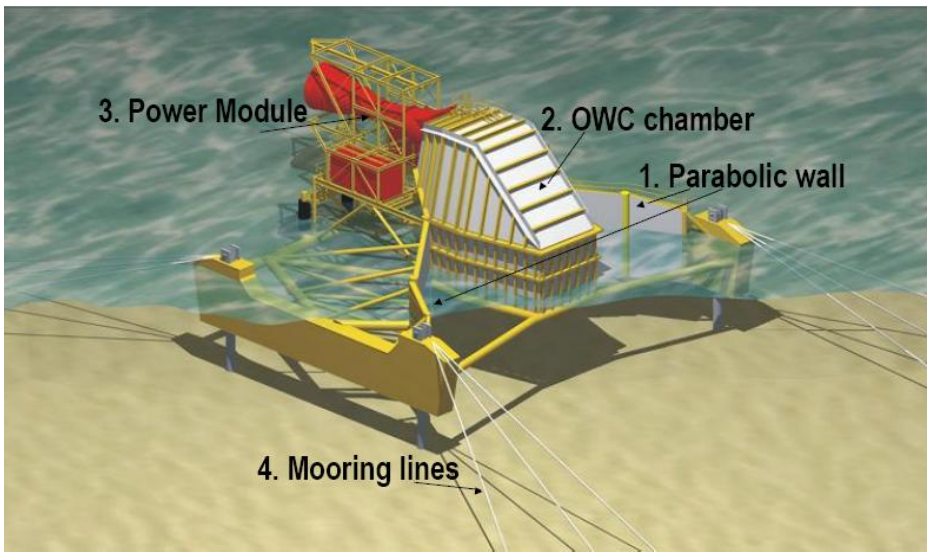

Figure 4.5 - Tethered OWC design by Energetech Australia [16]

4.2.4 Pros and Cons of Shoreline/Nearshore Technology

Avoiding the need for armoured subsea cables is one of the main advantages to building nearshore or shoreline WEC devices. These cables are costly, on the order of US $115,000 per km [89], and in the case of a farm of offshore devices, the distance between the shore and the farm may need to be covered multiple times depending on the number of WEC devices.

Another advantage to shoreline devices is the accessibility for maintenance and repair. While little data on this topic exists for WEC devices, since so few are in operation, this has already been identified as an issue for offshore wind farms [74, 75].

The major disadvantage to shoreline and nearshore technologies is the major decrease in wave power which occurs as waves enter shallow waters and approach the shores. This was discussed in section 3.4, and is the main reason that the trend towards offshore WEC devices has recently been noted [90].

With this in mind, the Pelamis device, which is an offshore WEC nearing commercialization, is described in the following section, and a model of this device is used to obtain simulation data to be compared to the Energetech and LIMPET OWC results.

4.3 Principles of Pelamis Operation

The Pelamis device, a design by Ocean Power Delivery (OPD) Ltd of Scotland, is made up of four hollow steel cylinders which are linked by hinged joints. At each joint is a power conversion module (PCM), which houses all the generation components, including the hydraulic motor and electrical generators. When the joints flex, either heaving (vertical motion) or swaying (horizontal motion), the motion is resisted by hydraulic rams, and high-pressure oil is pumped through smoothing accumulators and then through

a hydraulic motor. This motor then drives an electric generator, producing electricity [91]. Figure 4.6 shows the design of the Pelamis device.

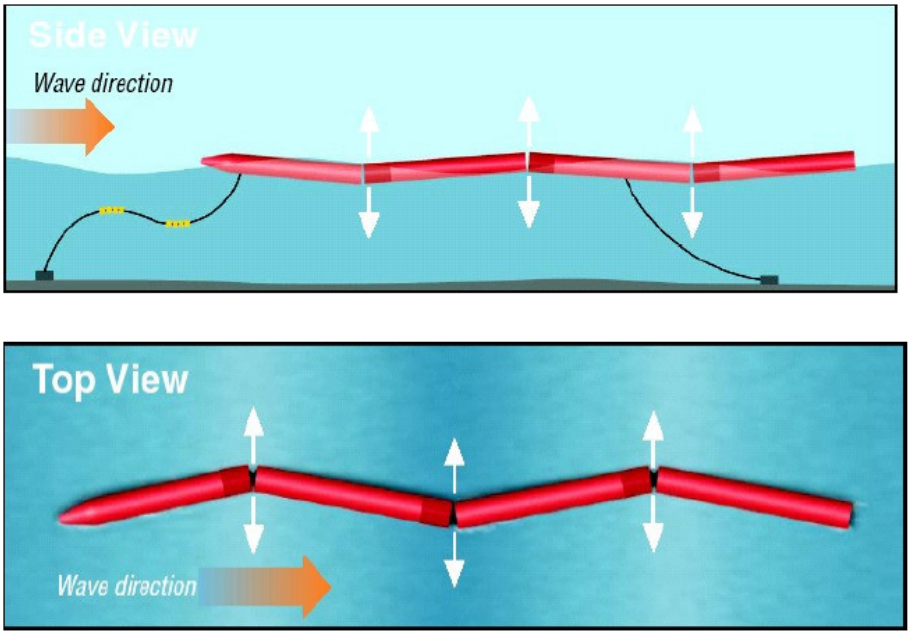

Figure 4.6 - The Pelamis wave energy converter [91]

The Pelamis WEC is slack-moored, with enough freedom for the device to swing in the direction of incoming waves, though it is tethered at both the front and the back to prevent any full 360º rotations. If multiple Pelamis devices operate in a cluster, they can be daisy-chained together with jumper cables; thus, the Pelamis devices can be wired such that only one connection is needed to a sub-sea junction box, where the connection is made to a cable running along the sea floor. The electrical connections are made right on the Pelamis device [91], avoiding the need for dive teams or automated underwater vehicles once the initial connection to the sub-sea junction box has been made. In this way, maintenance crews have easier access to most of the cables which interconnect the Pelamis devices [89].

The overall length of the Pelamis device is optimized for the predominant wave conditions at the site for which it is destined. In Scotland, where the first full-scale prototype is already in operation, a length of 120 m was chosen as optimal for the

conditions in that area. When given the data for several location in the United States, however, increasing the overall length to 150 m achieved better results. In both cases, the diameter of the device remained 3.5 m [91]. Since it has been demonstrated in section 3.5 that there are differences between the general wave climate in Vancouver Island and in Oregon, both configurations were initially tried in the simulations for this thesis, to determine which is more suited to the Vancouver Island wave climate.

OPD is just entering the commercialization phase of Pelamis development. The first full-scale prototype has been built and is in operation off the Orkney Isles in Scotland [91]. Its first commercial contract, for three Pelamis devices to be installed in Portugal, was signed in May 2005 [92]. While these devices will be manufactured in the UK and towed to Portugal, OPD has expressed a willingness to licence out the fabrication of Pelamis devices to companies local to a project site [91], which will significantly reduce costs that would have been associated with shipping Pelamis devices from the UK to the west coast of North America.

The economics of a wave energy project based on the Pelamis WEC will be briefly discussed in Chapter 8. The environmental implications of wave energy conversion devices, while certainly important, are beyond the scope of this thesis.

4.3.1 Rationale for Offshore Technology

One of the main reasons for considering offshore technologies is that more energy is available in deep water. This is because, as mentioned in section 3.4, energy is dissipated when a wave enters shallow water, through the processes of wave breaking and sediment transport. The Pelamis device was designed to take advantage of the fact that deep water waves are more energetic, by being optimally moored in waters from 60 to 150 m in depth [89]. The OWC devices mentioned in the previous section are limited to shallower water and less of the useful energy in waves can be converted by them.

On a related note, the survivability of the device is also impacted by the depth of the water at its location. Shallow-water or shoreline devices such as the OWC may be exposed to damaging breakers that deep-water devices would avoid.

The main disadvantage to offshore devices is the distance between the devices themselves, and the load or the distribution network to which they are connected. Effects include higher capital cost for longer cables, line losses which are related to the resistance of the cables (and in turn, the length of the cables), and more travel for maintenance crews. The Pelamis device has been designed to mitigate these disadvantages as much as possible [89, 91], though they cannot be completely eliminated.

The advantage of higher-power waves for offshore devices is significant enough to continue to consider these devices in a wave energy conversion project. Therefore, the Pelamis device will be simulated in this study, and the results will be compared to those from the LIMPET and Energetech OWC model simulations.

4.4 Preliminary Discussion on Comparisons between Devices

In this thesis comparisons are made between three different devices – the Pelamis, the LIMPET OWC, and the Energetech OWC, with models based on the power capture properties either measured or calculated for each device. The primary reason these devices were compared, rather than simply focusing on a single device, was a desire to determine whether a particular device might be more suitable to the geographic location and wave climate than another device. Since very few commercial wave energy projects currently exist, there is no obvious dominant technology in the field of wave energy. Also, since a multitude of wave energy devices are in existence, it can be useful to see the differences in behaviour and power output of different devices, given the same input. The number of devices was restricted to these three, however, because simulating all known devices would not only be a large undertaking beyond the scope of this thesis, but also because very few devices are currently at a design stage where power capture curves are readily known or available.

In this study, the comparison between devices will be based on the the installed capacity required to generate enough electricity to serve the Tofino/Ucluelet load over the course of a year, and also the grid penetration caused by the output of the devices. The most suitable candidate will be the device which minimizes both these factors – less installed capacity typically leads to lower capital costs, and lower grid penetration reduces the likelihood of problems occurring in a grid structure which was originally meant for one-way power distribution [43]. Each device will be tested with the same inputs of significant wave height and period, and residential load.

4.4.1 Comparison Conclusions from EPRI

The EPRI recently conducted a survey of offshore wave energy conversion technologies [62], using information about eight different devices to come to a conclusion about which device currently has the most potential for use in a commercial wave energy project. Of these eight devices, only the Pelamis device was deemed to be suitable for selection in any proposals for wave farms in the near future, though the Energetech OWC was short-listed as a possible contender with some improvements to mooring, deployment, and deeper water survivability. The LIMPET device was not part of EPRI's comparison because it is a shoreline device rather than an offshore device.

4.4.2 Information Availability

The amount of information available for each device used in the comparisons of this thesis varies. The LIMPET OWC, though relatively new, had a 75 kW predecessor about which several academic papers were written, both about the overall project [72, 78] and about its components, such as the Wells turbine (for example, [77, 93, 94]). Wavegen has also published several extensive reports on its website [82]. The power curves used in the simulations for this thesis were taken from these reports, though the only available curves were simulated output for a larger OWC than the existing LIMPET. Also, the curves exist for only two wave heights – 1 m and 2 m – and therefore more interpolation is necessary

for the LIMPET device model than in other models where a larger variety of wave heights are characterized.

The Pelamis device is just entering the commercialization phase, and has few academic papers written about it. Experimental and numerical results of its hydrodynamics were recently published by Retzler and Pizer [95], and OPD has been very cooperative in providing information to the EPRI for its studies of a potential Pelamis farm near San Francisco [89]. Included in the information made available to the EPRI are schematics, cost estimates, and the power capture curves used in this study.

Energetech has published limited data and specifications about its OWC, and because the first device has only just barely begun operating at the time of this writing, no experimental data are available upon which to base the simulations. Some information is available through EPRI's site design document for a hypothetical Energetech installation in San Francisco [62], including the power capture curve upon which this simulation is based.

4.5 Summary

The Oscillating Water Column (OWC) and Pelamis devices are both promising candidates for a wave energy project near Tofino/Ucluelet. Given the wave resource described in Chapter 3, and the wave energy conversion devices described in this chapter, the next step is to examine the size and characteristics of the load which will be serviced by these WEC devices. The next chapter provides a description and quantification of the Tofino/Ucluelet load upon which these simulations are based.

5 Load Profile for Tofino/Ucluelet Area

5.1 Introduction

One of the most important factors to be taken into account when sizing a wave energy installation is the fact that the load is not constant and can therefore not be accurately represented as an average number. The load characteristics change depending on the season, the day of the week, and the time of day. In this chapter, these changes are examined and characterized so that the input into the model is as representative of real conditions as possible.

5.2 Purpose of Load Data Synthesis

The system model developed for this thesis calculates hourly results, and therefore requires as input hourly load data for the community. Since hourly load data for the entire Tofino/Ucluelet community was not available, other data sets were combined to synthesize hourly data. Section 5.3 describes the known monthly load, and Section 5.4 discusses the known hourly load for an average Coastal BC home. Section 5.5 describes how these two data sets were combined to synthesize hourly community data.

5.3 Average Monthly Load in Tofino/Ucluelet

For the combined areas of Tofino and Ucluelet, BC Hydro has collected data on energy use for the years 2002-2003. Figure 5.1 shows the 2002 monthly figures, with separate traces for the residential, industrial, commercial, and total loads.

In this thesis, the object is to assess the feasibility of servicing the residential electrical load of the Tofino/Ucluelet area with wave energy devices. There are two main reasons

for choosing the residential load, rather than the commercial, industrial, or combined loads for the area:

1. Of the three classes of loads (commercial, industrial, residential), the residential electrical sales are the most stable and predictable, since the rate of electricity use grows at approximately the same rate as the population [2].
2. The wave resource, as seen in Chapter 3, is most plentiful in winter, and drops substantially in the summer. The shape of this resource profile is similar to the shape of the residential load profile for Tofino/Ucluelet, where demand for electricity is the highest in winter and dwindles in summer. Therefore the residential load was the most suitable for a first attempt at load servicing through wave energy in this area.

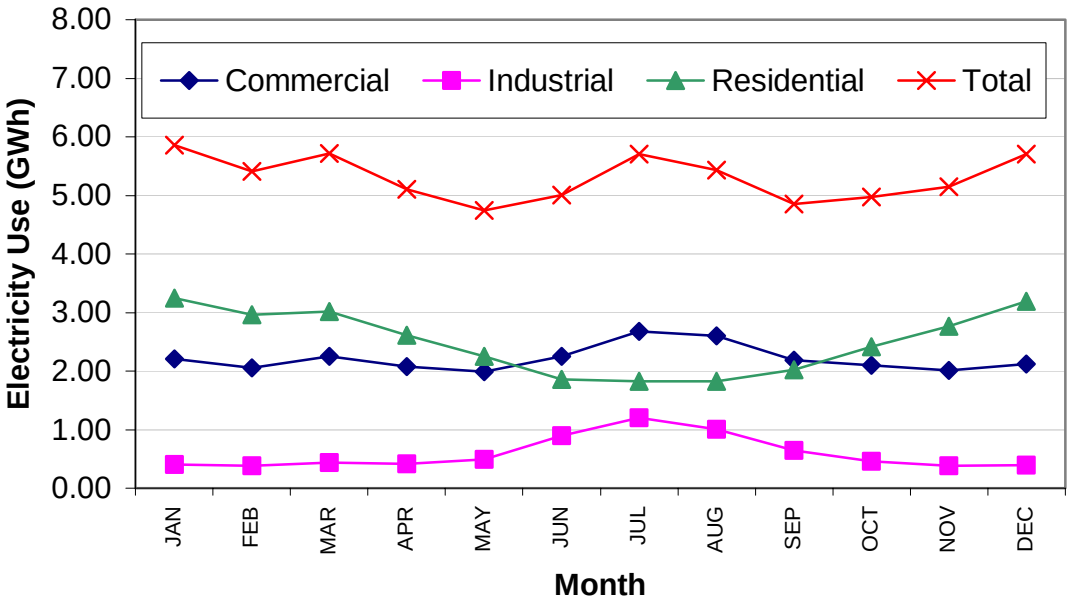

Figure 5.1 - Actual electricity use for the Tofino/Ucluelet area in 2002, by sector [96]

Figure 5.2 is also based on the BC Hydro monthly data for the area, and shows only the residential load values. The 2002 numbers are the values in the residential trace of Figure 5.1 divided by 1913, the total number of residential accounts in the Tofino/Ucluelet area. The 2003 values are included for comparison. Note that data for November and December of 2003 was not available and is thus absent from Figure 5.2.

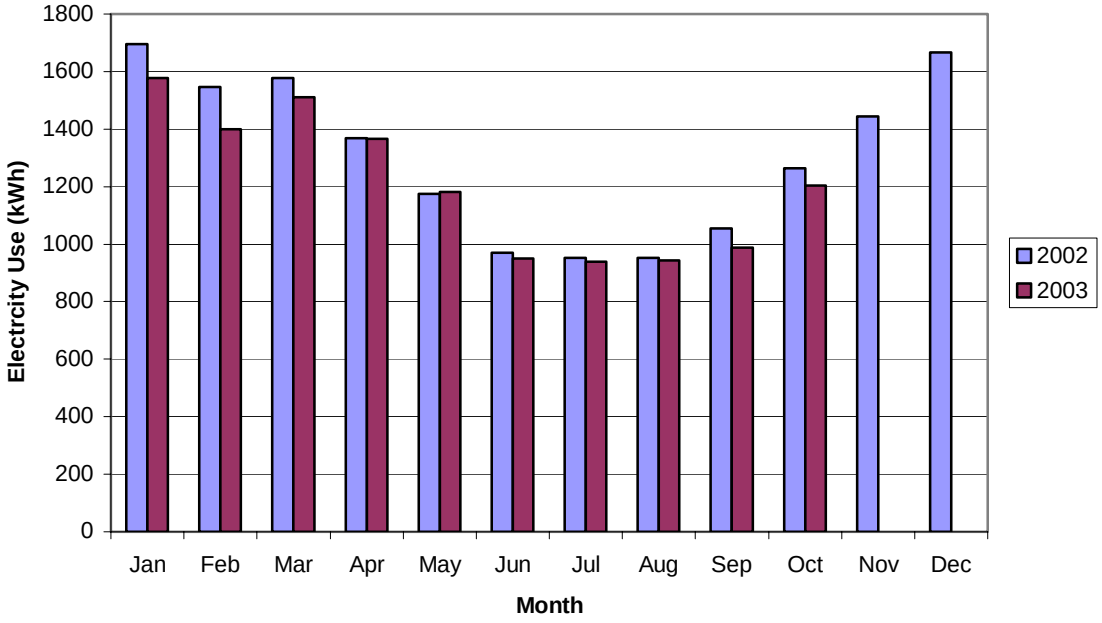

Figure 5.2 - Average energy use per residential account in Tofino/Ucluelet for 2002 and 2003

5.3.1 Load Growth

For Vancouver Island as a whole, BC Hydro projects that the average growth in residential electricity sales from 1998 to 2025 is approximately 1.9% per annum, as shown in Figure 5.3 [2]. This is slightly higher than the overall load growth (including commercial and industrial sectors) for Vancouver Island, as mentioned in the introduction to this thesis. In Figure 5.2, however, it is evident that there was a slight drop in residential electricity demand between 2002 and 2003, though a similar drop exists in BC Hydro's records (Figure 5.3). Therefore, a 1.9% annual growth in electricity demand can still be assumed when sizing a wave energy conversion system for the community.

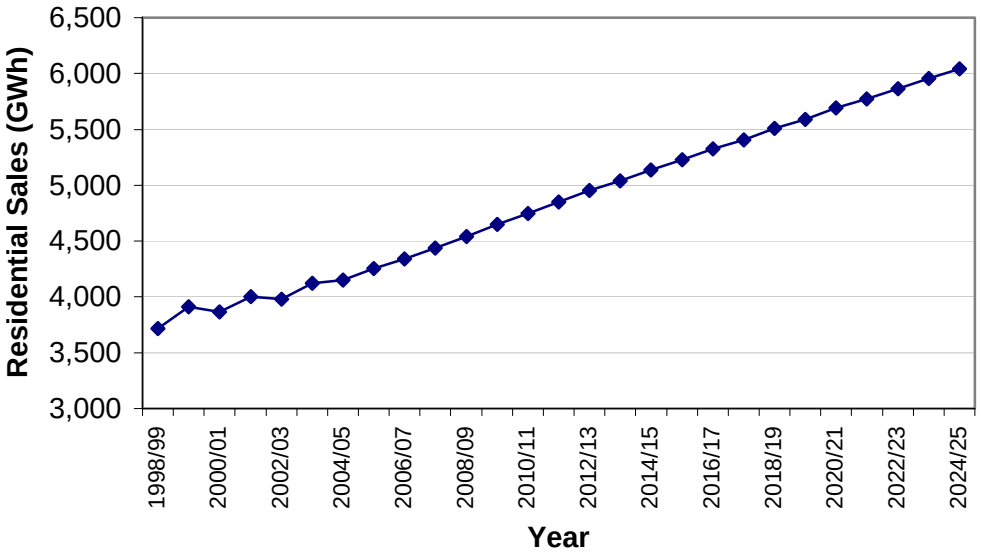

Figure 5.3 - Actual and predicted annual residential electricity sales on Vancouver Island [2]

5.4 Average Residential Hourly Load for Coastal BC

In British Columbia as a whole, 20% of households use electric space heaters; the remainder use some form of non-electric heating. This percentage is higher on Vancouver Island due to the limited availability of natural gas [2]. Whether a household is heated electrically greatly impacts the use of electricity, particularly in the winter months.

Available for this project were two sets of hourly data compiled by BC Hydro for typical Coastal BC households – one with electric heating, and the other with non-electric heating. These two data sets had different trends in their load profiles, particularly in the winter months when heating is necessary. Figure 5.4 shows the first two weeks of the load data of a typical non-electrically heated Coastal BC home.

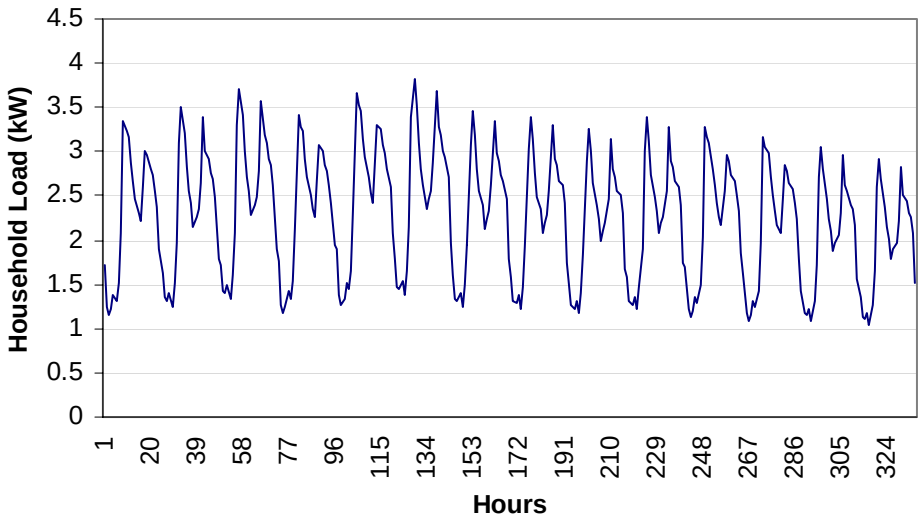

Figure 5.4 - Two weeks' non-electric household load data for a typical Coastal BC home

This household load data formed the basis of the hourly synthesized community load data for this study.

5.5 Generation of Synthesized Community Load Data

The hourly household load data was converted to monthly data by totalling the energy use for each month. This was done for both hourly data sets – the typical household with electric heating, and that with non-electric heating. Figure 5.5 shows the resulting plot for the non-electrically heated home. In other words, summing a month's worth of data points as illustrated in Figure 5.4 gives that month's point on the plot in Figure 5.5.

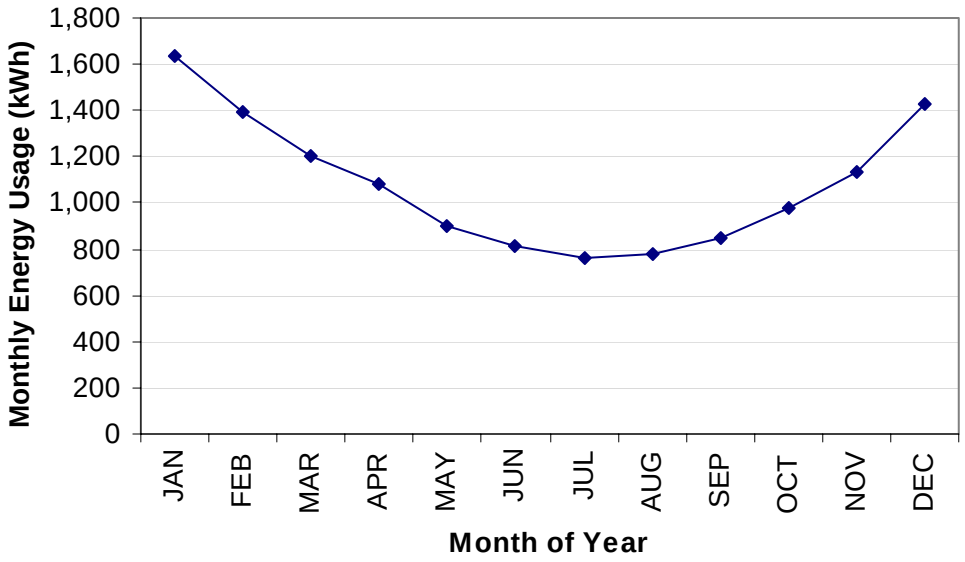

Figure 5.5 - Monthly electricity usage for an average Coastal BC non-electrically heated household

Since the Tofino/Ucluelet area consists of over 2000 households, a scaling factor was then applied to the single-household average values, adjusting the scaling factor to match the actual community data as closely as possible. This allows the simulation of multiple households based on the data for a single household. The result is shown in Figure 5.6. The BC Hydro monthly residential data trace is the same as the residential trace in Figure 5.1, which comes from BC Hydro's measured monthly load data for Tofino and Ucluelet. The points on the scaled household (non-electric) trace are the product of the points in Figure 5.5, multiplied by a constant factor representing the number of homes in the community. In this case, the scaling factor of 2300 (homes) is used.

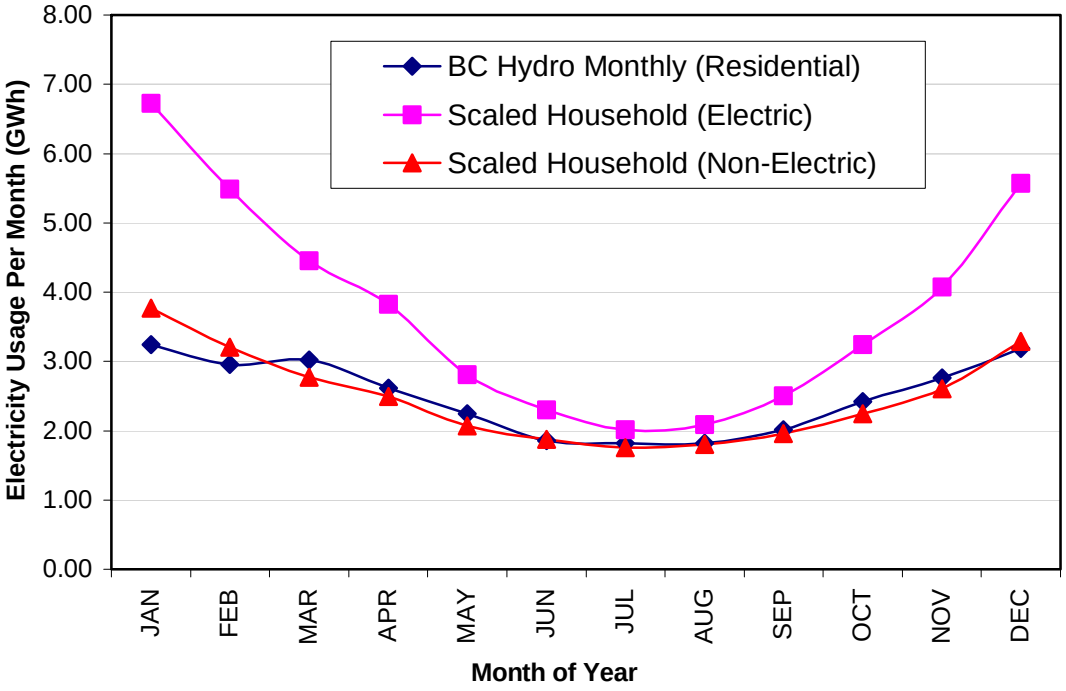

Figure 5.6 - Comparison of actual monthly data with converted hourly data for electrically and non-electrically heated households

Figure 5.6 shows that the shape of the load data for non-electric housing more closely matches the shape of the actual recorded data for the region, meaning that the majority of homes in the Tofino/Ucluelet area are non-electric. Therefore, the load data for an average non-electrically heated Coastal BC home will be used as the basis for the hourly community load data.

5.6 Summary

For the purposes of this research, the hourly load data for a non-electrically heated average Coastal BC home is used and a constant scaling factor of 2300 homes represents the approximate number of these households which make up the Tofino/Ucluelet community. By multiplying the hourly household load data by the scaling factor, hourly community load data can be approximated.

6 Simulation

6.1 Introduction

With the wave energy resource, conversion technologies, and load properties now known, this chapter introduces the system which will be used to perform the simulation and generate the results seen in Chapter 7. Section 6.2 examines the Ucluelet area for suitability as a wave energy site, and determines the site-specific information which will be important to the simulations. Section 6.4 gives an overview of the wind resource available in the area, which will be used for results comparisons later in the thesis. Section 6.5 lists the assumptions made in the model development, and 6.6 gives the overview of the model structure. The last two sections discuss the sensitivities which will be examined, and the power capture curves used for these simulations.

6.2 Geographical Suitability of the Ucluelet Area

The area near Ucluelet was originally selected by BC Hydro as one of two favourable sites for wave energy on the coast of Vancouver Island. The other site, at Winter Harbour near the Northern tip of Vancouver Island, may also be well-suited to wave energy conversion, but due to the remoteness of the area and the fact that two wave measurement buoys are located in the vicinity of Ucluelet, this site became the focus of the present study.

Figure 6.1 is a map of the Tofino/Ucluelet area with the location of the transmission lines roughly plotted. LBH is the Long Beach substation, from which two feeders extend – one towards Tofino, and the other to Ucluelet. Each of these feeders has a capacity of 15 MVA [97, 98]. Therefore, the grid capacity at the substation where the two feeders join is considered to be 30 MVA.

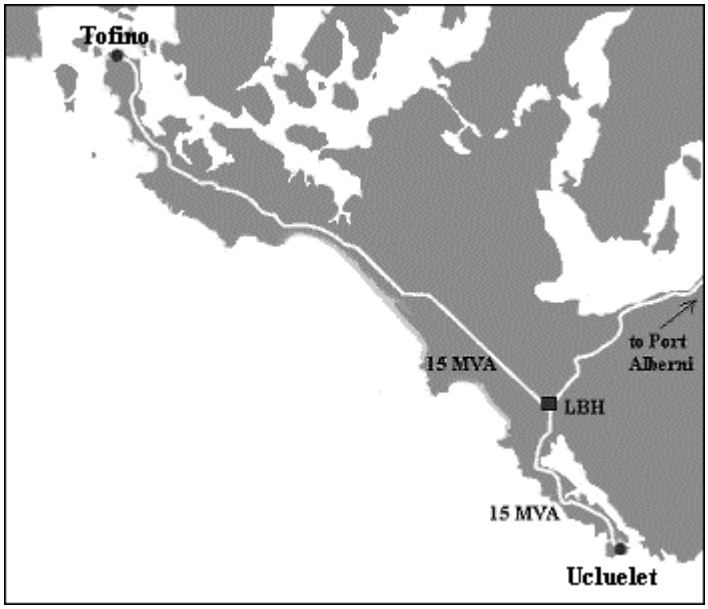

Figure 6.1- Tofino/Ucluelet area and location of transmission lines [97, 98], which generally follow the main roads (image modified from [99])

Figure 6.2 is a bathymetric map of the waters in the Tofino/Ucluelet area. The location of the Long Beach substation (code LBH) is shown. Since it is only at this location only where a perceived grid capacity of 30 MVA could be achieved, it would be advantageous to build a wave energy conversion system in a location easily accessible to the LBH.

Also shown in Figure 6.2 are the zones suitable for each device. The Pelamis device is an offshore WEC device whose target depth is 60 to 150 m. The Energetech device, on the other hand, is designed for waters from 5 to 50 m in depth. The black arrows are distances that have been measured for comparison in this study, and are of particular concern for any Pelamis project, given that a minimum depth of 60 m is suggested by the manufacturer [91]. Fortunately for Ucluelet, there is an undersea canyon near the shore in proximity to the Long Beach substation, allowing a Pelamis device to be placed closer to shore than would normally be possible. The total distance along that path is approximately 6.2 km, with 2.8 km of that distance under water, and the remaining 3.4 km on land. A second arrow indicates a more normal distances of 24.2 km between 60 m waters and the shoreline, all of which is undersea. Further transmission cables would be required to connect from the shoreline to the grid connection point.

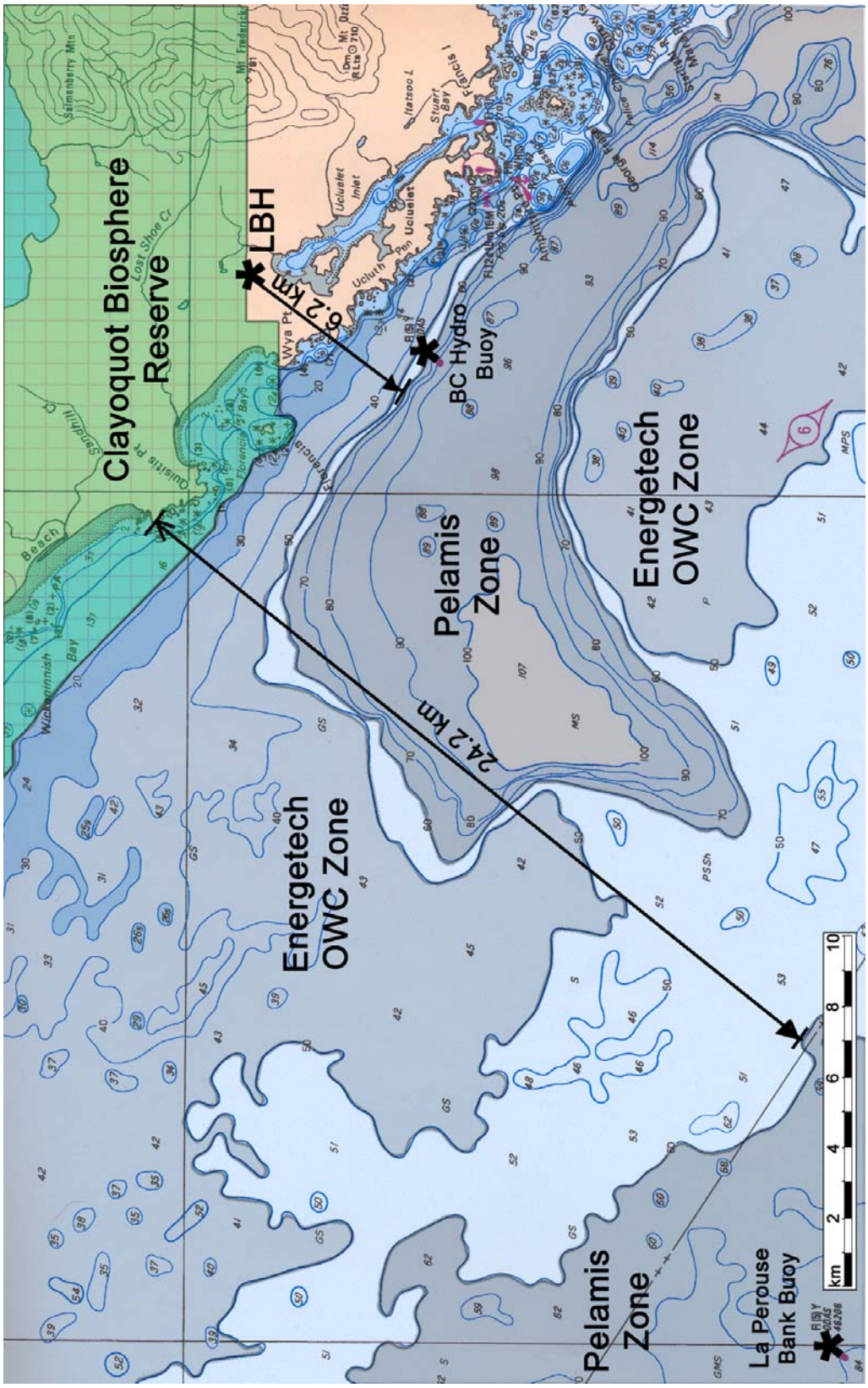

Figure 6.2 - Chart of Ucluelet area, buoys, Clayoquot Biosphere Reserve, and potential sites for WEC devices (base map from [100])

One potential constraint to the size and type of wave energy projects that could be constructed in near Ucluelet is the presence of the Clayoquot UNESCO Biosphere Reserve. This 350,000 hectare protected area extends across most of the area between Tofino and Ucluelet, and includes a marine area approximately extending to the 20 m depth contour. The location of the reserve in relation to Tofino and Ucluelet is shown in Figure 6.2. The biosphere reserve is in place to promote conservation, sustainable development, and research/education [101]. While it may still be possible to have a wave energy project within the boundaries of the reserve, WEC technologies deemed to have high environmental impacts, such as shoreline OWCs, may likely encounter opposition. Offshore devices such as Pelamis may not only be less invasive, but would be moored in waters deeper than that found in the area enclosed by the reserve.

Noise is not expected to be a major issue for animals [22], though shoreline OWCs may require design modifications for noise abatement. The average noise for the Energetech OWC turbine is 73 dB, for a distance 1 m from the turbine [102]. Since a breaking wave at a distance of 10 m is 90 dB [103], the Energetech OWC is not expected to cause noise problems for observers on shore. The LIMPET OWC required the installation of a noise attenuation chamber due to noise caused by airflow through the ducts and the turbine blades, particularly during stall conditions [104].

6.3 The Grid and the Concept of Grid Penetration

The physical location of the grid feeders and substation were described in Section 6.2, but the importance of figures such as grid capacity centres around the concept of grid penetration. In this thesis, grid penetration for each hour *i* of the simulation, is defined as:

$$Penetration_i = \frac{P_{renewable}}{Capacity_{grid}} \tag{6.1}$$

The grid penetration is calculated for each hour, with $P_{renewable}$ being that hour's power output from either the wind turbines or the WEC devices. The grid capacity is taken to be 30 MVA in all cases, which is the capacity at the Long Beach substation.

In addition to the hourly grid penetration just mentioned, two specific grid penetration numbers are used in results comparison – maximum grid penetration, and average grid penetration. These are both yearly values, and are calculated using the following two equations:

$$Penetration_{\max} = \max(Penetration_i) \tag{6.2}$$

$$Penetration_{ave} = \frac{\sum_{i=1}^{8760} Penetration_i}{8760} \tag{6.3}$$

In both cases *i* ranges from 1 to 8760, the number of hours in a year.

For renewable resources, which are usually intermittent and often difficult to accurately predict, grid penetration is often an issue because the variations in the resource level occur more rapidly than the ramping rates of baseload power plants, and often on too large a scale to be handled by the grid's infrastructure for handling short-term fluctuations. For small proportions of the total capacity, this is usually not a problem. However, as the average penetration level increases, unexpected changes in renewable power output could cause, on a short-term scale of a few hours, problems such as electricity shortage (if renewable power predictions were too high) or conversely, the overloading of the system (if renewable power predictions were too low) [42]. Comparing wind and wave resources, Energetech's Tom Denniss found that wind speed and wave height have roughly the same variability, but since wind power is proportional to the cube of the wind speed, while wave power is proportional to the square of wave height, Denniss showed that there is a higher probability that wind power at a site is more variable than wave power at a site [105]. Nevertheless, since wave power is still quite variable when compared to other sources such as hydro or tidal, the grid penetration tolerance level used in this thesis is based on that for wind power, which approximates a worst-case scenario.

This tolerance level is not clearly defined – in Denmark, the average grid penetration is 50% and some significant problems have been observed [42]. Weisser et al. [45] mention in reference to wind that penetrations of 15-20% should not be harmful, while in Northern Ireland a constraint of 10% was imposed on a recently proposed wind farm. [106] For the purposes of this thesis, an intermediate value of 15% will be used. Therefore, momentarily neglecting the effects of storage capacity, the maximum wave and wind power input value should be no greater than 4.5 MW for Tofino/Ucluelet's 30 MW grid.

6.4 Wind Resource Data for Comparison

To make a baseline comparison of the suitability of wave energy in the Tofino/Ucluelet area, the simulation was first run using wind turbines as the producers of renewable electricity, since their characteristics are better defined and understood.

Environment Canada has data sets [107] for three measurement sites in the general area of interest, as described in Table 6.1. Figure 6.3 is a map indicating the locations of these three sites.

Location	Measurement Dates	Notes
Amphitrite Point	Jan. 14, 1970 – June 15, 1978	No recent data
Cape Beale	Feb. 16, 1968 – July 1, 1997	On opposite side of Barkley Sound
Tofino Airport	Jan. 1, 1960 – Dec. 31, 2003	From 1978 onward, daytime measurements only

Table 6.1 - Locations and characteristics of Environment Canada wind data in area near Ucluelet

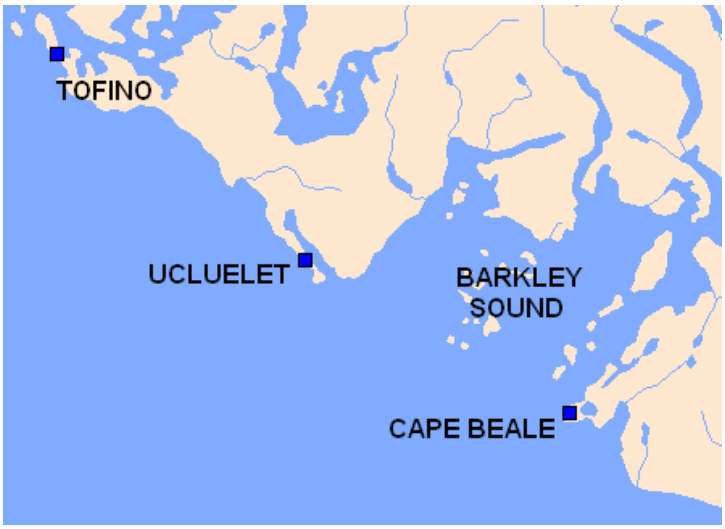

Figure 6.3 - Three Environment Canada wind measurement sites in the area of Ucluelet (map modified from [108])

While data from the Tofino Airport is the most up-to-date and has been collected since 1960, after 1977 data has only been collected in the daytime hours, making the data set useless for the purposes of this study. The Amphitrite Point data would have been the closest and was indeed recorded 24 hours a day, but the data set ends in 1978, a full decade before the beginning of the wave data collection at La Perouse Bank. Therefore, in order to obtain both wind and wave data for the same year, wind data from Cape Beale was used.

To determine the magnitude of the differences between the available data sets, 9-year averages for each of the three sites (see Table 6.2) were compared over the years 1969 (1970 for Amphitrite Point) to 1978, omitting 1974 due to large gaps in data. The mean wind speed at Cape Beale is on average 24% higher than at the Tofino Airport. The mean wind speed at Amphitrite Point, however, is an average of 11% higher than at Cape Beale.

These observations are consistent with the data available from the Canadian Wind Energy Atlas (CWEA) models, which are numerically-simulated statistical averages of wind speeds collected between 1953 and 2000 [109]. The mean wind speed values and the averages of the differences between the Cape Beale data and that of the other two locations are shown in Table 6.2. The mean wind speed values do not match exactly because the

Environment Canada data are recorded at a specific location, while the CWEA data are simulated for a 5 km x 5 km area.

Location	Mean Wind Speed (m/s)		Average difference with Cape Beale (%)	
	EC	CWEA	EC	CWEA
Amphitrite Point	5.61	6.03	+11 %	+11 %
Cape Beale	4.68	5.32	--	--
Tofino Airport	3.86	4.46	-24 %	-19 %

Table 6.2 - Mean wind speed comparison between Environment Canada (EC) and CWEA simulations

Since Amphitrite Point is the location closest to any potential wave project, the wind for this area was of interest. The Canadian Wind Energy Atlas also shows that the wind speed at Amphitrite Point is on average 11% higher than at Cape Beale [109].

However, no particular site had been identified for potential wind projects in the area. Consequently, the choice of wind data for use in this thesis was somewhat arbitrary, particularly since factors such as topography and land roughness [110] can play a large role in wind characteristics at a given location. The Cape Beale data was deemed suitable for a first estimate of wind energy, as the mean wind speeds there are roughly halfway between those of Tofino Airport and Amphitrite Point. The simulations are therefore based on data which is neither the best-case nor the worst-case scenario. Data for 1996 was used in the first set of simulations.

6.5 Assumptions

A number of assumptions were made during the implementation of the model, and these are described in this section.

1. The load profile used for this study was synthesized from the Tofino/Ucluelet residential load, consisting of 2300 average non-electrically heated homes (see

Section 5.5).

2. The waves near the coast of Ucluelet are likely to be spilling breakers, and thus the energy dissipated during breaking is likely in the range of 40% of the total wave energy [64]. However, since the actual energy left in the wave when it reaches the WEC is conjectural at best, without experimental testing at that particular location, the model errs on the side of caution and assumes a 50% energy dissipation for the OWCs, which operate in shallow water. This 50% energy dissipation was approximated by using the following modified value of the significant wave height:

$$H_{sig(shallow)} = \frac{1}{\sqrt{2}} H_{sig(deep)} \qquad (6.4)$$

Inserting this value into (3.16), the wave power equation, produces the required 50% reduction since the power is proportional to the square of the significant wave height. While the actual behaviour of the waves is significantly more complex and this may not be representative of what actually happens to the wave height, this rough approximation allows the simulation to account for a reduction in wave energy in some form.

3. No energy dissipation was assumed in the case of the Pelamis device, as it operates in water deep enough to be clear of the surf zone.

4. The placement of wind turbines over a large area tends to smooth some of the sharpness of variation in wind power production [111], since the prevailing wind conditions can vary substantially between regions. However, no attempt was made in this model to smooth the wave power output from multiple WEC devices. If in the future, multiple wave farms begin to contribute a substantial amount of power to Vancouver Island, this type of smoothing could potentially occur, but by that time, the effects of this will likely already be well known from studies on wind farms.

5. Finally, there were no transmission losses included in the model. Although any transmission cable has a finite resistance and this will contribute to losses, since there was no particular location in mind for the WEC devices in this project, the length of cable required would be conjectural at best. In the event that a project of this nature were to be considered, these losses would need to be accounted for. This model, then, is a best-case scenario as far as transmission is concerned, assuming no line losses and a power factor of 1.

6.6 Model Structure

TRNSYS was the software used to run the simulations for this study. Though originally designed for modelling heat transfer in buildings, over the years it has been adapted to also allow for the simulation of renewable energy systems. The building block of any system to be simulated in TRNSYS is the component, which is a generic model of a particular system element that can be customized to match the exact characteristics of the device to be simulated. These characteristics are defined by parameters of the component, which do not change with time over the course of the simulation. Components are linked to each other through their inputs and outputs. Version 16 of TRNSYS, the latest version available at the time of this writing, incorporates several renewable energy components including fuel cells, electrolyzers, photovoltaic panels, batteries, and wind turbines. While many of the components proved useful, several components needed to be developed specifically for this project. The overall model structure is described in the following sub-section, and the structure of each of the custom components is explained in further detail in the subsequent sub-sections.

6.6.1 Overall System Layout for Simulation

The system was laid out in TRNSYS as shown in the schematic of Figure 6.4. On the left are the input files which include the hourly renewable resource data (wind and/or wave, depending on the set-up), and the hourly load profile for a typical household. In these simulations, as explained in Section 5.5, the BC Hydro data for an average BC coastal

home using non-electric heating is used. On the far right of the diagram are the outputs of the model, usually in the form of graphs with corresponding text files. In this example, the wave resource file, which gives the significant wave height (H_{sig}) and wave period (T_{sig}) for each hour, provides the inputs to the WEC device model. The output of this model is the amount of power generated by the WEC device. This power is then multiplied by the number of devices to scale the output for multiple identical WECs. The household load profile and the output power from the WEC device(s) are both inputs to another set of equations, called "Resource/Load Balance Calculations" in the diagram. Here the household load profile is scaled up to represent an entire community, and the difference between the renewable energy input and the residential load is calculated. An integrator/summation component, marked with "Σ", uses these hourly values to calculate the cumulative values of excess or deficit electricity over the course of the year. The storage device also uses the net difference of renewable power and load to determine whether there is excess electricity, or a demand. A detailed explanation of the structure and behaviour of the storage component is given in Section 6.6.3. Since the storage component acts as a buffer between the renewable resource and the grid, calculations of the grid penetration uses output data from the storage component. If no storage is present, the output of the load calculations becomes the input to the grid equation, which calculates the grid penetration.

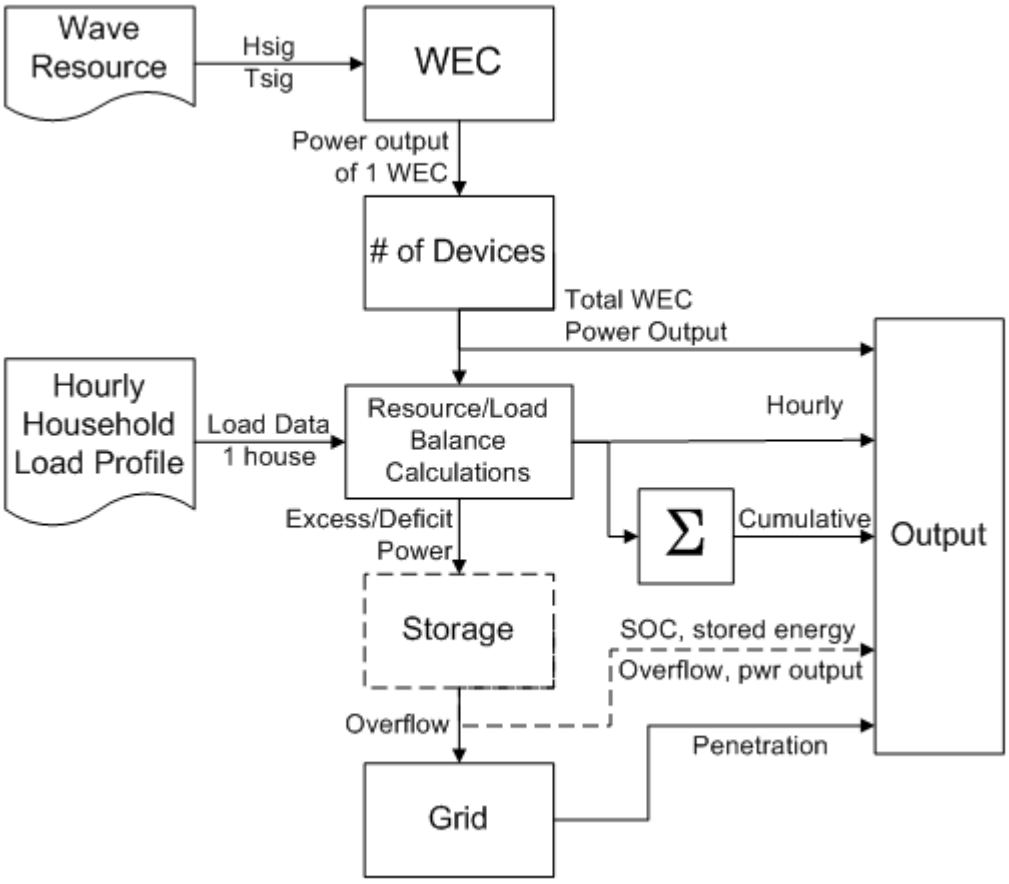

Figure 6.4 - TRNSYS model structure for WEC system simulation

The following sections describe in detail the two important components in this system – the WEC device, and the storage component.

6.6.2 Wave Energy Conversion Device Component Design

The WEC device component, shown at the top of the middle column in Figure 6.4, was a key component necessary for this project, as it was the pillar for the simulation of systems containing WEC devices. Since TRNSYS did not come with a WEC device component, it was necessary to design one for this thesis. Two options were considered in the fundamental structure of the component.

1. It could be designed to calculate power output analytically using the fundamental equations at each energy conversion interface.

2. Power capture curves, which are tables listing the power output of a device for specific significant wave heights and wave periods, could be given as a parameter to the component. In this way, the specific energy conversion mechanism and its corresponding equations are not important to the model. The component's internal process would therefore centre around interpolating power output values in the power capture curves for the given wave height and period inputs.

Each of these possibilities was explored over the course of the thesis research, and these are discussed in this section.

The original idea was to focus on the OWC and calculate power output analytically given the equations for energy transfer within the device. The following code structure was suggested:

1. Get wave data input from input of the model
2. Compute wave power from significant wave period (T_{sig}) and significant wave height (H_{sig})
3. Determine pneumatic power using non-linear scaling factor defining wave power to pneumatic power conversion efficiency
4. Interpolate turbine efficiency from plot of efficiency vs. angle of attack (α) on the blades, for that specific turbine design
5. Determine power extracted from the air flow using efficiency from previous step
6. Determine electrical power generated using turbine power and generator efficiency
7. Output the results of electrical power

The main difficulty with this code structure is that it is highly dependent on accurate and site- or device-specific data. For example, one of the major stumbling blocks is determining the angle of attack necessary in step 4, to look up efficiency on a graph of efficiency vs. angle of attack. For the Wells turbine, which is the turbine most commonly used in OWCs, turbine efficiency is affected by changes in blade sweep [112], blade

pitch [93], airfoil shape, the presence of guide vanes [113], and the number of rotors [77]. To further complicate the matter, not all OWCs use Wells turbines. The Energetech OWC uses a Denniss-Auld turbine which has variable-pitched blades [114], and thus the control strategy of the blades would also need to be known in the model to determine the angle of attack for efficiency calculations. Even if all this information were known, and the simulation was possible, it is likely that the simulation results would need to be validated against experimental data with the exact turbine configuration modelled. This validation is not possible for this thesis.

Other steps also had uncertainty associated with them. Raju et al. [115] determined that the entrance geometry of an OWC impacted the efficiency of energy absorption.

Also, since the data available from La Perouse bank was in the form of hourly averages of key characteristics, a wave spectrum would be needed to synthesize a record of individual waves to use as an input to the analytical model. No spectral model exactly matches the real frequency spectrum of the sea state, and there is no one model which is consistently the best approximation, depending on conditions and time of year [116].

The second option for the WEC device component design, which is implemented in this research, is to use a known power capture curve as a parameter, treating the actual mechanism for energy conversion as a black box. This has the advantage of being far less computationally intensive, and it also allows the same component to be used for any wave energy conversion device, OWC or otherwise. In TRNSYS, the wind turbine model is similar in its dependence on a pre-existing power capture curve for a particular make and model of wind turbine [117].

An external file defining the power capture curve(s) is specified as a parameter to the component in the project. As the simulation runs on an hour by hour basis, the significant wave height and wave period are passed to the component as inputs. If the specific combination of wave height and period do not correspond to a given point in the power capture parameter file, the power is determined by linear interpolation of the nearest

values in the power capture file. This process is illustrated in Figure 6.5, showing the calculations for hour 8668 (1:00 am, December 28).

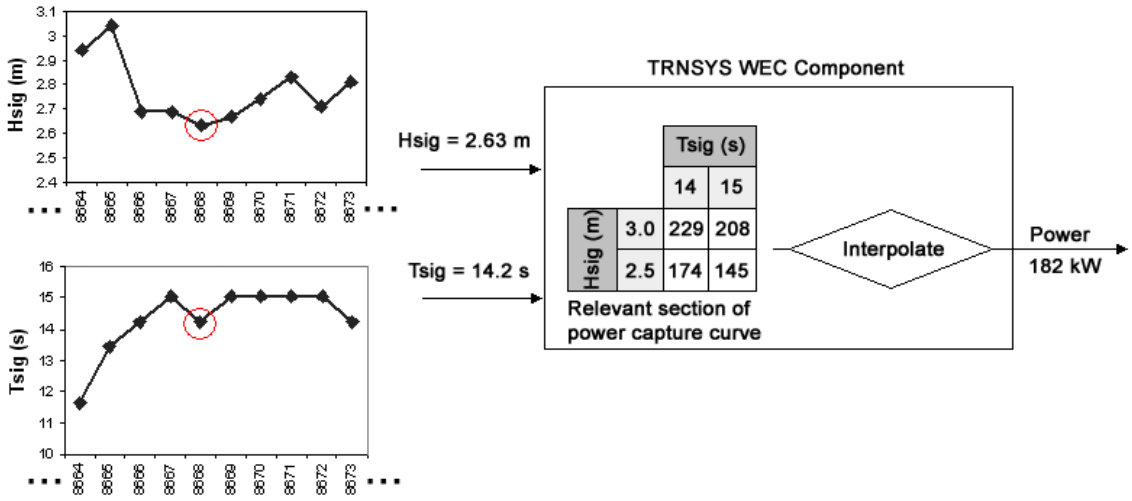

Figure 6.5 - Interpolation process within TRNSYS WEC component, showing process for hour 8668

Earlier, in section 3.7, it was mentioned that tides can affect the operation of shoreline devices such as OWCs. In the case of the LIMPET OWC, separate power capture curves exist for low, mean, and high water levels [118]. Since it was the only device in this study for which different files would have been necessary depending on water level, and since it would have been necessary to also have a separate input for tide levels, it was decided to use the power capture curve for mean water levels, leaving the tidal component out of the model. In the future the model could be refined to include the effects of the tides, if there is further interest in shoreline devices.

6.6.3 Storage Design

A component was designed for energy storage, based on the operation of the VRB Redox flow battery. This technology was chosen due to its known round-trip efficiency values and simple concept. In this way, the simulations could be distanced from the actual mechanism of energy storage, depending instead on input and output efficiencies to determine system sizing for both the WEC devices and the storage. If it were later determined that a hydrogen system will be used for a wave energy project, a preliminary

simulation could be done using either experimental or calculated efficiencies, and a more complex model could be substituted into the system simulation once more specifics are known.

The inputs, outputs, and parameters of the VRB storage component are shown in Table 6.3.

Input
Leftover power once load is serviced (W)
Outputs
Power exchanged to and from storage (W)
Energy stored within the storage component (kWh)
State of charge (%)
Overflow power exchanged with the grid (W)
Parameters
Storage capacity (kWh)
Maximum power in/out of storage at any given time (kW)
Input efficiency (%)
Output efficiency (%)
Off/On (storage or no storage)
Maximum state of charge (%)
Minimum state of charge (%)

Table 6.3 - Inputs, Outputs, and Parameters of storage component in TRNSYS

In the list of parameters, the storage capacity is one of the main parameters which has been varied during the simulations. The maximum power in/out of storage, or in other words the maximum rate of charge/discharge of the stored energy, can limit the amount of electricity which can be provided to the load, even though there may otherwise be enough stored energy to accommodate the demand. The product of the input and output efficiencies gives the round-trip efficiency. Since VRB claims a round-trip efficiency of 70-78 % for its VRB flow battery [23], this value was retained for this experiment. Both the input and output efficiencies were set to 87.5% so that the product, 76.5%, worked out to be within VRB's specifications. They were, however, separated into two parameters in order to allow the flexibility of specifying different input and output efficiencies.

While the VRB flow battery is the basis for the storage model, both lead-acid batteries and pumped hydro installations have similar round-trip efficiencies. Therefore, the results from using this storage model should be good approximations to the results obtained if the system were based on lead-acid or pumped-hydro storage.

Also specified by VRB were maximum and minimum states of charge, which were 85% and 15% respectively. This was also used in the model, and means that the battery cannot be charged to more than 85% of its capacity, or discharged to less than 15% of its capacity.

The one input is the difference between the renewable energy produced in a given hour, and the residential load for the hour. If the number is positive, an excess of renewable energy exists, and the storage component attempts to store what it can of this excess. If the number is negative, the load is greater than the renewable energy for the hour, and the storage component attempts to discharge enough energy to meet the remaining demand.

Four outputs have been built into the storage component. The first is the output power, which is the electricity exchanged between the storage component and the combination of load and WEC devices. Unlike the input power, this value can be zero or positive, but not negative. If there is excess energy from the WEC devices, the storage will attempt to absorb the excess energy and therefore will not discharge any energy back towards the load. In this case, the output power will be zero. If there is unmet demand from the load, and there is available energy stored, the storage component will discharge enough electricity to either meet the unmet demand, or until the resources of the battery are either depleted or the discharge rate limit is reached. In these cases, the output power is the amount of power discharged from the storage unit. This is measured in kW, though since it is an averaged value over the course of an hour, the amount of energy released from the battery can easily be converted to an energy value in kWh.

The second and third outputs are status indicator of the energy stored, and the state of charge of the device. If the system model were to be expanded to more than one type of

storage, or if for some reason an external system controller component is required, these outputs can be used in the decision-making of that controller. However, at this point, the storage component does its own control of charging and discharging, and does not require an external component to make sure charge/discharge restrictions are not breached.

The last output indicates how much power cannot be accommodated by the storage system, and is considered the overflow. Like the input power, this value can either be positive or negative. A positive number indicates how much power remains after the load is serviced and the storage is filled as much as possible. This is the amount which is fed to the grid, and contributes to grid penetration. A negative number indicates that the WEC and storage components together still cannot produce enough electricity to service the load, so this number indicates how much power would be required from the grid.

This makes up the basic model for energy storage in these simulations. The following sections provide background information also useful to this study.

6.7 Sensitivity

One of the main areas where the sensitivity of the system is measured is the size of the storage. In one scenario, the storage capacity is set large enough to be considered infinite, and the maximum input power limitation is varied to determine its impact on grid penetration when connected to a wave farm and a load. In a second scenario, the maximum input power is set large enough to be considered infinite, and the storage capacity is varied. The two results together provide insight into the design of a storage system which leads to acceptable penetration levels while minimizing the size of the storage facility necessary, thus reducing costs.

6.8 Power Capture Curves

As previously mentioned, the TRNSYS models of WEC devices are dependent on pre-existing power curves as lookup tables for calculation of output wave power. Figure 6.6 to Figure 6.9 show graphically the power capture curves of each of the four device configurations to be considered. Figure 6.6 shows the expected power capture curve of the Faroese LIMPET OWC. Since this power capture curve is based on experimental data rather than numerical simulation, only 15 combinations of wave height and period were characterized. The matrix was divided into 15 sections, with each section represented by a single wave power value. For this reason, the power capture curve for the LIMPET is not as detailed as for the other devices. For wave periods of 12 – 15 seconds, linear interpolation was possible for wave heights between 2 – 5 seconds; otherwise, no interpolation was performed to obtain the matrix in Figure 6.6.

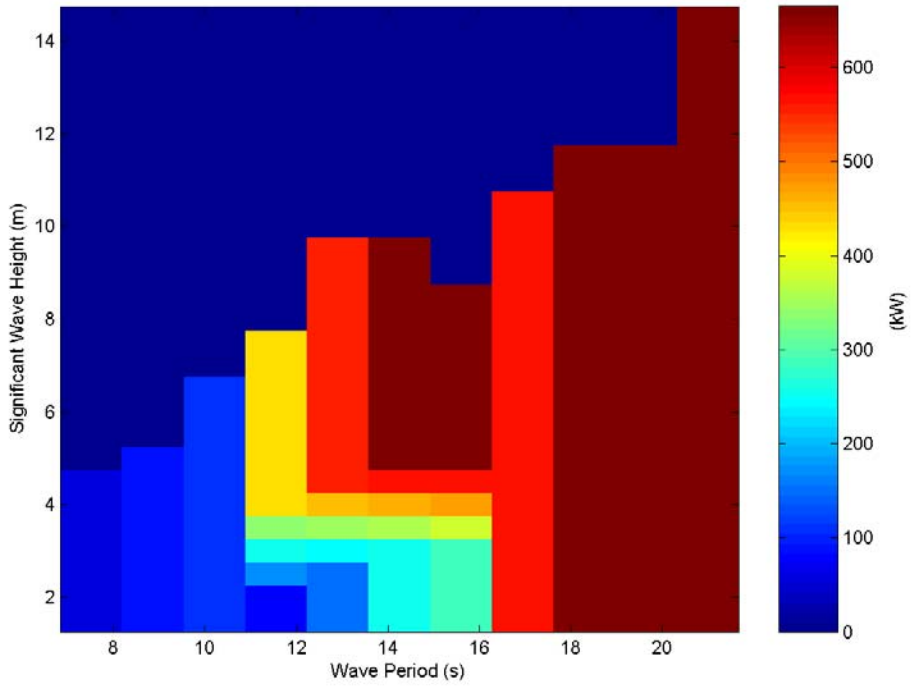

Figure 6.6 - Power capture curve of Faroese LIMPET OWC [83]

Figure 6.7 is the power capture curve for the Energetech OWC, which shows that maximum power is obtained from higher wave heights and longer periods. Figure 6.8, the power capture curve for the UK Pelamis configuration, and Figure 6.9, the power capture curve for the US Pelamis configuration, show the similar characteristic of better

performance for higher wave heights, though shorter wave periods generate the maximum power than is the case for the Energetech OWC.

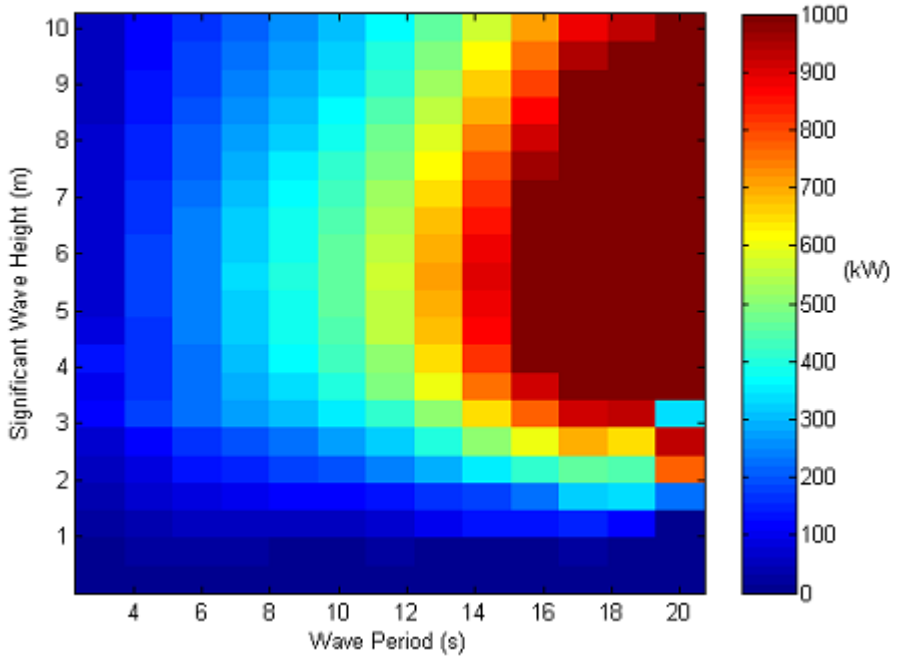

Figure 6.7 - Power capture curve of Energetech OWC [62]

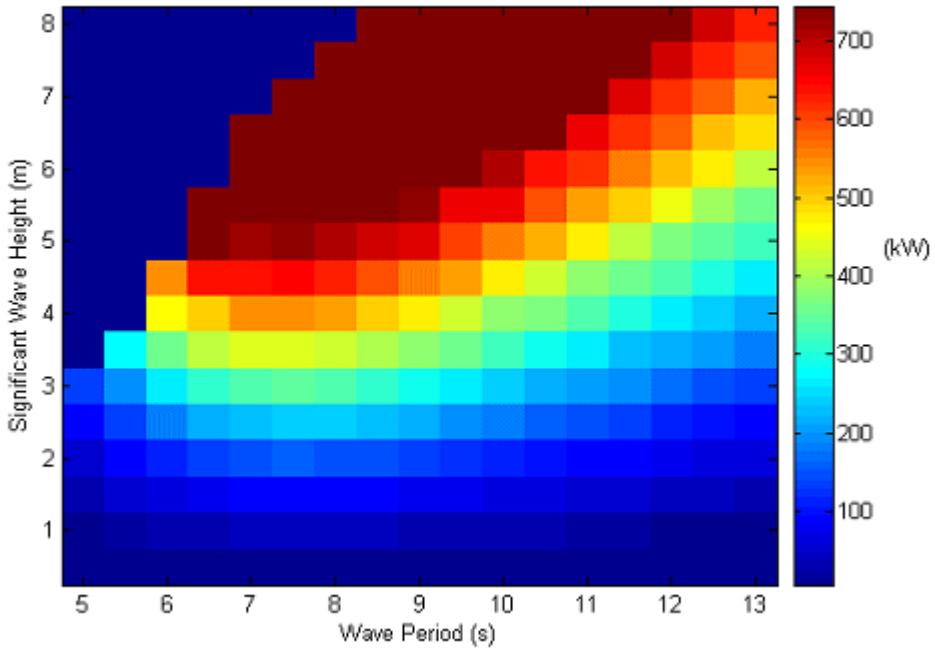

Figure 6.8 - Power capture curve for UK configuration of Pelamis Device [119]

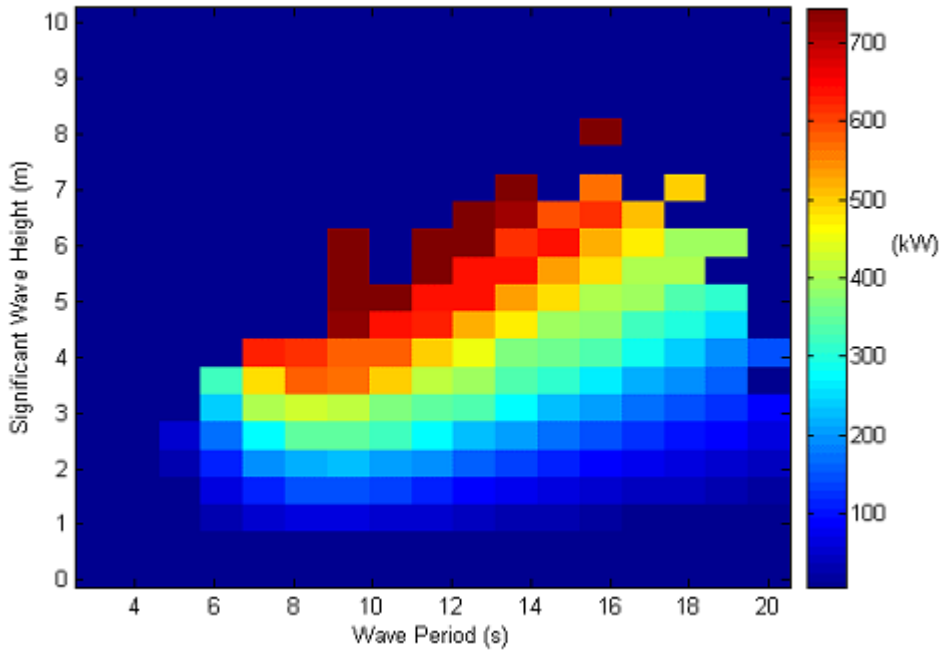

Figure 6.9 - Power capture curve of US configuration of Pelamis Device [91]

6.9 Summary

In this chapter, the important aspects of the simulation context and model design were examined. Many assumptions were made to simplify the model, as well as account for variables which are currently unknown due to lack of information. However, experimental or numerical data are used whenever possible, such as for the power capture curves. The following chapter discusses the results which were obtained using this model.

7 Results

7.1 Introduction

In this chapter, the results of the TRNSYS simulation are presented. The first section lays the foundation, using the wind resource to identify general problems when attempting to implement renewable energy in this area. Once this baseline is analyzed, the wave resource is then simulated and compared with wind, to determine the advantages and disadvantages of wave energy conversion systems. Finally, the wave energy conversion system is coupled with a storage medium, and its effects on grid penetration are characterized. The eight main scenarios simulated are summarized below in Table 7.1.

Resource	Device	Storage?	Purpose
Wind	Enercon E40 600/46	No	Determine number of devices required to service load
Wave	LIMPET OWC	No	Determine number of devices required to service load
Wave	Energetech OWC	No	
Wave	Pelamis (UK)	No	
Wave	Pelamis (US)	No	
Wave	LIMPET OWC	Yes	Determine effects of storage on grid penetration, and determine storage required for maximum 15% penetration
Wave	Energetech OWC	Yes	
Wave	Pelamis (US)	Yes	

Table 7.1 - Summary of simulations

7.2 Wind Only

The first step in this analysis was to analyze a system consisting of a grid-tied wind farm servicing the Tofino/Ucluelet load. This forms the baseline to which wave energy can be compared. The wind turbine parameters used were from the TRNSYS parameter file of the Enercon E40 600/46 model, a 605 kW wind turbine. While TRNSYS comes with parameter files for seven models of wind turbines ranging from 230 kW to 2 MW, the Enercon E40 600/46 was chosen for its relatively mid-range properties. Figure 7.1 shows

the power capture curves for all seven turbine models included with TRNSYS, and in this figure the Enercon E40 600/46 power curve is illustrated with a bold line.

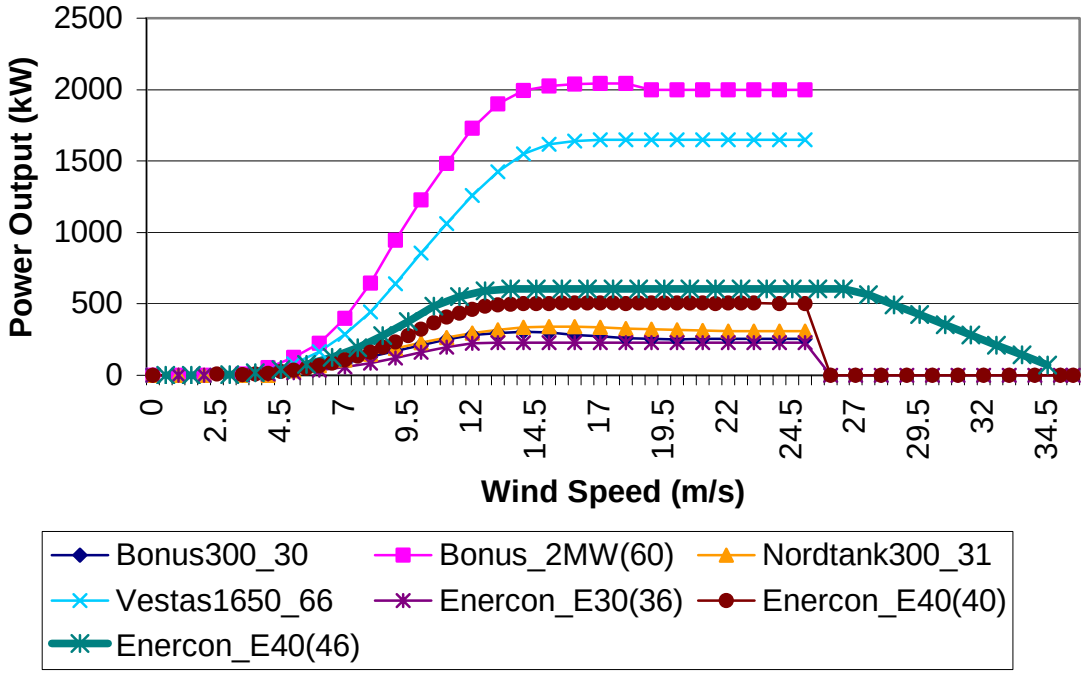

Figure 7.1 - Power capture curves for the seven turbine models in TRNSYS

Cape Beale wind data for 1996 was used as a specific test case, as it was the latest full year for which data was available. Using this Cape Beale data, Figure 7.2 was obtained, showing both the wind velocity (bottom trace and left axis), and the corresponding power available from the wind turbines (right-hand axis).

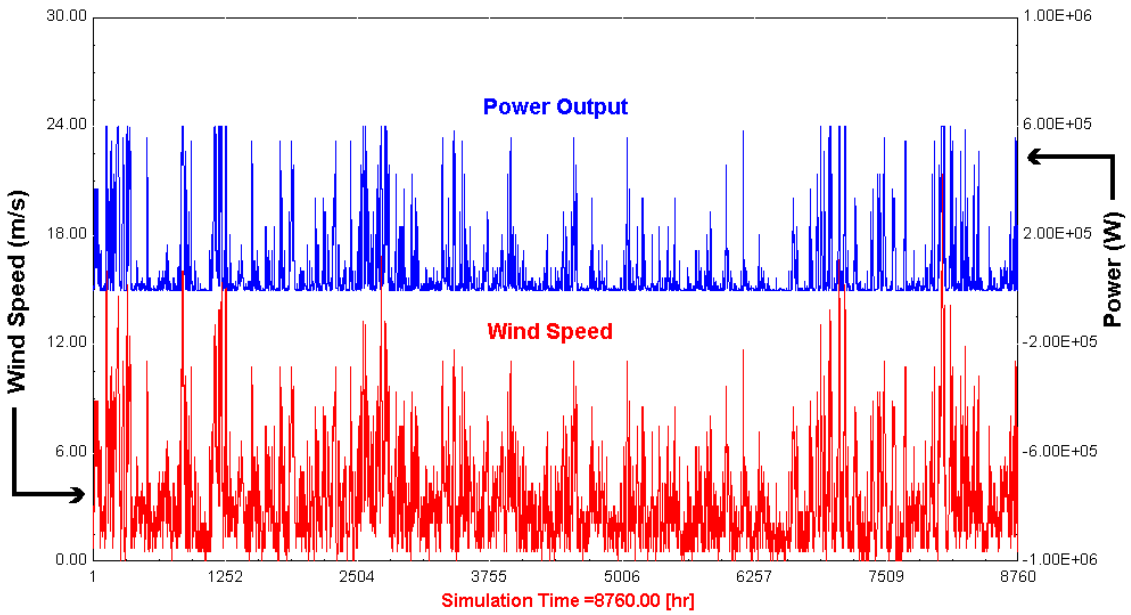

Figure 7.2 - Wind speed (bottom trace) and corresponding power output from Enercon 40 600/46

While the summer months in the middle portion of the plot show a slightly lower overall power than in the winter, in general there is no marked summer and winter trends.

When this wind resource was simulated for servicing the Tofino/Ucluelet load, it was found that considerable support from the grid was necessary to service the load. Furthermore, when the percentage of annual load serviced is increased, the percentage of time that the wind system can fully service the load does not increase at the same rate, as illustrated in Figure 7.3. Even when the total energy produced over the year is equal to the total energy required by the load, the grid must support part or all of the load 76% of the time. This is likely due to the dominance of low wind speeds in this area – while the mean wind speed for Cape Beale in 1996 was 3.6 m/s, the mode was 1.7 m/s, well below the cut-in wind speed of 2.75 m/s for the E40 600/46. Even when the turbine model was parameterized as an Enercon E30 230/36, a 230 kW turbine with a lower cut-in speed of 2.0 m/s, the results were not significantly altered.

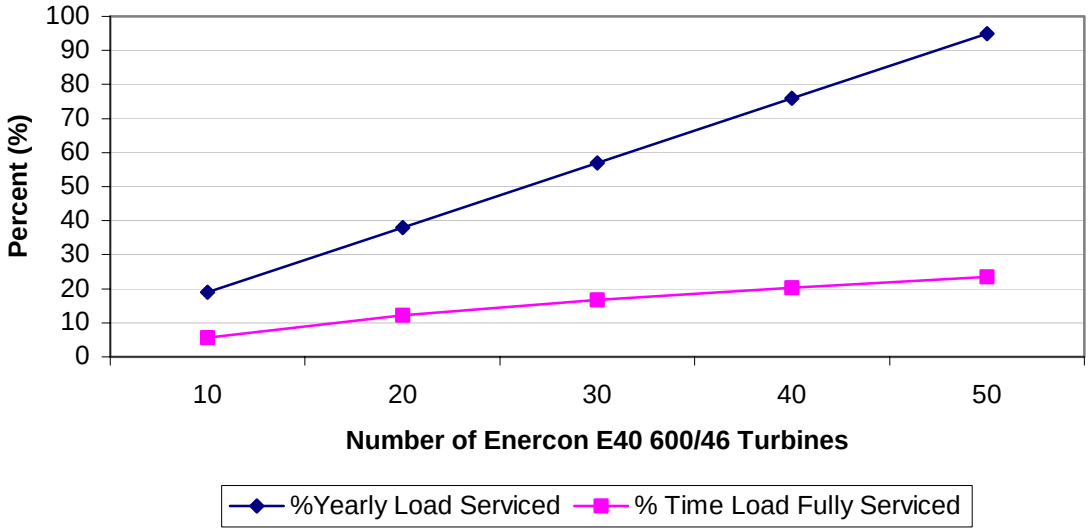

Figure 7.3 - Comparison of percent of load serviced with percent of hours of excess power

Figure 7.4 shows the difference between the load and available power for a farm of Enercon E40 600/46 wind turbines, where excess wind power is positive (above the horizontal line), and a power deficit is negative, requiring grid power to make up the difference. Figure 7.5 shows the cumulative value of power transferred to and from the grid, which is the sum of all the values in Figure 7.4 up to that point. In this thesis, wind and wave plants are sized such that this cumulative power to and from the grid is as close to zero as possible. In other words, as much power is transferred to the grid as is taken from it, over the course of a year. In Figure 7.5, this balance has been achieved with 53 of the Enercon E40 600/46 turbines. This represents 32 MW of installed nameplate capacity, which is approximately 3.6 times the peak residential load of 8.8 MW, and over nine times the average residential load of 3.4 MW.

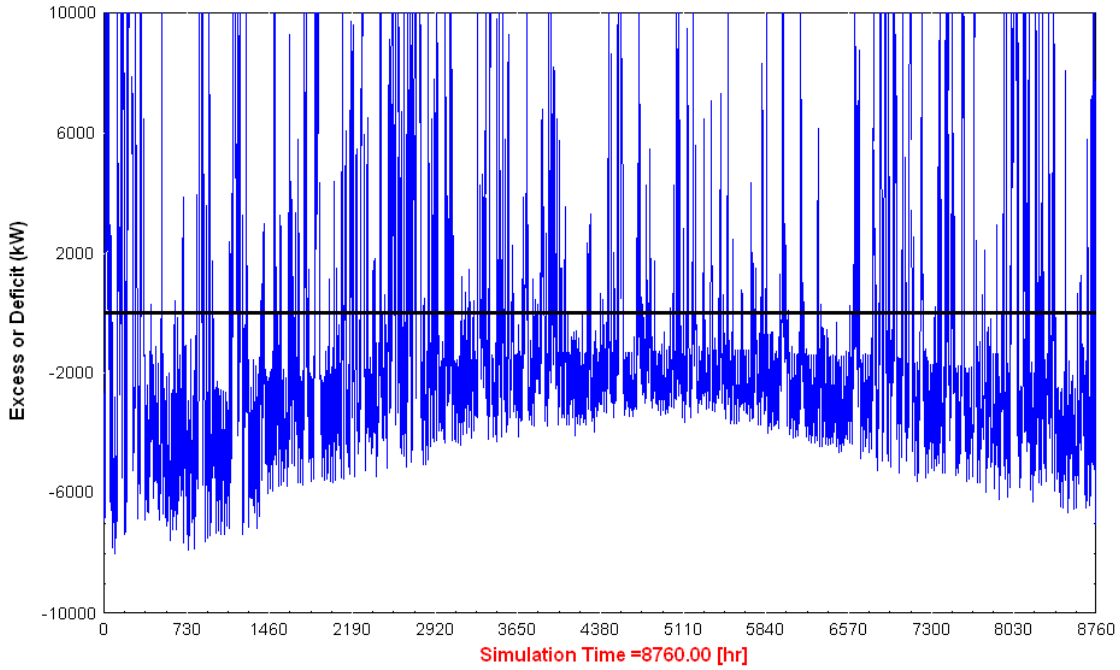

Figure 7.4 - 53 Enercon E40 600/46 turbines servicing Tofino/Ucluelet load - hourly values of excess and deficit power

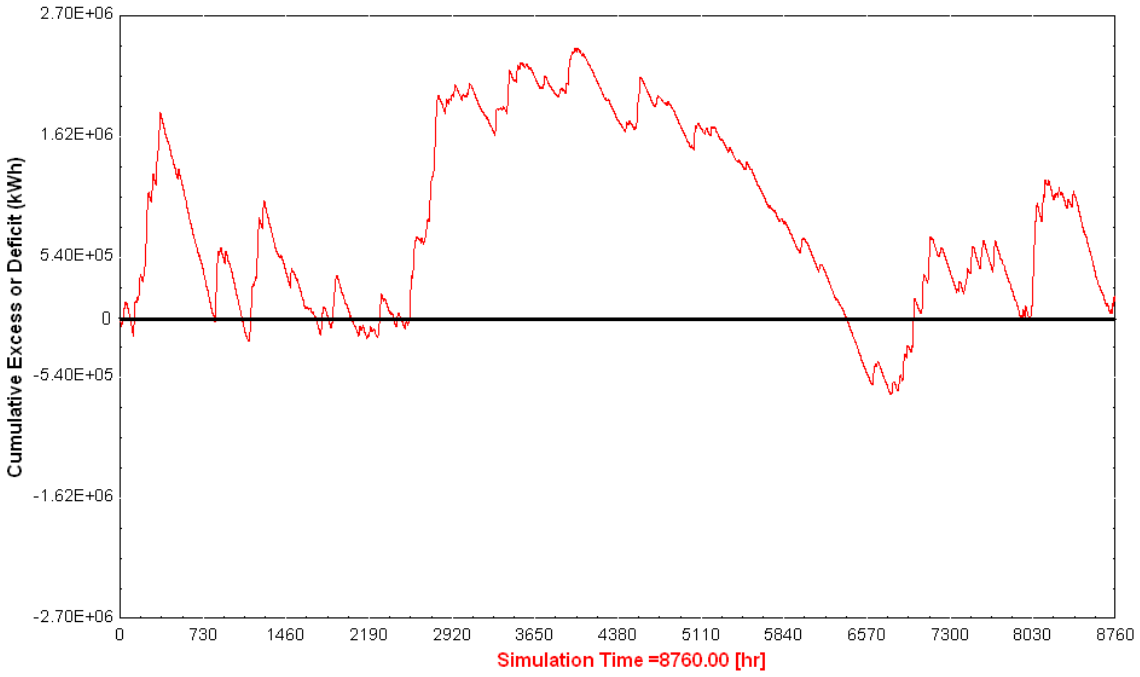

Figure 7.5 - 53 Enercon E40 600/46 turbines servicing Tofino/Ucluelet load - cumulative energy excess/deficit total

Even though it may seem theoretically possible to erect 53 of the turbines and arrive at an energy balance through the grid, a further problem becomes obvious upon inspection of a plot of the grid penetration, which is the amount of power fed to the grid as a percentage of the grid capacity. Figure 7.6 shows the grid penetration plot for the 53 Enercon E40 600/46 turbines. As discussed in the literature review of Chapter 2, significant penetration of intermittent renewable energies can cause grid disruption, particularly in the more remote areas with weak grid infrastructure. This simulation represents the best-case scenario, with:

- Unity power factor – a purely resistive load, meaning that none of the power is inaccessible due to capacitive or inductive effects, and
- Connection at the Long Beach substation – this is the only location in the area where the two 15 MVA feeders join to make 30 MVA accessible (see Section 6.2 for description of grid infrastructure).

The penetration of the wind energy averages 7%, and peaks near or even over 100%. This means that at times, the wind farm is attempting to dump more power than the grid's total capacity, neglecting the amount of power which may already be on the lines from other sources. If the wind farm connects to the grid at any location other than the Long Beach substation, the penetration values would automatically double, as the feeders towards Tofino and towards Ucluelet are each 15 MVA rather than the combined 30 MVA.

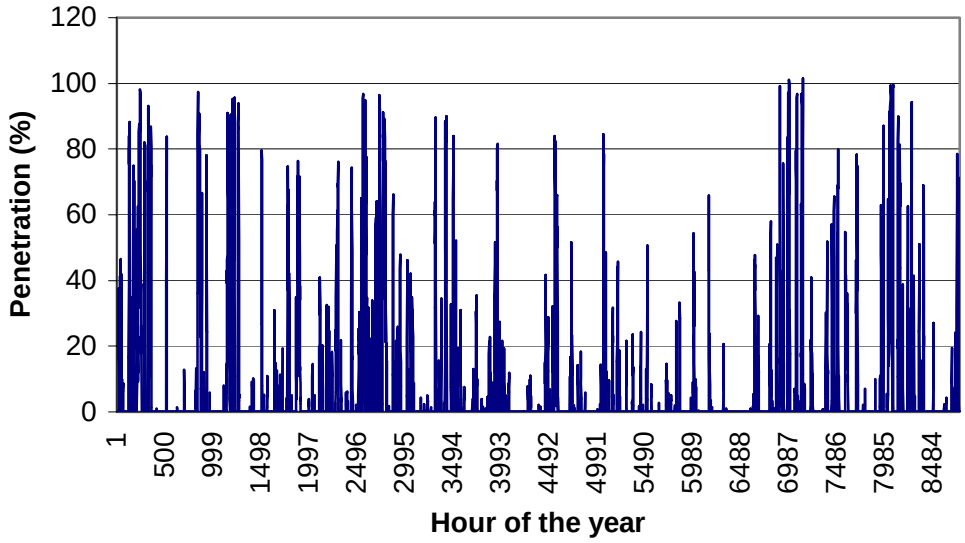

Figure 7.6 - Penetration of 30 MVA grid by 53 Enercon E40 600/46 turbines servicing Tofino/Ucluelet load

If the maximum grid penetration is limited to 15% (see section 7.4.1 for justification of the use of this number), only 10 turbines can be installed before storage becomes necessary to buffer the grid from the wind farm.

Clearly, a simple wind-only grid-connected solution is not acceptable due to the problems with penetration. This area could likely benefit from the addition of a secondary renewable resource for the times when the wind is calm, and some form of energy storage is also likely to be a necessity to act as a buffer between the grid and the wind farm.

The next step in this research was to determine the characteristics of a simple wave-only, grid-tied system, in order to compare the wind and wave systems.

7.3 Wave Only

A grid-tied, wave only system was simulated using the 1995 La Perouse Bank data. 1996 data would have been preferable in order to determine any correlation between wind and

wave resources, but the 1995 data set was among the most complete for the La Perouse Bank buoy – 1996, for example, was missing seven weeks' worth of data.

The system in Figure 6.4 (page 61) was run with four different configurations of WEC devices:

a) Pelamis (UK configuration)
b) Pelamis (US configuration)
c) Energetech OWC
d) LIMPET OWC (Faroese)

In all cases, the cumulative total of energy exchanged to and from the grid was brought as close to zero as possible, though integer numbers of devices were maintained. In the case where an integer number of devices did not come reasonably close to zero, such as in the case of the LIMPET, the number chosen was that which led to an excess of energy. Table 7.2 summarizes the results of the simulations. The last column indicates whether 50% of the energy was assumed to be dissipated due to breaking waves in shallow water, as discussed in section 6.5. The Pelamis devices operate in relatively deep water and were thus assumed to be exposed to the full energy of deep water waves.

Device	Rating	Number Required	Installed Capacity	50% Energy Reduction?
Pelamis (UK Config.)	750 kW	23	17 MW	No
Pelamis (US Config.)	750 kW	15	11 MW	No
Energetech OWC	1 MW	12	12 MW	Yes
LIMPET OWC	665 kW	16	11 MW	Yes

Table 7.2 - Summary of results for grid-connected WEC devices with no storage

Figure 7.7 shows a plot of the output of 15 Pelamis devices of the US configuration, in red, along with the residential load of Tofino and Ucluelet, in pink. Unlike the wind resource, the power extracted from the waves shows a significant drop in the summer period. This also corresponds with a drop in demand over the summer, as is also obvious from the plot. The wave power is similar to wind, however, in that short burst of high power output interspersed with periods of low production lead to a variability in power

output which could be problematic to network operators needing to predict the amount of generating capacity to have at any given time.

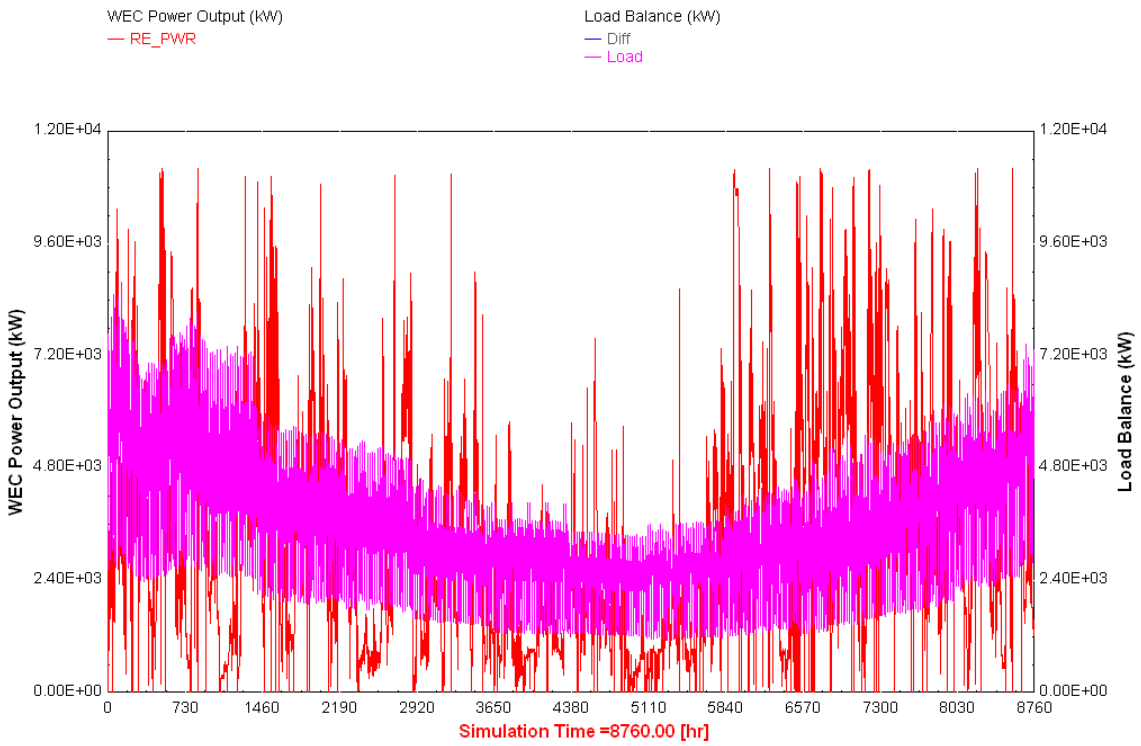

Figure 7.7 - Output of 15 Pelamis (US configuration) devices compared to Tofino/Ucluelet load

A plot of the penetration, Figure 7.8, for the same system with 15 US-Pelamis devices supports this claim. The maximum penetration level in this scenario is just under 32%, which is significantly better than in the case of the wind farm, where penetration at times theoretically exceeded 100%. However, given that any significant penetration to the grid can have a negative effect, 32% is still considerable, and further efforts should be made to reduce this penetration level as much as possible.

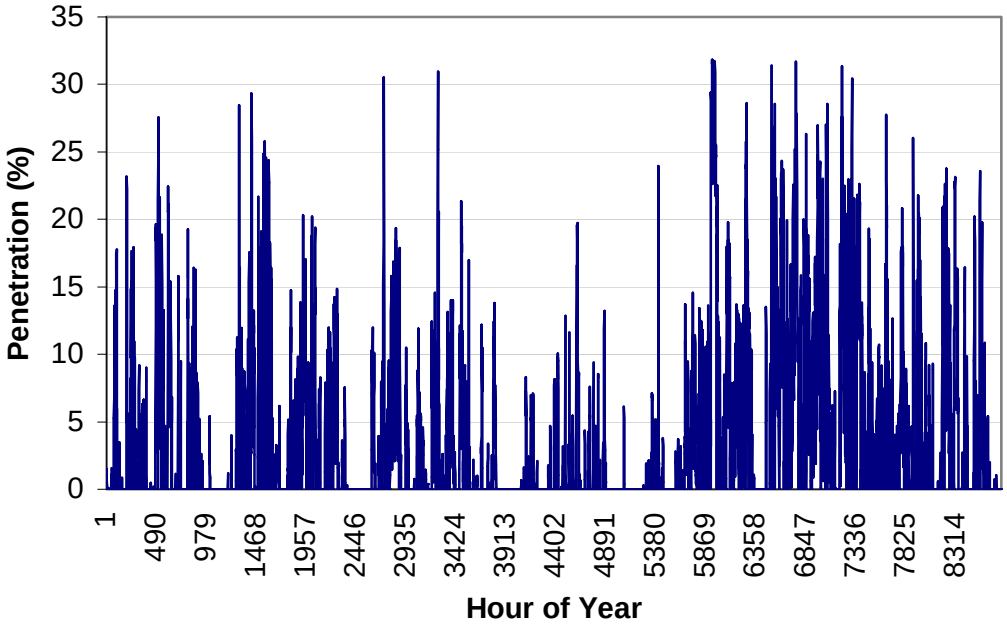

Figure 7.8 - Grid penetration for 15 US-Pelamis devices on 30 MVA grid

Table 7.2 shows a broad range of values for installed capacity, depending on the device. At the high end is the UK configuration of Pelamis, with approximately 17 MW of installed capacity required to service the Tofino/Ucluelet load, whose average demand is 3.4 MW. The high number of required Pelamis devices of UK configuration was anticipated, however, since the UK devices are tuned to different sea state conditions [91].

On the low end of installed capacity are the LIMPET and the Pelamis (US) devices, which both needed approximately 11 MW to service the Tofino/Ucluelet load.

Having a smaller installed capacity also means that in cases when the devices are at maximum output and the load is minimal, the difference between the two, which must be transferred to the grid, is lower. The penetration levels therefore are expected to be lower for the LIMPET and US-configuration Pelamis devices, and this expectation was supported by the simulation results, summarized in Table 7.3.

Device	Installed Capacity	Maximum Penetration (%)	Average Penetration (%)
Pelamis (UK Config.)	17 MW	51.5	3.9
Pelamis (US Config.)	11 MW	31.8	3.6
Energetech OWC	12 MW	35.2	4.0
LIMPET OWC	11 MW	31.5	3.8

Table 7.3 - Penetration values for WEC devices without storage

Table 7.4 gives the expected approximate dimensions of wave farms with the number of devices shown in Table 7.2. The Pelamis devices are spaced 150 m apart side by side, and 450 m apart end to end. [89] The Energetech OWCs are 35 m wide, and are also spaced 35 m apart. [62] The value for the LIMPET device is very approximate – the current LIMPET is 21 m wide and this is the value used for the calculation of the low end of the LIMPET range of dimensions. However, the power capture curves used for this simulation are for a future LIMPET device in the Faroe Islands, and its dimensions are not known. Wavegen has found, however, that a figure of 2-3 kW/m wavefront is the average electrical output for many devices that they have studied [83]. Ignoring storage and using the total requirement of the Tofino/Ucluelet area (30 GWh/year), the high figure in the LIMPET range of dimensions was obtained.

Device	Number of Devices	Dimensions of wave farm	Area (km^2)
Pelamis (UK Config.)	23	3300 m x 120 m 1050 m x 1260 m	0.40 1.32
Pelamis (US Config.)	15	2100 m x 150 m 600 m x 1650 m	0.32 0.99
Energetech OWC	12	805 m wide	--
LIMPET OWC	16	336 - 1700 m wide	--

Table 7.4 - Dimensions of WEC farms

In the case of the Pelamis devices, two sets of dimensions are given. The first corresponds to a case where the Pelamis devices are all in a single row, side by side. The second corresponds to a farm containing three rows of devices, or in other words a 5 x 3 matrix of US-type Pelamis devices, or an 8 x 3 matrix of UK-type devices. The OWCs do

not have calculated areas because the lengthwise dimension is negligible compared to the widthwide (side-by-side) dimension.

The number of devices which can be deployed without storage, given a maximum grid penetration limitation of 15%, is shown in Table 7.5. The corresponding value for the wind turbines from the previous section is also listed for comparison.

Device	Number	Installed Capacity
Pelamis (UK configuration)	8	6.0 MW
Pelamis (US configuration)	7	5.3 MW
Energetech OWC	5	5.0 MW
LIMPET OWC	8	5.3 MW
Enercon 40 600/46 Wind turbines (see Section 7.2)	10	6.1 MW

Table 7.5 - Number of devices permitted for maximum 15% grid penetration

When a grid penetration restriction is imposed, the WEC devices and the wind turbines do not differ significantly in the allowable installed capacity. Therefore, like wind farms, the WEC devices also require some form of storage to increase installed capacity while maintaining relatively low grid penetration.

From this point, knowing the size of the wave farm required, simulations were performed with system designs which included storage as a buffer between the renewable resource and the grid, with the goal of reducing penetration which servicing as much of the load as possible. Because the US Pelamis design fared better than the UK design in terms of number of devices required and penetration levels, the UK design was not considered in any further simulations.

7.4 Wave System with Energy Storage

The next step in the simulations was to add storage to the wave energy system. The major part of this work was to determine the response of the system to changes in both the overall storage capacity, and the maximum power input/output that the storage could

tolerate. Fortunately, in the VRB flow battery the two are independent of each other, and therefore each variable could be manipulated separately. The metrics used in the evaluation of the response were based on the grid penetration of the system, and this was further split into the yearly average penetration, and the maximum penetration – the highest one-hour penetration value seen in the simulation.

The simulations whose graphs are presented here were performed using the 15 US-configured Pelamis devices. The decision to use the Pelamis as the WEC for this simulation was based on the fact that it is the only one of the three which operates in deep water, and thus is the only one which does not have to contend with the uncertainty of the energy loss and wave behaviour of shallow waters off the coast of Ucluelet. Nevertheless, the results for the other two types of devices will be computed using the same process, and the final results of the storage requirements for all three devices will be tabulated at the end for comparison.

7.4.1 Varying Maximum Power Input to Storage

The first set of simulations were performed with the following conditions:

- Storage capacity was set to the total annual electricity generated by the wave farm – thus making it infinite for the purposes of the simulation
- No changes to load, wave resource, device type or number of devices
- Maximum input power to storage was the independent variable
- Average grid penetration and maximum grid penetration were the dependent variables

For each value of maximum input power to the storage device, the entire simulation was run, and the average and maximum grid penetrations over the course of the simulated year were calculated. These steps were repeated for all ten values of maximum input power. The resulting plots are shown in Figure 7.9 and Figure 7.11.

Note that the maximum input and the maximum output powers are assumed to be the same, so any subsequent mention of maximum power input also implies the maximum power output. This is based on the fact that VRB flow batteries can be charged at the same rate they are discharged [40].

Figure 7.9 shows the linear relationship between maximum grid penetration and the maximum power input level. As mentioned in Section 6.3, the maximum grid penetration is the single highest penetration value over the course of the entire year. Since none of the penetration in this set of simulations is due to storage being full, any hourly penetration is due to a limitation of the power input to the storage. This is illustrated for a sample of 10 hours in Figure 7.10. Any increase in the maximum power input to the storage is therefore matched by a corresponding decrease in the maximum penetration, producing the linear effect. The slight deviation from the linear between the last two values on the plot are due to the fact that the maximum penetration is reduced to zero at some point between 9 and 10 MW, but is only measured at a value of 10 MW.

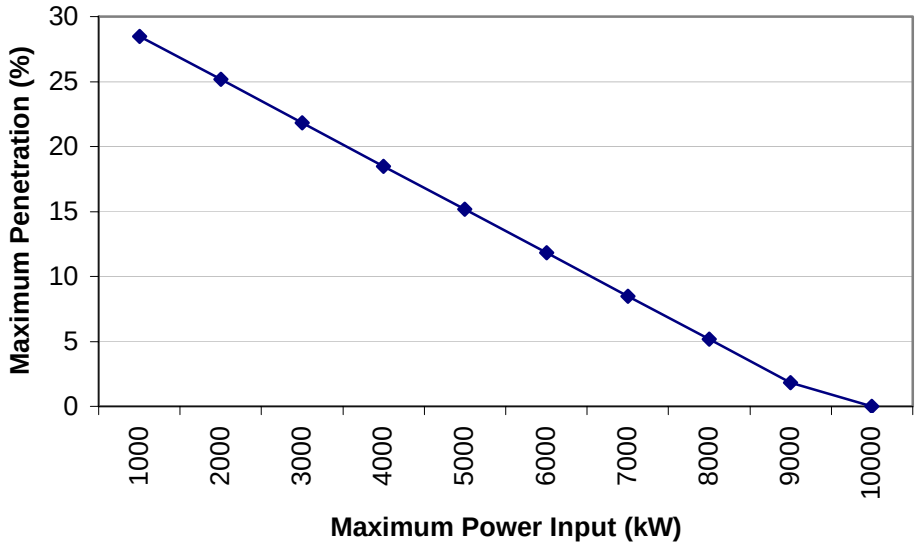

Figure 7.9 - Effect of maximum power input on maximum grid penetration

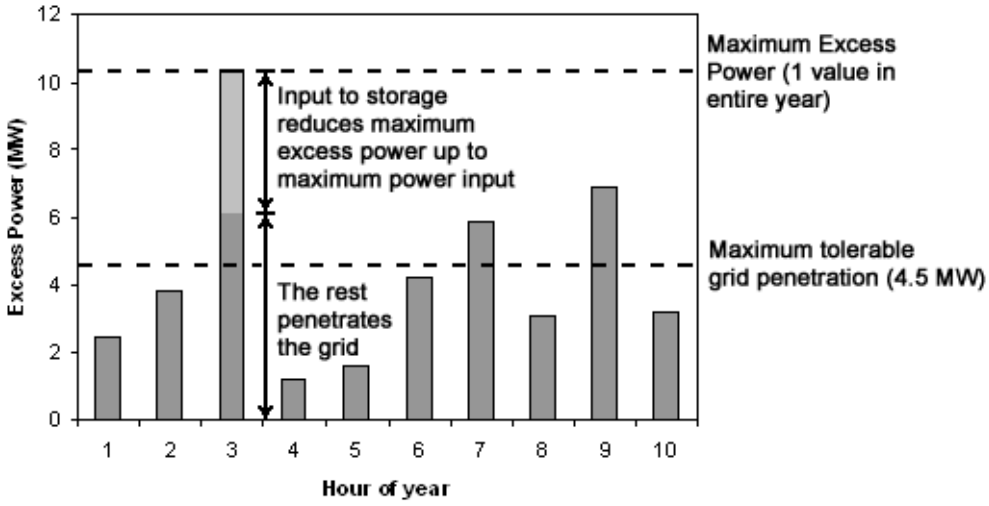

Figure 7.10 - Effect of maximum power input on grid penetration

While the situation with maximum penetration is relatively straightforward, Figure 7.11 demonstrates that the response of average penetration is entirely different. The original data shows an exponential decay relationship between the average grid penetration and the maximum input power tolerated by the storage component. More specifically:

$$AvgPenetration \propto \frac{1}{(MaxPowerInput)^4} \tag{7.1}$$

When the curve in Figure 7.10 is fitted with a 4th-order polynomial trendline, the R^2 value is unity, indicating a perfect fit.

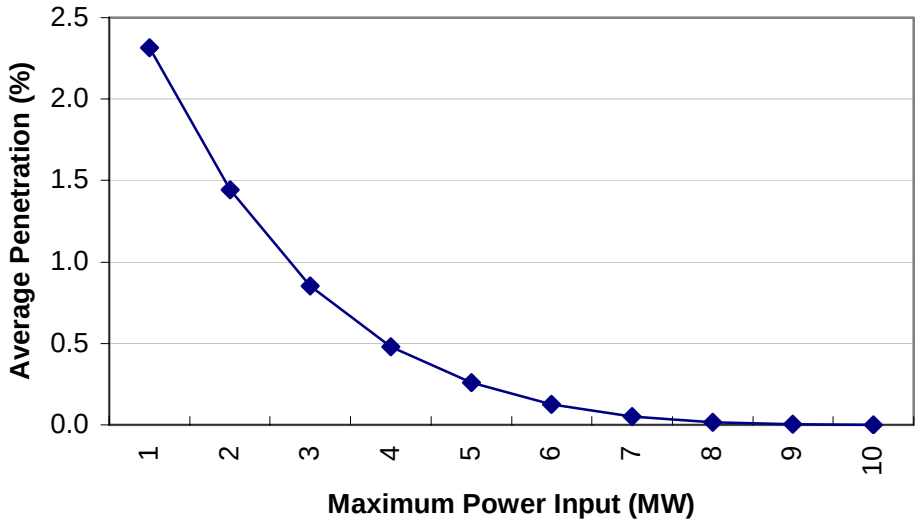

Figure 7.11 - Effect of maximum power input on average grid penetration

The conclusion from these results is that the maximum power input should be set to a level such that:

$$MaximumExcessPower - MaximumPowerInput \leq MaximumTolerableGridInput \quad (7.2)$$

With reference to Figure 7.10, this means that the maximum power input should be at least as large as the span between the two dashed lines. For Ucluelet's 30 MVA grid, the maximum tolerable input is 4.5 MVA, if 15% grid penetration is allowed. Also, increasing the storage size is originally highly beneficial in reducing grid penetration, but has diminishing returns as the maximum power input begins to approach the maximum excess power production.

The choice of maximum power input for the storage component, assuming technical feasibility, would mainly be constrained by the maximum penetration level as seen in Figure 7.9, in order not to exceed the maximum tolerable penetration set by the utility operating the grid. In this case, as described in Section 6.3, the maximum tolerable penetration is 15%.

7.4.2 Varying Storage Capacity

The second set of results looks at the effects of varying the storage capacity itself. In this case, the maximum power input was set high enough to be able to absorb the largest amount of excess power seen in the dataset, effectively making maximum power input infinite. The results in this case were quite different from those of the previous section. In Figure 7.12, the effect of the changing storage capacity on the maximum grid penetration level is shown to be relatively ineffective until a threshold level is hit, at which point the maximum grid penetration drops dramatically and quickly reduces to zero. The reason for this sharp drop only becomes clear in the plot of the state of charge of the storage component. The penetration occurs when the state of charge is at the maximum, and any attempt to add more energy results in grid penetration as the excess is redirected to the grid. It only takes a single hour for a reasonably large penetration to register. As soon as the storage becomes large enough to store that final amount of energy, a dramatic reduction in the maximum grid penetration is observed.

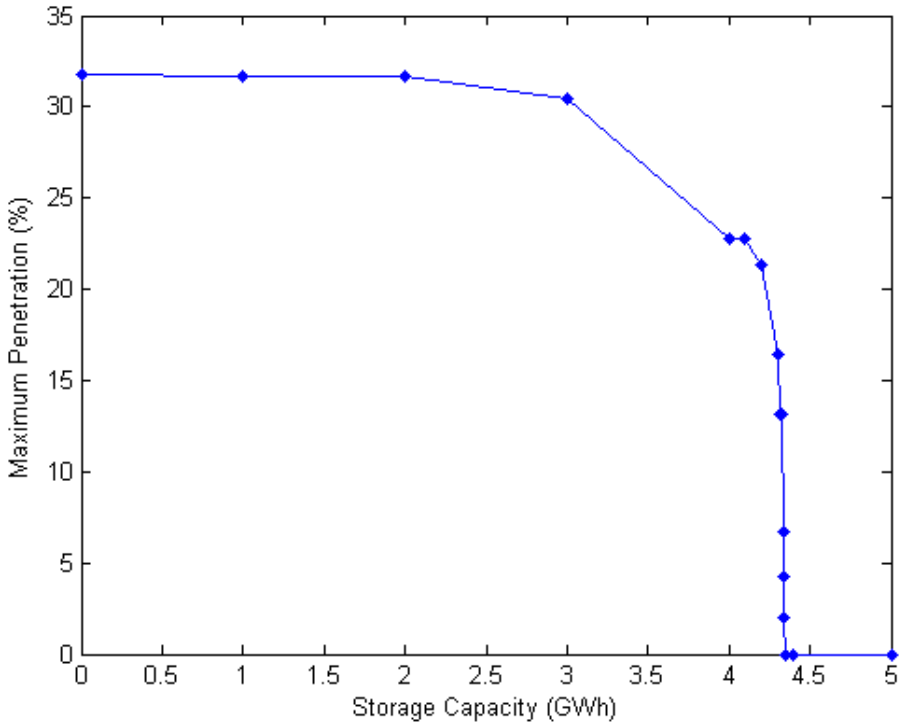

Figure 7.12 - Effect of storage capacity on maximum grid penetration

On the other hand, in Figure 7.13 which plots the relationship of storage capacity on the average grid penetration, a near-linear relationship is observed, except at the extremes of the graph. The sharp decrease in penetration between the values of 0 and 1 GWh of storage may indicate that a small amount of storage is sufficient to take care of most of the small-amplitude differences between the renewable energy produced and the load serviced. The larger levels of grid penetration, on the other hand, respond gradually and linearly to larger and larger storage capacities until there is enough capacity to absorb all the power that needs to be stored at any given hour during the year. In the case of this system, grid penetration is reduced to zero once the storage capacity is set at 4.345 GWh. Assuming the same penetration limit of 15% as in the previous section, and neglecting for the moment the effects of maximum power input, the minimum storage capacity should be 4.32 GWh, from Figure 7.12.

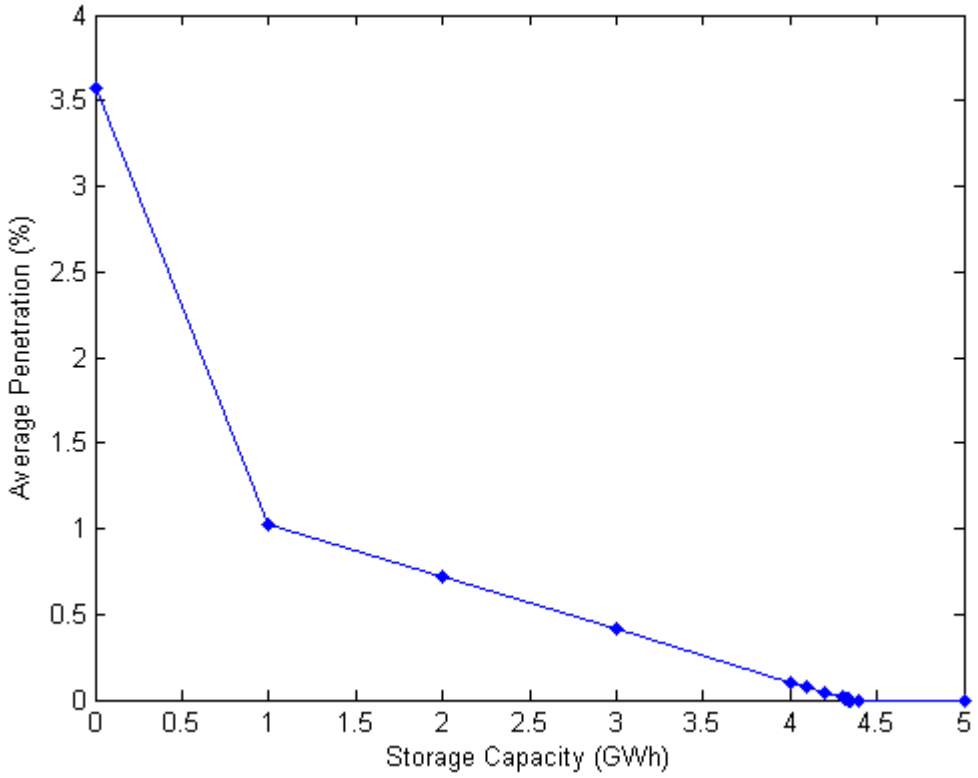

Figure 7.13 - Effect of storage capacity on average grid penetration

7.4.3 Optimizing the Storage Option

At this point, the effects of both storage capacity and maximum input power have been determined. The results from the previous two sub-sections were then simulated together, in order to eliminate the assumption that either storage capacity or maximum input power are infinite. Figure 7.14 shows the graph of the penetration over the course of the year, using a storage component whose maximum input power is 5.1 MW and whose storage capacity is 4.32 GWh.

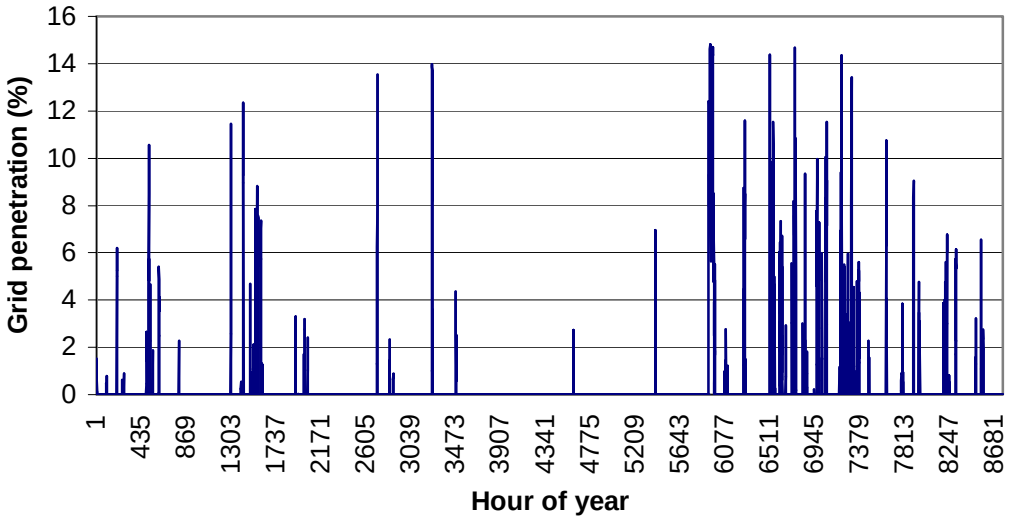

Figure 7.14 - Combined minimum storage capacity and maximum input power values

Since the storage capacity and maximum input power to this type of storage are independent, through the simulation illustrated in Figure 7.14, it was shown that satisfying each variable independently leads to a storage system that overall also satisfies the grid penetration condition. In the above example, the maximum penetration is 14.8%, with an average penetration of 0.24%.

Similar calculations were made for the LIMPET and Energetech OWCs. The results of these calculations are given in Table 7.6.

Device	Storage Capacity (GWh)	Maximum Power Input (MW)	Maximum Penetration (%)	Average Penetration (%)
Pelamis	4.32	5.1	14.8 (31.8)	0.24 (3.6)
Energetech OWC	5.96	6.1	14.9 (35.2)	0.35 (4.0)
LIMPET OWC	3.46	5.0	14.8 (31.5)	0.58 (3.8)

Table 7.6 - Summary of storage characteristics for each device (original values without storage given in parentheses)

Unsurprisingly, the storage system required for the Energetech OWC is the largest of the three, as the original penetrations (both average and maximum) were the highest of the three. The LIMPET OWC and the Pelamis storage requirements are similar, which is in keeping with their similar installed capacities.

To put these storage characteristics in perspective, it is useful to make a couple of comparisons. The maximum power input/output requirements for the WEC devices are approximately on the same scale as the nameplate capacities of BC Hydro's smallest hydroelectric facilities, such as the one at Shuswap Falls (5 MW). However, the storage capacity required by the WEC devices is much smaller than the average dependable capability of these hydro facilities, the smallest of which are 30 GWh [3].

While the storage capacity required may be an order of magnitude smaller than what is typical of a hydro facility, this storage capacity is at the same time well over three times as large as even the largest VRB flow batteries conceived of by VRB Systems, and over 20 times larger than the largest VRB actually built by that company [23]. These two facts build a case for the idea of pairing hydro and wave energy together. Rather than attempting to store as much of the excess wave-generated electricity in a storage device, a shorter-term, smaller storage could be used to even out fluctuations. With that, hydro electricity could be used at times when wave energy is not particularly abundant, such as in the summer, while wave energy could take over during the winter when an excess is usually available. Determining which proportions of storage to hydro dependence is not within the scope of this thesis, and is certainly intricately linked to project economics, but it certainly would be interesting to pursue for future work.

Another option would be to use a smaller storage and either implement a smaller WEC system, or shut down the WECs during periods of high seas, thus avoiding the high penetration levels seen at these times. Again, studying this option would involve extensive simulation and the development of a control strategy, and was thus beyond the scope of this thesis.

7.5 Summary

The results presented in this chapter indicate that the scale of a wave energy conversion system to service the Tofino/Ucluelet residential load range between 11 and 17 MW of installed capacity, depending on the device modelled. The amount of storage necessary to keep penetration below 15%, however, is nearly on the scale of a small hydroelectric facility. While this may be technically feasible, the next chapter gives a brief overview of the economics, which adds a new perspective to the feasibility of the project both with and without storage.

8 Economic Overview

8.1 Introduction

This chapter is a brief overview of the economics of wave energy conversion projects. It is not meant to be an in-depth analysis, but rather attempts to give a general idea of the scale of the project, and to estimate a ballpark figure for the cost of electricity, comparing this to the status quo of electricity sold by BC Hydro. The general assumptions are first listed, and a basic discounted cash flow analysis follows.

8.2 General Assumptions

Several assumptions were made in this study to simplify the calculations and accommodate uncertainties. These are described in the list below.

- An **8% nominal discount rate** is used. This is the figure used in the UK for its public sector investments, [11] and BC Hydro used the same number in its Vancouver Island Generation Project (VIGP) Call for Tenders [120].
- The **exchange rate** for conversion of $US to $CDN is assumed to be a constant 1.2096, which is the March 31, 2005 value quoted by the Receiver General for Canada [121].
- The **capital costs** are assumed to all be incurred in one lump sum rather than spread out over multiple years.
- **Inflation** is assumed to be 2.1% per annum [120]. This gives a real discount rate of 5.8%.
- **No externalities** (e.g., costs associated with visibility impact, noise, and the like) are included in the cost, as their estimation is vague at best, even with established technologies [11].
- The **lifetime of the project** is assumed to be 20 years, in line with BC Hydro's original estimate for an Energetech wave energy project near Ucluelet [12].

- No **subsidies** are included, nor are **income taxes**. This means that it is assumed that this project is carried out by BC Hydro, which does not pay taxes, as opposed to independent power producers (IPPs), which do [122].
- **Operation and Maintenance (O&M)** are assumed to be 1.5% of the capital cost annually, which is another assumption used by BC Hydro in its Ucluelet wave project study. [12] While van Bussel [75] estimates a much higher figure of up to 25% for offshore wind farms, there is no evidence at this point that wave energy converters are subject to such high O&M costs. Once more commercial wave farms are in operation, it is likely possible to get a better estimate for this figure. Until then, the BC Hydro figure will be used.
- All figures will be given in **2004$**, as many of the useful figures for this study come from two reports by the EPRI, [62, 89] both of which use 2004$.
- The electrical output of the devices are considered to be steady over the years – no variation in output is taken into account at this stage. Harrison et al. [123] suggest that global warming could contribute to an increase in wave power and a corresponding decrease in the unit cost of wave energy, but until the rate of change of wave energy can be quantified, this cannot be included in this type of analysis.

Now that the general assumptions used in this assessment have been identified, the following section presents the analysis of wave energy in which these assumptions are used. Several specific assumptions were made regarding particular values in the analysis, and these will be noted as they become important in the next section.

8.3 Discounted Cash Flow Analysis

A discounted cash flow analysis was performed for both the Pelamis and the Energetech OWC options. Little information is available for the costs associated with the LIMPET OWC, and it was therefore left out of this analysis.

Table 8.1 summarizes the discounted cash flow analysis for the Pelamis system disregarding storage, which will be dealt with separately afterwards. Many of the values used to obtain the total plant cost, the O&M, and the overhaul cost are based on those from the study done by EPRI on a potential system for San Francisco [89]. Since the San Francisco system consists of 213 devices, while only 15 are necessary for the Ucluelet/Tofino area, most of the values were scaled proportionally. The transmission/grid interconnection and facilities costs, however, remained the same, as they would not be divisible by unit.

Description of factor	Value ($CDN)
Total plant cost (Capital cost + installation, management)	$ 38,652,000
Overhaul and replacement cost, net present value	$ 2,405,000
Total of one-time costs (total plant cost + overhaul)	$ 41,057,000
Annuitized value of one-time costs	$3,516,000
Annual operation and maintenance (O&M)	$1,766,000
Total cost per year (annual payments + O&M)	$5,281,000
Amount of energy produced per year (kWh)	29,800,000
Cost in $/kWh	**$0.18**
Cost in $/kWh if O&M is simply assumed 1.5% capital cost	$0.14

Table 8.1 - Summary of discounted cash flow analysis on Pelamis wave farm

The last line in the table makes reference to BC Hydro's original calculations, where the O&M costs were assumed to be 1.5% of the total plant cost. However, when the O&M costs were further broken down by EPRI in their study of the San Francisco area, the O&M costs worked out to be higher, approximately 4.5%. Currently, since no large commercial wave farms exist, this value will be very approximate until real data can prove what the operating costs of a wave farm might be. Therefore, depending on which values are used, and using the numbers provided by EPRI, the cost of electricity from a bank of 15 Pelamis devices near Ucluelet would be between $0.14 and $0.18.

The same calculations were done for the case of 12 Energetech devices. Once again, most of the figures are adapted from the EPRI report where a hypothetical wave farm was proposed for the San Francisco area [62]. The results for Ucluelet are shown in Table 8.2.

Description of factor	Value ($CDN)
Total plant cost (Capital cost + installation, management)	$ 40,321,000
Overhaul and replacement cost, net present value	$ 1,401,000
Total of one-time costs (total plant cost + overhaul)	$ 41,721,000
Annuitized value of one-time costs	$3,572,000
Annual operation and maintenance (O&M)	$1,797,000
Total cost per year (annual payments + O&M)	$5,370,000
Amount of energy produced per year (kWh)	29,800,000
Cost in $/kWh	**$0.18**
Cost in $/kWh if O&M is simply assumed 1.5% capital cost	$0.14

Table 8.2 – Summary of discounted cash flow analysis on Energetech wave farm

Interestingly, both the Pelamis and the Energetech options work out to the same cost of $0.14 to $0.18 per kWh. These are well above the BC Hydro rates of $0.06 per kWh, though a direct comparison cannot be made without considering all factors such as subsidies.

In the wave energy figures quoted above, the costs of storage have yet to be considered. If the VRB flow battery storage is used, as assumed in the simulations, its cost must be factored into the system cost. Table 8.3 gives an overview of the basic costs of a VRB storage system. The figures used in these calculations come from VRB Power Systems, converted to Canadian dollars [40, 124].

Description of Factor	Value ($CDN/kWh)
Capital costs of VRB system	$410
Cost of disposal, adjusted to net present value	$118 - $255
Operation and Maintenance (O&M) annual cost	$0.01
Total fixed, one-time costs	$528 - $665

Table 8.3 - Unit costs, per kWh, for VRB storage

One more assumption was used in the calculations specifically to storage. As mentioned in the simulation and results chapters, the storage capacity and the maximum power input/output to the VRB are independent of each other, and the sizing of the storage is dependent on finding values for both these characteristics. However, the costs of a VRB system are given only in terms of storage capacity; therefore, the assumption is that the

costs associated with including a large enough maximum power input are included in the storage capacity costs, as the figure given is for the whole system and not just the electrolyte itself. Table 8.4 illustrates the calculations made only for the best case scenario, i.e., the smallest storage capacity required by any of the devices in the storage simulations. In this case, it is the Pelamis devices, at 4.32 GWh (4.3×10^6 kWh) which require the smallest storage.

Description	Unit Cost ($CDN)	Value ($CDN)
Storage cost, with most expensive disposal	$665 / kWh	$2,870,000,000
Storage cost, with cheapest disposal	$528 / kWh	$2,280,000,000
Storage cost, ignoring disposal	$410 / kWh	$1,770,000,000
Cheapest of the three options: no disposal	$410 / kWh	$1,770,000,000
Annuitized over 20 year project lifespan	--	$152,000,000/year
Total annual cost of Pelamis with storage	--	$157,000,000/year
Cost per kWh, assuming 29.8 GWh/year	--	**$5.27 / kWh**

Table 8.4 - Costing the storage option for the Pelamis devices

Adding VRB storage leads to a massive increase of nearly 30 times the original cost without the storage, and this is the best-case scenario, where disposal costs are entirely omitted and the smallest storage is used. The largest storage, required by the Energetech device, would lead to a cost of over $11 per kWh. Including the cost of disposal would significantly raise the cost again.

8.4 Summary

From these calculations, it is conceivable that with subsidies, process improvement, and economies of scale, wave energy conversion could eventually become competitive with other forms of energy generation. However, attempting to use storage such as a VRB to buffer such a system with a constraint of 15% maximum grid penetration would be highly impractical, both technically and financially. Therefore, the possibility of using wave energy in conjunction with hydroelectric facilities, as mentioned at the end of Chapter 7, merits further investigation.

9 Conclusions

The object of this study was to determine how much wave power can feasibly be converted for use in servicing the residential load in the Tofino/Ucluelet area of Vancouver Island, and the impacts of such an undertaking in terms of infrastructure. To generate useful information which could be used to answer the question, the problem was broken down into three main sections.

First of all, the magnitude of the energy resources available and the load to be serviced were determined. BC Hydro's real monthly data for the Tofino/Ucluelet area loads were combined with the hourly load of a typical coastal BC residence in order to generate hourly data for the entire area. The residential load was chosen for its similarity to the resource profile of wave energy, which is higher in winter and lower in summer. The wave resource was determined by using data collected from an Environment Canada buoy at La Perouse Bank, approximately 34 km off the coast of Ucluelet. At a depth of approximately 75 m, this buoy is considered to be in deep water and the measurements are thus directly used to determine wave power for deep water devices such as the Pelamis. For shallow or shoreline devices, such as the OWCs, the wave height values were modified such that the calculated wave power was one-half its original value. This 50% figure is an estimate for the amount of energy dissipation as the water enters shallow water.

Three types of wave energy conversion devices were studied – the Pelamis "sea snake", which uses the flexion of its joints and hydraulics to produce electricity, and two types of OWCs – the LIMPET, which is one of the older research projects in wave energy conversion, as well as the Energetech OWC, a device which is just entering the commercialization stage. Models of these devices were used in system simulation in the TRNSYS software. A system model using wind energy was also run in TRNSYS, in order to give a baseline comparison with a better-known technology. A storage component model was later developed, to be used as a buffer between the irregular output of the WECs and the grid, which can be sensitive to the large power swings.

Finally, the economics of wave energy projects and the associated storage were briefly examined in broad terms. While the analysis is far from rigorous and many uncertainties exist in the figures, the purpose was to determine a ballpark figure for the cost of electricity generated from wave energy.

9.1 Conclusions from Simulations

9.1.1 Key Findings for Model Scenarios

The following conclusions are specific to the scenarios modelled in the simulations.

1. The installed capacity of wind turbines required to service the load was found to be 32 MW, while the installed capacity required for WECs was between 5 and 17 MW, depending on the device. Furthermore, while the grid penetration for the wind-only system at times exceeded 100%, the worst-case scenario for wave energy was just over 50%.

2. Despite having lower grid penetration than wind, the grid penetration levels for wave are still unacceptable. Acceptable values vary, but are usually in the range of 10-20%. Therefore, in order to have a wave power generation facility capable of producing enough electricity to service the entire Tofino/Ucluelet residential load, some form of energy storage is necessary.

3. With maximum grid penetration constrained to 15%, the system storage capacity required was between 3.46 and 5.96 GWh. These values are larger than any VRB ever built and the maximum input/output powers were in the range of some of the nameplate capacities of BC Hydro's smallest hydroelectric facilities.

   The maximum input/output power was found to be directly dependent on the

single largest hourly penetration value in the dataset, while the storage capacity was generally linearly dependent on the average grid penetration.

4. Using VRB storage as a buffer between the WEC devices and the grid is economically infeasible at this scale. Options include coupling the WEC farm with hydroelectric facilities, or reducing the scale of the WEC system.

9.1.2 General Wave Energy Conclusions

1. The residential load profile for temperate areas such as Vancouver Island correlates well with the wave energy resource availability, as both peak in the winter months. Wave energy is therefore a good candidate for servicing residential loads in this area.

2. The cost of wave energy (without storage) was found to be high, but not unreasonable, being in the range of $0.14 - $0.18 per kWh. This is high compared to BC Hydro's rates of $0.06 per kWh, but these cannot be directly compared due to differences in assumptions, particularly relating to possible government subsidies for renewable energy.

9.1.3 Conclusions Regarding Model

Several issues have been identified with the model, which would need to be overcome to develop more accurate information on which to base decisions.

1. Wave data for shallow water should be collected at any specific location where a shallow-water (or shoreline) WEC device installation is proposed. It would be beneficial to know the wave climate characteristics more exactly before beginning simulations or other preparation for a project of that nature, to reduce the number

of assumptions and approximations.

2. Experimental power capture curves for full-scale devices would be useful to obtain more accurate predicitions of device behaviour. Difficulties in comparing devices occurred in this research due to availability of power capture data, particularly experimental data. This lack of data is due to the small number of existing WEC devices, as well as the proprietary nature of information on commercial or pre-commercial devices.

9.1.4 Summary

Given the above conclusions, and keeping in mind the shortcomings, it can be concluded that while wave energy conversion technologies are nowhere near mature, a significant potential exists for the extraction of wave energy off the coast of Vancouver Island for a relatively reasonable cost. However, the problem of finding reasonable and compatible storage remains, and should be an important factor in any decisions to implement large-scale wave energy projects.

9.2 Future Work

This thesis has been a first step in determining the viability of wave power on Vancouver Island, but there is still much work that can and should be done before wave energy projects should proceed. First and foremost, as mentioned in the previous section, storage is an important issue, and further study is required to determine solutions which are both possible and economically viable.

The economic analysis was not a focus of this thesis, and since the attractiveness of this type of project to investors is highly dependent on its economics, it is important to conduct a more thorough and detailed investigation into the costs and sensitivies of the factors contributing to the overall cost of electricity produced from wave energy.

The wave climate in the area, while quantified somewhat in this thesis, could use a detailed investigation into shallow-water behaviour, as well as further study regarding the changes of the wave climate over a number of years.

None of these hurdles should prevent Vancouver Island from someday tapping into its 8.25 TW of average wave energy. However, one final important factor which should not be overlooked but is beyond the scope of this thesis is energy policy. No wave energy projects are currently on the drawing board in Canada, and it is up to engineers, policy makers, economists, and a variety of others from multiple disciplines to come together and find a way to make it happen.

References

[1] "2001 Census Profile of British Columbia's Regions: Vancouver Island," BC Stats [Online document], [cited 2005, August 30], Available HTTP: http://www.bcstats.gov.bc.ca/data/cen01/profiles/VanIslnd.pdf.

[2] "Resource Expenditure and Acquisition Plan," BC Hydro, Vancouver March 7 2005.

[3] "Making the Connection: The BC Hydro Electric System and How it is Operated," BC Hydro 1995.

[4] "Response to Staff Information Request No. 1.7.3.," Vancouver Island Energy Corporation [Online document], [cited 2005, February 23], Available HTTP: http://www.bchydro.com/rx_files/vigp/vigp5010.pdf.

[5] "Vancouver Island Transmission Reinforcement Project: Project Description," British Columbia Transmission Corporation (BCTC) [Online document], [cited 2005, February 28], Available HTTP: http://www.eao.gov.bc.ca/epic/output/documents/p250/d19554/1107276158426_ae8fa289472b4ae8a982c94c9f97a3ac.pdf.

[6] "Vancouver Island Generation Project: Major Capital Project Plan," BC Hydro [Online document], [cited 2005, February 28], Available HTTP: http://www.bchydro.com/rx_files/info/info4484.pdf.

[7] "Vancouver Island Generation Project," BC Hydro [Online document], [cited 2005, February 23], Available HTTP: http://www.bchydro.com/info/vigp/vigp1002.html.

[8] "Order E-1-05," British Columbia Utilities Commission (BCUC) [Online document], [cited 2005, February 28], Available HTTP: http://www.bcuc.com/Documents/Orders/2005/DOC_6941_E-1-05_BCH%20VICFT%20Electricity%20Purchase%20Agrmnt.pdf.

[9] "Continued appeals force BC Hydro to abandon Duke Point Power Project," BC Hydro [Online document], [cited 2005, June 20, 2005], Available HTTP: http://www.bcuc.com/Documents/Proceedings/2005/DOC_7723_B-8_CFT%20News%20Release.pdf.

[10] "Hydro becalms 'green' wave-power project," Independent Power Producers' Association of British Columbia (IPPBC) [Online document], [cited 2005, February 28], Available HTTP: http://www.ippbc.com/329/1588.

[11] G. Boyle, *Renewable Energy: Power for a Sustainable Future*. Oxford: Oxford University Press, 1996.

[12] *2004 Integrated Electricity Plan. Part 3: Resource Options*: BC Hydro, 2003.

[13] "AXYS Environmental Systems Signs Agreement with BC Hydro to Monitor Ocean Wave Potential off Vancouver Island, B.C. (Press Release)," Axys Environmental Systems [Online document], February 13, 2002, [cited 2004, August 2], Available HTTP: http://www.axystechnologies.com/news/feb_2002_bc_hydro_partnership_release.pdf.

[14] "Media - What's New," Energetech Australia Pty Ltd. [Online document], 2004, [cited 2004, August 2], Available HTTP: http://www.energetech.com.au/index.htm?http://www.energetech.com.au/content/new.html.

[15] "British Columbia Utilities Commission Information Request No. 1.2.10," BC Hydro [Online document], January 23, 2004, [cited 2004, June 15], Available HTTP: http://www.bchydro.com/reg_files/rev_reqs_bch/bcuc_1_002_10.pdf.

[16] T. Thorpe, "Ocean Wave Energy: Energetech," presented at 5th BASE International Investment Forum, Bonn, Germany, June 2004.

[17] "Vancouver Island Map," Tourism Victoria [Online document], 2004, [cited 2004, August 1], Available HTTP: http://www.tourismvictoria.com/Content/EN/1070.asp.

[18] A. Westwood, "Ocean power: Wave and tidal energy review," *Refocus*, vol. 5, pp. 50-55, 2004.

[19] S. H. Salter, "Wave Power," *Nature*, vol. 249, pp. 720-724, 1974.

[20] J. P. Kofoed, P. Frigaard, E. Friis-Madsen, and H. C. Sorensen, "Prototype Testing of the Wave Energy Converter Wave Dragon," presented at World Renewable Energy Congress VIII (WREC 2004), 2004.

[21] Y. Washio, H. Osawa, and T. Ogata, "The open sea tests of the offshore floating type wave power device "Mighty Whale" -characteristics of wave energy absorption and power generation," 2001.

[22] T. W. Thorpe, "A Brief Review of Wave Energy," ETSU-R120, 1999.

[23] "Corporate Brochure," VRB Power Systems Incorporated [Online document], [cited 2005, September 11], Available HTTP: http://www.vrbpower.com/pdfs/VRB%20Corporate%20Brochure.pdf.

[24] A. Shibata, S. Kanji, and M. Nakajima, "Development of vanadium redox flow battery for photovoltaic generation system," 1994.

[25] S. Miyake and N. Tokuda, "Vanadium redox-flow battery for a variety of applications," 2001.

[26] S. Miyake, "Vanadium Redox-Flow Battery (VRB) for a Variety of Applications," Sumitomo Electric Industries, Ltd. [Online document], [cited 2005, September 11], Available HTTP: http://www.electricitystorage.org/pubs/2001/IEEE_PES_Summer2001/Miyake.pdf.

[27] "The VRB Energy Storage System - A Case Study in Utility Network Planning Alternatives," VRB Power Systems Incorporated [Online document], [cited 2005, May 12], Available HTTP: http://www.vrbpower.com/pdfs/VRB-ESS%20-%20Case%20Study%20Rural%20Feeder.pdf.

[28] "Application Note: Vanadium Redox Flow Battery - Key Features," HILTech Developments Limited [Online document], [cited 2005, September 11], Available HTTP: http://www.hiltechdevelopments.com/downloads/vanadium_redox.pdf.

[29] A. Bergen, N. Djilali, L. Pitt, A. Rowe, and P. Wild, "Renewable Regenerative Energy Systems: Practical Integration Challenges," presented at International Green Energy Conference, Waterloo, Ontario, 2005.

[30] K. Agbossou, M. L. Kolhe, J. Hamelin, E. Bernier, and T. K. Bose, "Electrolytic hydrogen based renewable energy system withoxygen recovery and re-utilization," *Renewable Energy*, vol. 29, pp. 1305-1318, 2004.

[31] A. Mills and S. Al-Hallaj, "Simulation of hydrogen-based hybrid systems using Hybrid2," *International Journal of Hydrogen Energy*, vol. 29, pp. 991-999, 2004.

[32] B. Sørensen, A. Hauge Petersen, C. Juhl, H. Ravn, C. Sondergren, P. Simonsen, K. Jorgensen, L. Henrik Nielsen, H. V. Larsen, and P. Erik Morthorst, "Hydrogen as an energy carrier: scenarios for future use of hydrogen in the Danish energy system," *International Journal of Hydrogen Energy*, vol. 29, pp. 23-32, 2004.

[33] S. R. Vosen and J. O. Keller, "Hybrid energy storage systems for stand-alone electric power systems: optimization of system performance and cost through control strategies," *International Journal of Hydrogen Energy*, vol. 24, pp. 1139-1156, 1999.

[34] Z. Yumurtaci and E. Bilgen, "Hydrogen production from excess power in small hydroelectric installations," *International Journal of Hydrogen Energy*, vol. 29, pp. 687-693, 2004.

[35] S. Gair, "Hydrogen on the Isle of Islay (Personal communication)," 2005.

[36] "Exploring Vancouver Island's Energy Future: A Workshop with BC Hydro and Rocky Mountain Institute," Rocky Mountain Institute 2003.

[37] E. D. Castronuovo and J. A. P. Lopes, "Optimal operation and hydro storage sizing of a wind-hydro power plant," *International Journal of Electrical Power & Energy Systems*, vol. 26, pp. 771-778, 2004.

[38] B. Sørensen, *Renewable Energy*. London: Academic Press, 2000.

[39] M. Perrin, Y. M. Saint-Drenan, F. Mattera, and P. Malbranche, "Lead-acid batteries in stationary applications: competitors and new markets for large penetration of renewable energies," *Journal of Power Sources*, vol. 144, pp. 402-410, 2005.

[40] "The VRB Energy Storage System - A Comparison with Lead-Acid Batteries," VRB Power Systems Incorporated [Online document], [cited 2005, May 12], Available HTTP: http://www.vrbpower.com/pdfs/VRB-ESS%20%20%20Lead%20Acid%20Comparison.pdf.

[41] D. Anderson and M. Leach, "Harvesting and redistributing renewable energy: on the role of gas and electricity grids to overcome intermittency through the generation and storage of hydrogen," *Energy Policy*, vol. 32, pp. 1603-1614, 2004.

[42] J. K. Jensen, "A Balancing Act: What demands does wind power make on a grid?" *Renewable Energy World*, vol. September-October, pp. 57-69, 2002.

[43] P. A. Østergaard, "Modelling grid losses and the geographic distribution of electricity generation," *Renewable Energy*, vol. 30, pp. 977-987, 2005.

[44] H. Bindner and P. Lundsager, "Integration of wind power in the power system," 2002.

[45] D. Weisser, R.S. Garcia, "Instantaneous wind energy penetration in isolated electricity grids: concepts and review," *Renewable Energy*, vol. 30, pp. 1299-1308, 2005.

[46] R. K. Jardan, I. Nagy, T. Nitta, H. Ohsaki, "Power factor correction in a turbine-generator-converter system," *Conference Record - IAS Annual Meeting (IEEE Industry Applications Society)*, vol. 2, pp. 894-900, 2000.

[47] S. N. Liew, G. Strbac, "Maximizing penetration of wind generation in existing distribution networks," *IEE Proceedings on Generation, Transmission and Distribution*, vol. 149, pp. 256-262, 2002.

[48] J. O. G. Tande, "Grid Integration of Wind Farms," *Wind Energy*, vol. 6, pp. 281-295, 2003.

[49] A. F. d. O. Falcao, "Control of an Oscillating-Water-Column Wave Power Plant for Maximum Energy Production," *Applied Ocean Research*, vol. 24, pp. 73-82, 2002.

[50] I. Glendenning, "Wave Power - A Real Alternative?" *Ocean Management*, vol. 4, pp. 207-240, 1978.

[51] "Islay LIMPET Project Monitoring Final Report," Wavegen. ETSU V/06/00180/00/Rep, 2002.

[52] N. I. Meyer, Nielsen, K., "The Danish Wave Energy Programme Second Year Status (2000)," [Online document], [cited Available HTTP: http://www.waveenergy.dk/wave_forside/4english/papers/paper_aau00.pdf.

[53] R. R. T. Stallard, A. Bradshaw, and G. Aggidis, "Comparison of Equivalent Capacity Wave Energy Schemes," presented at World Renewable Energy Congress (WREC), Aberdeen, Scotland, 2005.

[54] "Results from the European Thematic Network on Wave Energy," WaveNet: Energy, Environment and Sustainable Development (EESD) ERK5-CT-1999-20001, 2003.

[55] M. L. Khandekar, *Operational Analysis and Prediction of Ocean Waves*. New York: Springer-Verlag, 1989.

[56] R. M. Sorensen, *Basic Coastal Engineering*. New York: John Wiley & Sons, Inc., 1978.

[57] B. LeMéhauté, *An Introduction to Hydrodynamics & Water Waves*. New York: Springer-Verlag, Inc., 1976.

[58] E. W. Weisstein, "Scienceworld - Wavenumber," Wolfram Research [Online document], [cited 2005, March 31], Available HTTP: http://scienceworld.wolfram.com/physics/Wavenumber.html.

[59] R. H. Stewart, "Introduction to Physical Oceanography," Department of Oceanography, Texas A&M University [Online document], [cited 2005, June 1], Available HTTP: http://oceanworld.tamu.edu/resources/ocng_textbook/contents.html.

[60] N. F. Barber, *Water Waves*. London: Wykeham Publications Ltd., 1969.

[61] R. M. Sorensen, *Basic Wave Mechanics: For Coastal and Ocean Engineers*. New York: John Wiley & Sons, Inc., 1993.

[62] M. Previsic, R. Bedard, G. Hagerman, O. Siddiqui, "System Level Design, Performance and Costs - San Francisco California Energetech Offshore Wave Power Plant," Global Energy Partners, LLC., E2I EPRI -- 006B - SF, 2004.

[63] C. Song, A.I. Sirviente, "A Numerical Study of Breaking Waves," *Physics of Fluids*, vol. 16, pp. 2649-2667, 2004.

[64] M. S. Kabdasli, U. Türker, "The wave breaking phenomena as a tool for environmental friendly shore protection," *Water Science and Technology*, vol. 46, pp. 153-160, 2002.

[65] W. K. Melville, P. Matusov, "Distribution of Breaking Waves at the Ocean Surface," *Nature*, vol. 417, pp. 58-63, 2002.

[66] "Search and Rescue - SAR Seamanship Reference Manual - Chapter 8," Canadian Coast Guard, Fisheries and Oceans Canada [Online document], [cited 2005, August 1], Available HTTP: http://www.ccg-gcc.gc.ca/sar/nsm-msn/ichapter_08_e.htm.

[67] R. Nicoll, "EOS 530 Final Report: Ocean Wave Energy Extraction near Vancouver Island, Canada," University of Victoria 2004.

[68] M. Previsic, R. Bedard, G. Hagerman, and O. Siddiqui, "System Level Design, Performance, and Costs - Oregon State Offshore Wave Power Plant," Global Energy Partners, LLC. E2I EPRI Global -- WP - 006 -- OR Rev 1, 2004.

[69] "Fisheries and Oceans Canada - Marine Environmental Data Services - Wave Data for C46206," [Online document], [cited 2005, August 28], Available HTTP: http://www.meds-sdmm.dfo-mpo.gc.ca/meds/Databases/Wave/idxMAP/DownLoadData_e.asp?medsid=C46206.

[70] R. E. Thomson, and S.E. Allen, "Time series acoustic observations of macrozooplankton diel migration and associated pelagic fish abundance," *Canadian Journal of Fisheries and Aquatic Sciences*, vol. 57, pp. 1919-1931, 2000.

[71] "Fisheries and Oceans Canada, Marine Environmental Data Services - CSV Format Description for Wave Data," [Online document], [cited 2005, August 28], Available HTTP: http://www.meds-sdmm.dfo-mpo.gc.ca/meds/Databases/Wave/Products/csv_e.htm.

[72] T. J. T. Whittaker, W. Beattie, S. Raghunathan, A. Thompson, T. Stewart, and R. Curran, "The Islay Wave Power Project: An Engineering Perspective," *Proceedings of the Institution of Civil Engineers, Water Maritime and Energy*, vol. 124, pp. 189-201, 1997.

[73] "Tide and Water Level," Fisheries and Oceans Canada, Marine Environmental Data Services [Online document], [cited 2005, August 27], Available HTTP: http://www.meds-sdmm.dfo-mpo.gc.ca/meds/databases/TWL/TWL_e.htm.

[74] G. J. W. v. Bussel, and C. Schöntag, "Operation and Maintenance Aspects of Large Offshore Windfarms," Institute for Wind Energy, Delft, Holland IW-98135, 1998.

[75] G. J. W. v. Bussel, "The Development of an Expert System for the Determination of Availability and O&M Costs for Offshore Wind Farms," Institute for Wind Energy, Delft, Holland IW-99155R, 1999.

[76] P. Osborne, "Electricity from the Sea," Fujita Corporation [Online document], July 2000, [cited 2004, August 2], Available HTTP: http://www.fujitaresearch.com/reports/tidalpower.html.

[77] S. Raghunathan, "The Wells Air Turbine for Wave Energy Conversion," *Progress in Aerospace Sciences*, vol. 31, pp. 335-386, 1995.

[78] T. J. T. Whittaker, "Learning from the Islay Wave Power Plant," presented at IEE Colloquium on Wave Power; An Engineering and Commercial Perspective, 13 March 1997.

[79] Wavegen, "Islay Limpet Project Monitoring Final Report," ETSU V/06/00180/00/Rep, 2002.

[80] "High-Resolution Image of LIMPET Plant," Department of Trade and Industry (DTI) UK [Online document], 2004, [cited 2004, August 2], Available HTTP: http://www.dti.gov.uk/renewable/hires/Completed_LIMPET.jpg.

[81] QUB, "Islay LIMPET Wave Power Plant," JOR3-CT98-0312, 2002.

[82] "Wavegen," Wavegen [Online document], [cited 2005, September 1], Available HTTP: http://www.wavegen.co.uk.

[83] T. Heath, "LIMPET Power Capture (personal communication)," September 30, 2005.

[84] "Portugal - Extract from the Survey of Energy Resources 2001," World Energy Council [Online document], 2003, [cited Available HTTP: http://www.worldenergy.org/wec-geis/edc/countries/Portugal.asp.

[85] H. C. Soerensen, L. K. Hansen, and R. Hansen, "Final Report - Planning," European Thematic Network on Wave Energy, Copenhagen, Denmark NNE5-1999-00438, 2003.

[86] "Introduction - Shoreline OWC Pilot Plant on the Island of Pico/Azores," Maretec Wave Energy [Online document], [cited 2004, August 3], Available HTTP: http://hidrox.ist.utl.pt/maretec/wave_energy/intro/intro05_e.htm.

[87] "Energetech: Technology," Energetech Australia Pty Ltd. [Online document], 2004, [cited 2004, August 4], Available HTTP: http://www.energetech.com.au/content/tech.html.

[88] "Initial Port Kembla Project Results," Energetech Australia Pty Ltd. [Online document], [cited 2005, August 31], Available HTTP: http://www.energetech.com.au/attachments/MediaUpdate_July2005.pdf.

[89] M. Previsic, R. Bedard, G. Hagerman, O. Siddiqui, "System Level Design, Performance and Costs for San Francisco California Pelamis Offshore Wave Power Plant," Global Energy Partners, LLC. E2I EPRI Global - 006A - SF, 2004.

[90] G. Bhyuan, "(Personal Communication)," Powertech Labs, March 11, 2005.

[91] "Submission of Pelamis WEC for E2I/EPRI Offshore Wave Feasibility Demonstration Project," Ocean Power Delivery, Ltd. 2004.

[92] "Order Signed to Build World's First Wave Farm in Portugal," Ocean Power Delivery, Ltd. [Online document], [cited 2005, September 10], Available HTTP: http://www.oceanpd.com/docs/OPD%20Enersis%20Press%20Release.pdf.

[93] T. Setoguchi, S. Santhakumar, M. Takao, T. H. Kim, and K. Kaneko, "A Modified Wells Turbine for Wave Energy Conversion," *Renewable Energy*, vol. 28, pp. 79-91, 2003.

[94] C. E. Tindall and M. Xu, "Optimising a Wells-Turbine-Type Wave Energy System," *IEEE Transactions on Energy Conversion*, vol. 11, pp. 631-635, 1996.

[95] C. H. Retzler, D.J. Pizer, "The Hydrodynamics of the Pelamis Wave Energy Device: Experimental and Numerical Results," presented at 20th International Conference on Offshore Mechanics and Arctic Engineering, Rio de Janeiro, Brazil, 2001.

[96] J. Seto, "Bamfield/Anacla Data Request [email]," BC Hydro, February 21, 2005.

[97] "Distribution Operating Diagram Index Map: Circuit 2551 LBH," BC Hydro, 2004.

[98] "Distribution Operating Diagram Index Map: Circuit 2552 LBH," BC Hydro, 2005.

[99] "Tofino Time," [Online document], [cited 2005, June 20], Available HTTP: http://www.tofinotime.com/main.htm?maps/MP-Pfrm.htm~BDfrm.

[100] "Ucluelet Inlet to/à Nootka Sound (chart 3603)," Canadian Hydrographic Service, Minister of Fisheries and Oceans Canada, 2002.

[101] "Clayoquot Biosphere Trust," [Online document], [cited 2005, August 29], Available HTTP: http://www.clayoquotbiosphere.org/.

[102] "Marine Energy Challenge: Oscillating Water Column Wave Energy Converter Evaluation Report," The Carbon Trust 2005.

[103] "Characteristics of Sound and the Decibel Scale," The Government of Hong Kong - Environmental Protection Department [Online document], [cited 2005, September 28], Available HTTP: http://www.epd.gov.hk/epd/noise_education/web/ENG_EPD_HTML/m1/intro_5.html.

[104] "Islay LIMPET Wave Power Plant," The Queen's University of Belfast. JOR3-CT98-0312, 2002.

[105] T. Denniss, "Comparing the Variability of Wind Speed and Wave Height Data," Energetech Australia Pty Ltd., Sydney, Australia 2005.

[106] "Proposed Wind Farm, Lough Hill, Curraghmacall, Castle Craig and Drummahon, County Tyrone: Supplementary Information under Article 15 of EA Regulations," B9 Energy Services Ltd. Planning Reference K/2001/0458, 2002.

[107] D. Robinson, "Tofino Wind Data [email]," Environment Canada, February 11, 2005.

[108] "West Coast Vancouver Island Atlas," Clayoquot Sound Energy [Online document], [cited 2005, August 12], Available HTTP: http://www.shim.bc.ca/tofino/main.cfm?sector=energy&name=Clayoquot%20Sound%20Energy&lat=49.260757&Lon=-126.000643&scale=600000.

[109] "Canadian Wind Energy Atlas," Environment Canada [Online document], [cited 2005, August 20], Available HTTP: http://www.windatlas.ca/en/index.php.

[110] "Information About Wind Energy," Environment Canada [Online document], [cited 2005, September 16], Available HTTP: http://www.on.ec.gc.ca/pollution/fpd/technologies/t-1000-e.html.

[111] H. Holttinen, "Hourly Wind Power Variations in the Nordic Countries," *Wind Energy*, vol. 8, pp. 173-195, 2005.

[112] T. H. Kim, T. Setoguchi, K. Kaneko, and S. Raghunathan, "Numerical investigation on the effect of blade sweep on the performance of Wells turbine," vol. 25, pp. 235-248, 2002.

[113] A. Brito-Melo, L. M. C. Gato, and A. J. N. A. Sarmento, "Analysis of Wells Turbine Design Parameters by Numerical Simulation of the OWC Performance," *Ocean Engineering*, vol. 29, pp. 1463-1477, 2002.

[114] T. Denniss, "Ocean Wave Energy Extraction System and Components Thereof," U.S. Patent 20020066269A1, June 6, 2002.

[115] V. S. Raju, M. Ravindran, and U. A. Korde, "Experiments on the Oscillating Water Column Wave Energy System," *OCEANS*, vol. 16, pp. 938-943, 1984.

[116] P. H. LeBlond, S.M. Calisal, and M. Isaacson, *Wave Spectra in Canadian Waters*: Marine Environmental Data Services Branch, Department of Fisheries and Oceans Canada, 1982.

[117] *TRNSYS Volume III: Introduction to TRNSYS with IISiBat (Manual)*: Solar Energy Laboratory, University of Wisconsin, Madison.

[118] "Research into the Further Development of the LIMPET Shoreline Wave Energy Plant," Wavegen, ETSU V/06/00183/REP, 2002.

[119] "Power Matrix Graph," Ocean Power Delivery Ltd. [Online document], [cited 2005, September 16], Available HTTP: http://www.oceanpd.com/Pelamis/Powermatrixgraph.html.

[120] "Vancouver Island - Call for Tenders: Quantitative Evaluation Methodology," BC Hydro [Online document], 6 August 2004, [cited 2005, September 16], Available HTTP: http://www.bchydro.com/rx_files/info/info14505.pdf.

[121] "Receiver General for Canada - Bank and Exchange Rates," Public Works and Government Services Canada [Online document], [cited Available HTTP: http://www.pwgsc.gc.ca/recgen/text/bankrt-e.html.

[122] "2005 Integrated Electricity Plan - Analysis of Dollar Costs of Resources in IEP: Summary of Current Thinking," BC Hydro [Online document], [cited 2005, September 16], Available HTTP: http://www.bchydro.com/rx_files/info/info22820.pdf.

[123] G. P. Harrison and A. R. Wallace, "Climate sensitivity of marine energy," *Renewable Energy*, vol. 30, pp. 1801-1817, 2005.

[124] "The VRB Energy Storage System - The VRB-ESS and Wind Power Generation," VRB Power Systems [Online document], [cited 2005, September 10], Available HTTP: http://www.vrbpower.com/pdfs/VRB-ESS%20Wind%20Application.pdf.